ORNL-3108
UC-34 – Physics

THE CARRIER-RECOMBINATION BEHAVIOR AND ANNEALING PROPERTIES OF RADIATION-INDUCED RECOMBINATION CENTERS IN GERMANIUM

O. L. Curtis, Jr.
J. H. Crawford, Jr.

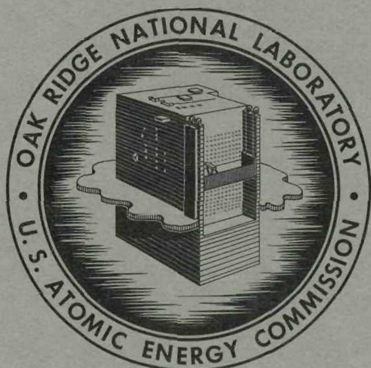

OAK RIDGE NATIONAL LABORATORY

operated by

UNION CARBIDE CORPORATION

for the

U.S. ATOMIC ENERGY COMMISSION

DISCLAIMER

This report was prepared as an account of work sponsored by an agency of the United States Government. Neither the United States Government nor any agency Thereof, nor any of their employees, makes any warranty, express or implied, or assumes any legal liability or responsibility for the accuracy, completeness, or usefulness of any information, apparatus, product, or process disclosed, or represents that its use would not infringe privately owned rights. Reference herein to any specific commercial product, process, or service by trade name, trademark, manufacturer, or otherwise does not necessarily constitute or imply its endorsement, recommendation, or favoring by the United States Government or any agency thereof. The views and opinions of authors expressed herein do not necessarily state or reflect those of the United States Government or any agency thereof.

DISCLAIMER

Portions of this document may be illegible in electronic image products. Images are produced from the best available original document.

Printed in USA. Price $2.50. Available from the

Office of Technical Services
Department of Commerce
Washington 25, D.C.

LEGAL NOTICE

This report was prepared as an account of Government sponsored work. Neither the United States, nor the Commission, nor any person acting on behalf of the Commission:

A. Makes any warranty or representation, expressed or implied, with respect to the accuracy, completeness, or usefulness of the information contained in this report, or that the use of any information, apparatus, method, or process disclosed in this report may not infringe privately owned rights; or

B. Assumes any liabilities with respect to the use of, or for damages resulting from the use of any information, apparatus, method, or process disclosed in this report.

As used in the above, "person acting on behalf of the Commission" includes any employee or contractor of the Commission, or employee of such contractor, to the extent that such employee or contractor of the Commission, or employee of such contractor prepares, disseminates, or provides access to, any information pursuant to his employment or contract with the Commission, or his employment with such contractor.

ORNL-3108

Contract No. W-7405-eng-26

SOLID STATE DIVISION

THE CARRIER-RECOMBINATION BEHAVIOR AND ANNEALING PROPERTIES OF RADIATION-INDUCED RECOMBINATION CENTERS IN GERMANIUM

O. L. Curtis, Jr.

J. H. Crawford, Jr.

DATE ISSUED

JUN 1 - 1961

Submitted as a thesis to the Graduate Council of The University of Tennessee in partial fulfillment of the requirements for the degree Doctor of Philosophy

OAK RIDGE NATIONAL LABORATORY
Oak Ridge, Tennessee
operated by
UNION CARBIDE CORPORATION
for the
U.S. ATOMIC ENERGY COMMISSION

ACKNOWLEDGMENTS

Association with the members of the Solid State Division of the Oak Ridge National Laboratory has contributed greatly to the success of this work. Drs. J. H. Barrett, H. C. Schweinler, D. K. Holmes, O. S. Oen, and Mr. J. W. Cleland (to mention only a few) have been helpful. Mr. S. Othmer, a student under the co-operative plan of Virginia Polytechnic Institute, assisted in much of the experimental work. The outstanding help of Miss M. Vannoy in preparing the manuscript is greatly appreciated.

TABLE OF CONTENTS

CHAPTER		PAGE
I.	INTRODUCTION	1
II.	EXPERIMENTAL PROCEDURE	9
III.	RESULTS	17
	Exploratory Measurements	17
	Detailed Measurements for Gamma Irradiation	21
IV.	DISCUSSION	43
	The Recombination Process	43
	The Annealing Behavior	73
	Comparison with Other Results	90
V.	SUMMARY	107
BIBLIOGRAPHY		111

LIST OF TABLES

TABLE PAGE

I. Hall Measurements of Arsenic-Doped Material 94

II. Determination of Capture Probability and Cross Section . . . 96

LIST OF FIGURES

FIGURE PAGE

1. (a) General Arrangement of Equipment 11

   (b) Schematic Diagram of Light Source 11

   (c) Construction of Flash Tube 11

   (d) Details of Sample Arrangement 11

2. A Schematic Diagram of the Temperature-Control Apparatus . . 14

3. Fraction of Damage Remaining following Successive Four-Hour Anneals 18

4. The Recombination Behavior of 2.0 Ohm-cm, Antimony-Doped Germanium following Irradiation by Reactor Neutrons and Successive Four-Hour Anneals 20

5. The Recombination Behavior of 2.0 Ohm-cm, Antimony-Doped Germanium following Irradiation by Co^{60} Gamma Rays and Successive Four-Hour Anneals 22

6. The Recombination Behavior of 11 Ohm-cm, Antimony-Doped Germanium following Irradiation by Co^{60} Gamma Rays and Successive Four-Hour Anneals 23

7. The Recombination Behavior of 15 Ohm-cm, Antimony-Doped Germanium following Irradiation by Reactor Neutrons and Successive Four-Hour Anneals 24

8. Fraction of Damage Remaining following Successive One-Hour Anneals, Antimony-Doped Germanium 26

9. Fraction of Damage Remaining following Successive One-Hour Anneals, Arsenic-Doped Germanium 27

FIGURE PAGE

10. Fraction of Damage Remaining following Successive Anneals for One Indium- and Two Antimony-Doped Specimens 28

11. The Recombination Behavior of 15 Ohm-cm, Antimony-Doped Germanium following Irradiation by Co^{60} Gamma Rays and Successive One-Hour Anneals 30

12. The Recombination Behavior of 3.7 Ohm-cm, Antimony-Doped Germanium following Irradiation by Co^{60} Gamma Rays and Successive One-Hour Anneals 32

13. The Recombination Behavior of 2.3 Ohm-cm, Antimony-Doped Germanium following Irradiation by Co^{60} Gamma Rays and Successive One-Hour Anneals 34

14. The Recombination Behavior of 1.3 Ohm-cm, Antimony-Doped Germanium following Irradiation by Co^{60} Gamma Rays and Successive One-Hour Anneals 35

15. The Recombination Behavior of 0.44 Ohm-cm, Antimony-Doped Germanium following Irradiation by Co^{60} Gamma Rays and Successive One-Hour Anneals 36

16. The Recombination Behavior of 20 Ohm-cm, Arsenic-Doped Germanium following Irradiation by Co^{60} Gamma Rays and Successive One-Hour Anneals 37

17. The Recombination Behavior of 5.4 Ohm-cm, Arsenic-Doped Germanium following Irradiation by Co^{60} Gamma Rays and Successive One-Hour Anneals 38

FIGURE PAGE

18. The Recombination Behavior of 2.6 Ohm-cm, Arsenic-Doped Germanium following Irradiation by Co^{60} Gamma Rays and Successive One-Hour Anneals 39

19. The Recombination Behavior of 8.3 Ohm-cm, Indium-Doped Germanium following Irradiation by Co^{60} Gamma Rays and Successive One-Hour Anneals 41

20. The Temperature Dependence of the Terms Involved in the Recombination Equation 52

21. The Result of Adding Three Terms of the Recombination Equation, Including the Effect of Intrinsic Carriers . . 53

22. A Different Combination of Terms from the Recombination Equation 57

23. The Recombination Behavior of Antimony-Doped Germanium following Irradiation by 14-Mev Neutrons. From Reference 6 60

24. The Recombination Behavior of Gallium-Doped Germanium following Irradiation by Co^{60} Gamma Rays. From Reference 5 64

25. The Recombination Behavior of Gallium-Doped Germanium following Irradiation by Reactor Neutrons. From Reference 5 65

26. The Recombination Behavior of Gallium-Doped Germanium following Irradiation by 14-Mev Neutrons. From Reference 6 66

FIGURE PAGE

27. The Energy-Level Structure Proposed to Explain the Recombination Behavior of n-Type Germanium Exposed to Various Kinds of Irradiation 71

28. Isothermal Annealing Curves for 3.7 Ohm-cm, Antimony-Doped Germanium following Co^{60} Gamma Irradiation 79

29. Isothermal Annealing Curves for 1.3 Ohm-cm, Antimony-Doped Germanium following Co^{60} Gamma Irradiation 80

30. Corrected Isothermal Annealing Curves. Data of Figure 29 . 82

31. Corrected Isothermal Annealing Curves for 1.3 Ohm-cm, Antimony-Doped Germanium following Various Co^{60} Gamma Irradiations 83

32. The First-Order Rate Constants as Obtained from Isothermal Anneals for 1.3 and 3.7 Ohm-cm, Antimony-Doped Germanium Plotted Logarithmically as a Function of Reciprocal Temperature 84

33. Isothermal Annealing Curves for 5.4 Ohm-cm, Arsenic-Doped Germanium following Co^{60} Gamma Irradiation and One Hour at 126°C 89

34. Comparison of Isothermal Anneals Performed on Arsenic-Doped Germanium Using Lifetime and Conductivity Data following Co^{60} Gamma Irradiation and Electron Irradiation, Respectively. Conductivity data from References 9 and 10 . . . 92

35. Isothermal Annealing Behavior in the Temperature Range just above Room Temperature of Antimony-Doped Germanium Irradiated with 1-Mev Electrons at 79°K. From Reference 8 . 97

FIGURE PAGE

36. A Semi-Logarithmic Plot of a Portion of the Data of the Preceding Figure, before and after Subtracting the Fraction 0.32 99

37. Four of the Isothermal Annealing Curves of Figure 35 Plotted as in Figure 36 but Time-Normalized to the Data of Figure 36 100

38. First-Order Rate Constant as a Function of Reciprocal Temperature from the Preceding Figure. The indicated activation energy is 0.79 ev 102

39. Isothermal Annealing Curves (56°C) Showing the Difference in Annealing Behavior among Specimens with Different Chemical Doping. From Reference 8 103

ABSTRACT

An investigation has been made of the carrier-recombination behavior and annealing properties of radiation-induced recombination centers in germanium. In order to analyze the recombination behavior, it has been necessary to treat the problem of recombination in the presence of trapping. A model which explains the experimental results in both n- and p-type material for various sorts of irradiation is presented. On the basis of this model, recombination occurs at an energy level 0.36 ev above the valence band in gamma-irradiated, n-type germanium. The position of this level is shifted slightly downward for neutron-irradiated material. Trapping levels occur in arsenic-doped germanium 0.17 ev above the valence band which are not present in antimony-doped material. An energy level apparently present in unirradiated material acts as a trapping center in p-type germanium. It is difficult to obtain a value for capture cross sections, but under certain assumptions a value for the electron-capture cross section in n-type material is obtained: 7×10^{-19} cm^2. The annealing behavior of antimony-doped germanium is grossly different from that of arsenic-doped material. Although the annealing behavior is rather complicated, the results are consistent with the following model. Irradiation produces three major types of defects: interstitials, vacancies, and vacancy-interstitial pairs. The vacancy-interstitial pair evidently is responsible for a trapping level located 0.25 ev above the valence band. Both the interstitial and vacancy act as acceptors. The recombination level at 0.36 ev belongs to the vacancy. The interstitial

becomes mobile above room temperature and either anneals or forms a complex with an impurity atom. It is thought that the trapping level located 0.17 ev above the valence band might be due to an arsenic-interstitial pair. The activation energy of motion for the interstitial is about 0.8 ev. At a somewhat higher temperature the vacancy becomes mobile with an activation energy of motion of approximately 1.1 ev. In antimony-doped material the vacancy disappears by association with an antimony atom. This process does not occur in arsenic-doped material, and higher temperatures are required to produce annealing.

CHAPTER I

INTRODUCTION

The study of radiation-induced defects has been of great assistance in obtaining an understanding of the structure of solids. Because of the high sensitivity of their electrical characteristics to structural imperfections, semiconductors have proven especially useful in such studies.[1] Annealing experiments have played an important role in our present understanding of radiation damage. It is hoped through the studies herein reported to resolve some of the questions which remain concerning radiation-induced defects, especially as they act as centers for the recombination of excess carriers in germanium.

Defect solid-state studies comprise one of the most active fields in solid state physics. The reason for this great interest is the fact that many of the more important physical properties of solids are strongly influenced by various types of defects. Defects may occur during the formation of a crystalline solid, or they may be introduced subsequently. Defects may be introduced mechanically (e.g., by plastic deformation), by thermal treatment (e.g., by quenching), or by irradiation with energetic particles. The production of defects by irradiation has several advantages. First, the relative amount of damage can be easily controlled. Various types of irradiation can

---

[1] See, for instance, J. H. Crawford, Jr., and J. W. Cleland, in Progress in Semiconductors, Vol. 2 (John Wiley and Sons, New York, 1957), pp. 69-107.

be chosen to give different sorts of damage. Using the proper type of irradiation, damage can be introduced quite homogeneously, which is difficult, if not impossible, using other methods. Of course, radiation-damage studies have considerable practical importance since materials are required to fulfill many functions in the presence of radiation fields.

There are a number of electrical properties of semiconductors which have been used in radiation-effect studies. Probably the most extensive studies have been made using conductivity and Hall-effect measurements which yield the concentration and mobility of carriers in the crystal.[1] Hall-effect measurements give the number of free carriers which, in turn, provides information concerning the number of acceptors or donors introduced into the lattice. (In n-type material a defect is a donor when it provides an energy level in the forbidden gap of the semiconductor from which an electron associated with the defect may be thermally excited, providing an additional carrier. It is an acceptor, on the other hand, when it introduces an empty level into the forbidden gap and an electron may be removed by occupying this level.) Knowing the carrier concentration, one may obtain the carrier mobility from the conductivity, thus providing information about the scattering properties of the introduced defects, which, in turn, yields values for the charge state.

Another electrical property of semiconductors is becoming very important in defect studies. That property is minority-carrier lifetime, the time constant associated with the recombination of excited

hole-electron pairs. Reviews of work in the field of radiation effects using measurements of carrier lifetime in silicon and germanium have recently appeared.[2,3] One might suppose that after an electron has been excited from the valence band across the forbidden gap into the conduction band, providing a hole-electron pair, it would quickly return because the process is so favorable energetically. However, this direct recombination is highly forbidden because of the requirement of momentum conservation. The value of the momentum associated with the photon produced by such a transition will not be equal to that possessed by an arbitrary hole-electron pair. The direct recombination process is so highly forbidden that it cannot be observed in germanium. (The lifetime associated with direct recombination is about 0.1 second for material having a carrier concentration of 10^{14} cm^{-3}.) Rather, recombination occurs via recombination levels lying in the forbidden gap. This work is devoted primarily to a study of these recombination levels.

Lifetime measurements have a great advantage over other electrical measurements because of their sensitivity to radiation-produced defects; very low concentrations of defects playing the role of recombination centers can be detected. The reason that lifetime measurements are more sensitive than those depending upon carrier concentration is that, in a well-prepared, unirradiated crystal, the number of recombination centers present is very small compared with the carrier concentration.

---

[2] G. K. Wertheim, J. Appl. Phys. 30, 1166 (1959).

[3] O. L. Curtis, Jr., J. Appl. Phys. 30, 1174 (1959).

This high sensitivity proves especially useful when one uses gamma rays as a source of radiation damage. Using the most powerful Co^{60} sources available, the time required to produce sizeable carrier-concentration changes in, say, one ohm-cm germanium is prohibitively long, while order-of-magnitude changes in lifetime are accomplished in only a few hours. Thus, lifetime measurements are useful over a greater range of carrier concentration (and, consequently, impurity concentration). Perhaps of equal importance in the choice of lifetime measurements is the possible simplification of the analysis of annealing kinetics for such low concentrations since processes higher than first order are less likely to occur.

In the analysis of lifetime measurements in terms of radiation-induced defects, there are both advantages and disadvantages as compared with conductivity or carrier-concentration measurements. An advantage is that, although there may be several types of defects present, all of which affect the carrier concentration and conductivity, one of these is likely to dominate in the recombination process and, therefore, may be singled out for separate examination. The primary disadvantage is that the relationship between lifetime and number of defect sites is not as direct as in the case of carrier concentration.

One naturally expects a difference in the nature of radiation damage, depending upon the nature and energy of the bombarding particle. This difference has demonstrated itself quite strikingly in the case of minority-carrier-lifetime measurements in germanium, where the recombination behavior is dependent upon whether the bombarding particles are

Co^{60} gamma rays, fission neutrons, or 14-Mev neutrons.[3-6] A brief study has been made to ascertain the nature of the dependence of annealing behavior on bombarding particles and it was shown that, indeed, there is a strong dependence.[7] However, it is not the purpose of this work to study in any detail these differences. Rather, the case in which the simplest type of damage is expected, irradiation by Co^{60} gamma rays, has been singled out in hopes that there might be a better chance of understanding the observations.

Irradiation by Co^{60} gamma rays has the advantage over charged-particle irradiation in that gamma rays are not appreciably attenuated in the sample and, thus, produce damage homogeneously. Gamma-ray irradiation may properly be called "internal-electron bombardment." The energetic photons produce Compton and photoelectric electrons in the crystal, which subsequently produce atomic displacement through collision with the crystal atoms. Irradiation by gamma rays also has an advantage over neutron irradiation in that essentially all of the damage consists of single displacements because the energy transferred to a recoiling atom by a Compton electron is small (near the displacement threshold). However, there may be a complication due to the higher

---

[4] O. L. Curtis, Jr., J. W. Cleland, J. H. Crawford, Jr., and J. C. Pigg, J. Appl. Phys. 28, 1161 (1957).

[5] O. L. Curtis, Jr., J. W. Cleland, and J. H. Crawford, Jr., J. Appl. Phys. 29, 1722 (1958).

[6] O. L. Curtis, Jr., and J. W. Cleland, J. Appl. Phys. 31, 423 (1960).

[7] O. L. Curtis, Jr., and J. H. Crawford, Jr., Bull. Am. Phys. Soc. (II) 5, 196 (1960).

degree of correlation in distance of separation between vacancy-interstitial pairs so produced. Although this study includes some measurements on p-type germanium, the primary emphasis is on n-type material. The principal reason for this choice is that the recombination process in p-type germanium appears to be more complicated and less subject to analysis.[5]

The investigation of the annealing behavior of a defect is useful in ascertaining the nature of the defect and of the crystal in which it is produced and annihilated. The effect of crystal properties and defect concentration (order of the process) on the annealing, the structure of annealing curves, and the activation energies obtained all give clues concerning the defect structure. In this study of defects in solids use has been made of these tools already mentioned: irradiation by energetic gamma rays to produce simple defects, homogeneously distributed in the crystal; measurement of minority-carrier lifetime, which is the most sensitive method available for observation of these defects; and annealing studies to provide information about these defects. Minority-carrier-lifetime measurements were not used simply as a means of following the annealing behavior. Rather, from the recombination process itself information was obtained about the defects in their role of recombination centers. Although in this study lifetime measurement have been used as an indication of degree of crystalline perfection, an attempt has been made to correlate these results with those of others using different types of measurements.

A number of studies of radiation damage, including annealing behavior, have been made. One such study is especially significant to this work and will be referred to often in the discussion. This is the work of Brown, Augustyniak, and Waite (Bell Telephone Laboratories) made upon electron-irradiated germanium.[8] These authors shall be referred to hereafter as BAW. BAW found that the chemical nature of the doping agent present in quantities of approximately 10^{15} cm^{-3} had gross effects upon the annealing behavior. These results indicate that previous analyses[9,10] made on the basis of annihilation of interstitials with their parent vacancies are invalid. In contrast to the present work, BAW primarily used conductivity as an indication of the amount of damage present. They used electrons with energies of the order of a million electron volts, which would be expected to produce damage similar to that produced by gamma rays since, as noted above, in gamma irradiation the actual damage is caused by the Compton and photoelectric electrons. However, their defect concentrations were much larger than those required for annealing studies based on recombination behavior. A brief study of the near-room-temperature annealing of 15 ohm-cm, n-type germanium irradiated with Co^{60} gamma rays also

---

[8] W. L. Brown, W. M. Augustyniak, and T. R. Waite, J. Appl. Phys. 30, 1258 (1959).

[9] W. L. Brown, R. C. Fletcher, and K. A. Wright, Phys. Rev. 92, 591 (1953).

[10] T. R. Waite, Phys. Rev. 107, 463, 471 (1957).

has been made.[11] However, the results were analyzed on the basis of direct recombination of vacancy-interstitial pairs, which BAW have shown cannot occur. Annealing studies, also very brief, have been made on high-resistivity germanium irradiated with 14-Mev neutrons.[12]

This work is concerned with the annealing of defects that are stable at room temperature. Since BAW found annealing effects at room temperature, it is known that some rearrangement of the defects may have already occurred. As is obvious, there is a wide variety of ways in which a study of radiation-damage annealing can be approached. This work does not provide a complete solution to the problems involved. However, it is believed that it does provide a significant contribution to the understanding of radiation-induced defects, especially in their role as recombination centers.

---

[11] T. Asada, H. Saito, K. Omura, T. Oku, and M. Oka, J. Phys. Soc. Japan 15, 93 (1960).

[12] R. F. Konopleva, T. V. Mashovets, and S. M. Ryvkin, Fiz. Tverdogo Tela, Sbornik [Supplement] II, 11 (1959).

CHAPTER II

EXPERIMENTAL PROCEDURE

The method of lifetime measurement utilized the exponential decay of excess carriers following injection by a light pulse. The time constant of this decay was taken as the minority-carrier lifetime. A constant current was passed through the sample, and a change in the voltage drop across the sample was assumed to be proportional to the number of excess carriers present. The field inside the sample was kept small to minimize the sweeping out of injected carriers. The injection level at the time of measurement was low, of the order of 0.1 to 1 per cent of the carrier concentration, in order to minimize errors due to the dependence of lifetime upon injection level.

In order to minimize surface effects, large samples were used, at least seven millimeters in the smallest dimension. The surfaces were prepared by etching with CP-4 etch* and washing with distilled water or distilled water plus ethyl alcohol. Each time the samples were irradiated or heat treated they were re-etched and dried in a vacuum overnight before performing lifetime measurements. Ohmic contacts were produced by using a lead-tin solder containing 2 per cent antimony. The melting point of this solder was approximately 180°C; therefore, when higher temperature heat treatments were used, the

---

*CP-4 etch consists of the following: twenty parts concentrated nitric acid, twelve parts 50 per cent hydrofluoric acid, twelve parts glacial acetic acid, and one-half part bromine.

solder was removed and replaced, following the heat treatment, by a high indium-content solder with a melting point of approximately 110°C.

Figure 1(a) indicates schematically the experimental arrangement used in obtaining lifetime measurements. The temperature was controlled by circulating dry helium through the sample chamber. Light pulses were admitted through a window in the front of the chamber. A regulated power supply in series with a high resistance resistor provided a constant current through the sample. The signal was fed (through a pre-amplifier, if necessary) to a Tektronix Type 545 oscilloscope. The non-reproducibility of light-pulse intensity required the observation of single pulses. This was the purpose of the Hughes memoscope, an instrument capable of retaining an oscilloscope trace indefinitely. This particular instrument had no sweep circuit but was driven from the Tektronix oscilloscope.

The light source used in these measurements utilized a xenon flash tube.[13] Figure 1(b) is a schematic diagram of the light source. The capacitor was charged to about five kilovolts. The setting of the Variac controlled the repetition rate of the discharge while a resistance in series with the capacitor limited the peak current through the rectifier tube. The duration of discharge was about one-half microsecond, with a peak current of the order of one thousand amperes. The intensity available from such a source is very high and is the only source found capable of use with a germanium filter in front of the

[13] J. N. Aldington and A. J. Meadocroft, J. Inst. Elec. Engrs. (London) 95, 671 (1948).

UNCLASSIFIED
ORNL-LR-DWG 48272

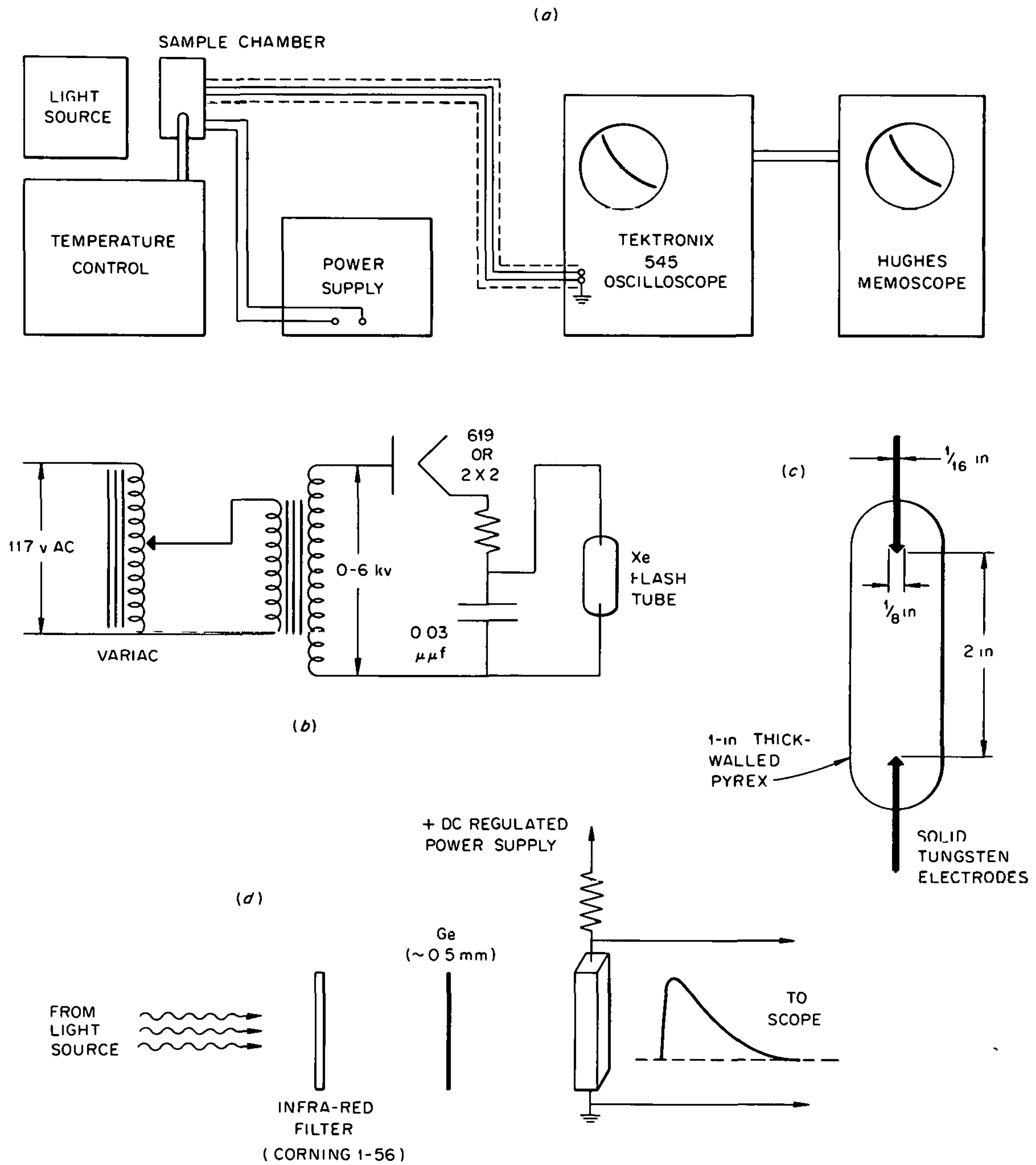

Figure 1. (a) General Arrangement of Equipment. (b) Schematic Diagram of Light Source. (c) Construction of Flash Tube. (d) Details of Sample Arrangement.

sample.* Figure 1(c) illustrates a typical geometry for the flash tube. A one-inch-diameter Pyrex tube was filled with xenon to a pressure of about one-half atmosphere. The primary difficulty associated with such a light source was the non-reproducibility of light intensity already mentioned.

Although the decay of the light flash had an initial time constant, as observed with a vacuum photodiode, of less than one microsecond, there was associated with it a considerably slower infrared afterglow capable of exciting carriers in germanium. This afterglow could be largely eliminated by using an infrared filter, such as Corning Type 1-56, in front of the sample. In order to remove the less penetrating short wave-length light, a thin germanium filter was also inserted. (In these experiments the germanium filter was omitted for specimens having resistivities less than three ohm-cm because of the difficulty in obtaining sufficient light intensity.†) The arrangement used is shown in Fig. 1(d), which also indicates the manner in which the signal was obtained from the specimen. The resistor shown had a value very large compared with the sample resistance.

---

*It is desirable to use such a filter in order to eliminate the less penetrating portion of the light (that having photon energies greater than the fundamental absorption edge). This prevents very large gradients in the photo-production of electron-hole pairs near the surface of the specimen with possible complications in recombination behavior.

†In this case large gradients in the concentration of excited carriers were avoided by waiting for the total number of excited carriers to decay to a small fraction of the initial value.

Figure 2 is a schematic diagram of the temperature controller. This apparatus was patterned after a similar design used at Oak Ridge National Laboratory by D. O. Thompson.[14] By means of a compressor, dry helium was continuously circulated through the sample chamber. The temperature was controlled by mixing hot and cold helium which had passed through a heater or cooling dewar, respectively. A Leeds and Northrup Speedomax, Type H recorder with a DAT controller, determined the ratio of hot to cold flow by operating solenoids in the hot and cold lines and at the same time recorded the temperature of a copper-constantan thermocouple soldered to the end of the sample. In order to obtain more accurate temperature values than were available from the recorder, a second thermocouple was also attached to the end of the sample and the temperature read with a Rubicon precision potentiometer. Either liquid nitrogen or a mixture of dry ice and alcohol was used in the cooling dewar, depending upon the lowest temperature desired. (Actually, dry ice and alcohol was sufficient for all measurements herein reported.) Other details of the apparatus are shown in the figure.

Most of the annealing was carried out in a silicone-oil bath. A mercury-to-wire temperature controller was capable of maintaining the temperature to $\pm$ 0.1°C. The temperatures were read with a copper-constantan thermocouple or a mercury thermometer. The estimated accuracy of annealing temperatures was $\pm$ 0.5°C. The time required for the specimens to attain temperature equilibrium after being placed in the

---

[14] D. O. Thompson, private communication.

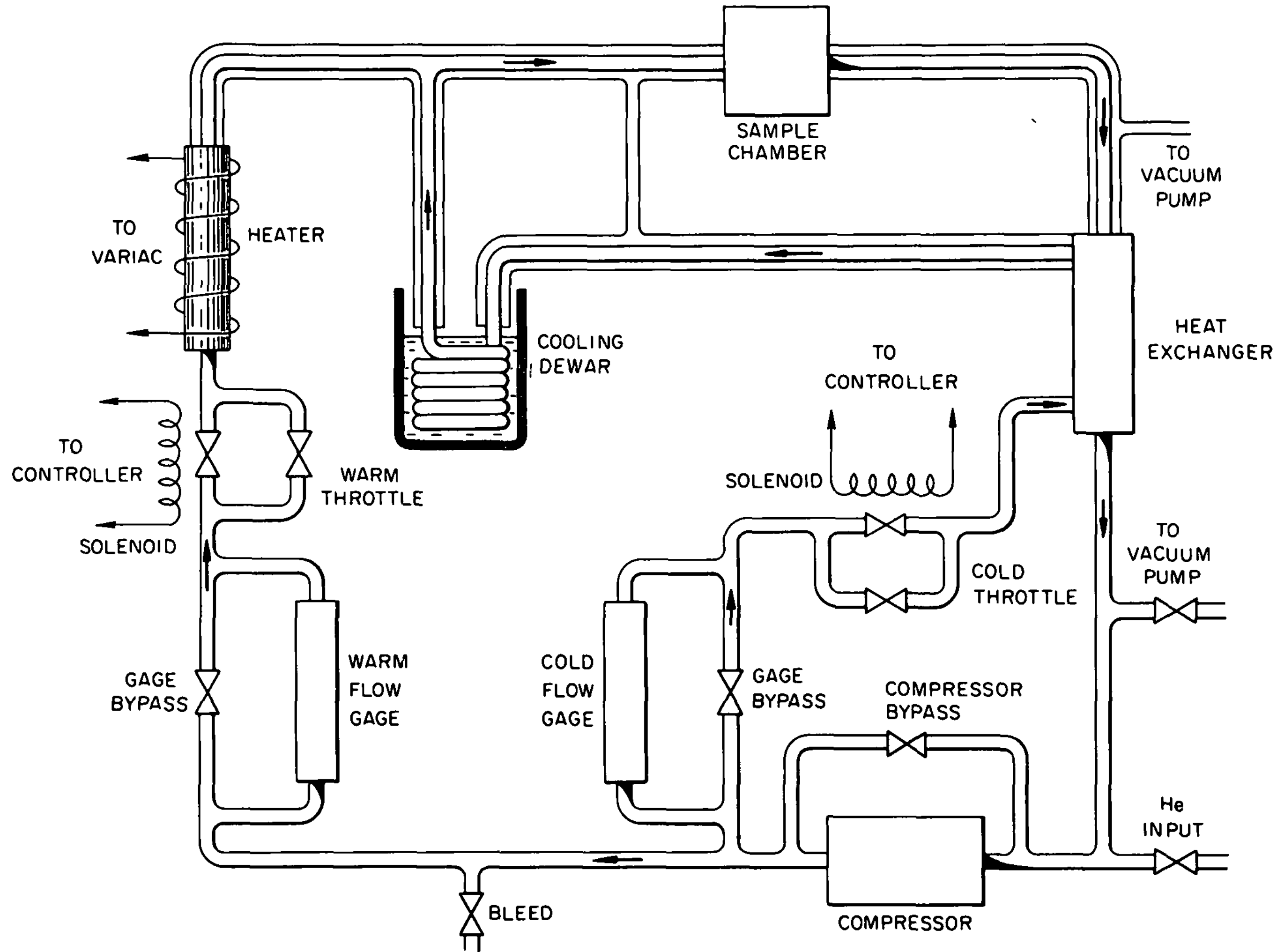

Figure 2. A Schematic Diagram of the Temperature-Control Apparatus.

oil was observed on a recorder. From this the estimated accuracy of time of anneal was ± one minute. The silicone oil used in the oil bath was nominally stable to about 250°C. Therefore, for higher temperatures it was necessary to use a salt bath.* The accuracy of temperature measurements using the salt bath was estimated to be about ± 1°C. It was necessary to seal the specimens in an evacuated Pyrex tube, thus lessening the thermal contact with the bath. However, the error in annealing time was estimated to be only about ± three minutes in this case. For the first series of measurements, which were exploratory in nature, to determine the nature of the annealing behavior for different types of radiation and sample characteristics, the anneals were carried out in a vacuum oven. In this case the temperature control was rather poor, and the error in the temperature of anneal may have been of the order of ± 5°C. These were all four-hour anneals, with an estimated inaccuracy in the time determination, due to the slow response of the oven, of ± one-half hour.

The gamma irradiations were carried out in a Co^{60} source of approximately 1,500 curies, providing approximately 2×10^{6} roentgens per hour or approximately 3×10^{15} gammas per cm^{2} per hour at the sample. The temperature of irradiation was approximately 35°C. The fission neutrons were obtained from a low-flux facility of the Oak Ridge Graphite Reactor. The temperature of irradiation was about 28°C.

---

*The use of this salt bath and the associated control equipment was kindly furnished by M. S. Wechsler and R. H. Kernohan, of the Solid State Division, Oak Ridge National Laboratory.

The 14-Mev neutrons were obtained using the $T(d,n)He^4$ reaction. The energetic deuterons necessary for the reaction were provided by a Cockroft-Walton accelerator.* At a distance of 7.5 cm from the target an irradiation time of from one to two hours was required to produce 10^{11} neutrons per cm^2 at the sample, with an accuracy in the flux determination of 5 to 10 per cent. Greater fluxes could be obtained closer to the tube with resultant decrease in the accuracy of flux determinations. The neutron flux was determined independently by two methods: the neutrons were counted directly by a long counter located some distance from the target, and the alpha particles produced simultaneously with the neutrons were detected by a second counter.

The material used was obtained from three sources. Antimony-doped material was obtained commercially from the Eagle Picher Company and United Mineral and Chemical Corporation. The arsenic- and indium-doped material, as well as part of the antimony-doped material, was grown under a special contract by National Carbon Research Laboratories.

---

*M. L. Randolph and D. L. Parrish, of the Biology Division, Oak Ridge National Laboratory, generously supplied the 14-Mev-neutron irradiations used in this work.

CHAPTER III

RESULTS

I. EXPLORATORY MEASUREMENTS

As a preliminary to making a detailed study of annealing behavior, a survey-type experiments was made in order to provide a general view of the behavior to be expected.[7] Three types of irradiating particles were used: 14-Mev-monoenergetic neutrons, fission neutrons, and Co^{60} gamma rays. In each case three specimens were used: two ohm-cm p-type, two ohm-cm n-type, and fifteen ohm-cm n-type. Figure 3 summarizes the results of these measurements. In this figure the fraction of damage remaining,* as determined from the room-temperature-lifetime values, is plotted as a function of the annealing temperature. Three temperatures were used: 104, 143, and 201°C. The type and resistivity of the material are indicated by the symbols used for the points; the type of irradiation by solid, dashed, and dotted lines. The n-type samples were antimony doped; the p-type samples were indium doped.

Several conclusions can be drawn immediately from this plot. The annealing behavior depends markedly both on the type of irradiation and the properties of the material. Two ohm-cm n-type material annealed more readily than fifteen ohm-cm n-type material regardless of the

---

*The fraction of damage remaining in the crystal was taken to be $f = (1/\tau - 1/\tau_o)(1/\tau_i - 1/\tau_o)^{-1}$, where τ_o is the pre-irradiation lifetime, τ_i is the post-irradiation lifetime, and τ is the lifetime following anneal.

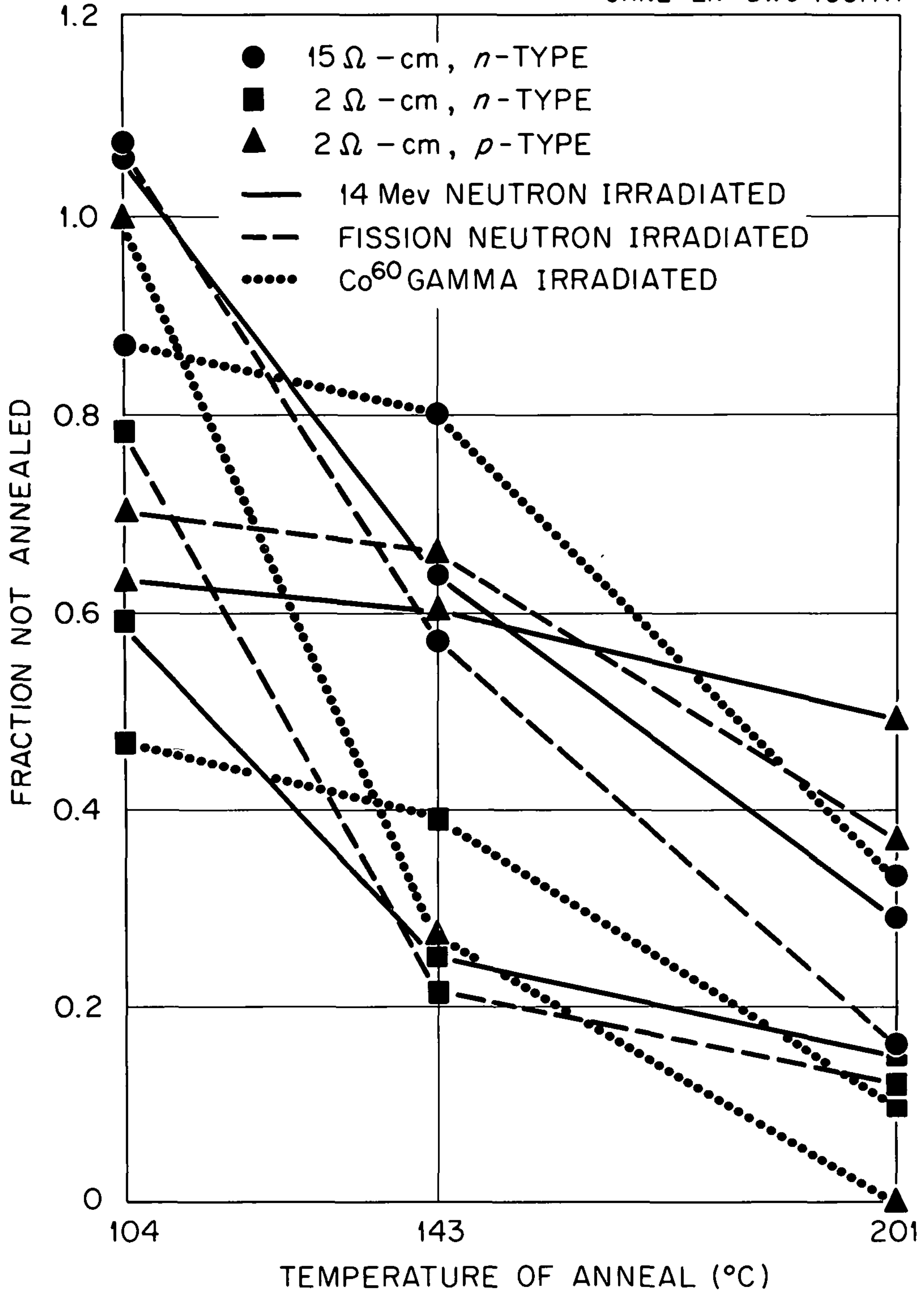

Figure 3. Fraction of Damage Remaining following Successive Four-Hour Anneals.

irradiation used. (The fifteen ohm-cm value is nominal. Although the three specimens were from the same ingot, the values ranged from eleven to fifteen ohm-cm.) The most striking difference between types of irradiation was demonstrated by the p-type material. Here, throughout the annealing range, the annealing behavior for material irradiated by Co^{60} gamma rays was much different from the two specimens irradiated by neutrons.

One must be cautious with a plot such as Fig. 3 since the annealing may produce a change in the recombination process and thus render a number for the fraction of damage remaining not very meaningful. In fact, a change in process (i.e., a change in temperature dependence of lifetime) was indicated in some cases. To determine any such change, lifetime measurements were made as a function of temperature at each of the points indicated on the graph. There was no appreciable change in process indicated for p-type material nor for 14-Mev-neutron irradiated, n-type material. However, for some fast-neutron and gamma-irradiated specimens, there seemed to be a change. Figure 4 shows the data for the two ohm-cm, n-type specimens irradiated with fast neutrons.* The 0.35 ev slope observed immediately following irradiation was reported earlier for this sample.[3] However, it should be noted that for a number of samples having higher resistivities a slope of about 0.24 ev has been

---

*The following sample designation will be used: the first two letters denote the source of the material; EP, the Eagle Picher Company; NC, the National Carbon Research Laboratories; and UM, the United Mineral and Chemical Corporation. The next two letters are the chemical symbol for the doping agent, and the number is the resistivity in ohm-cm.

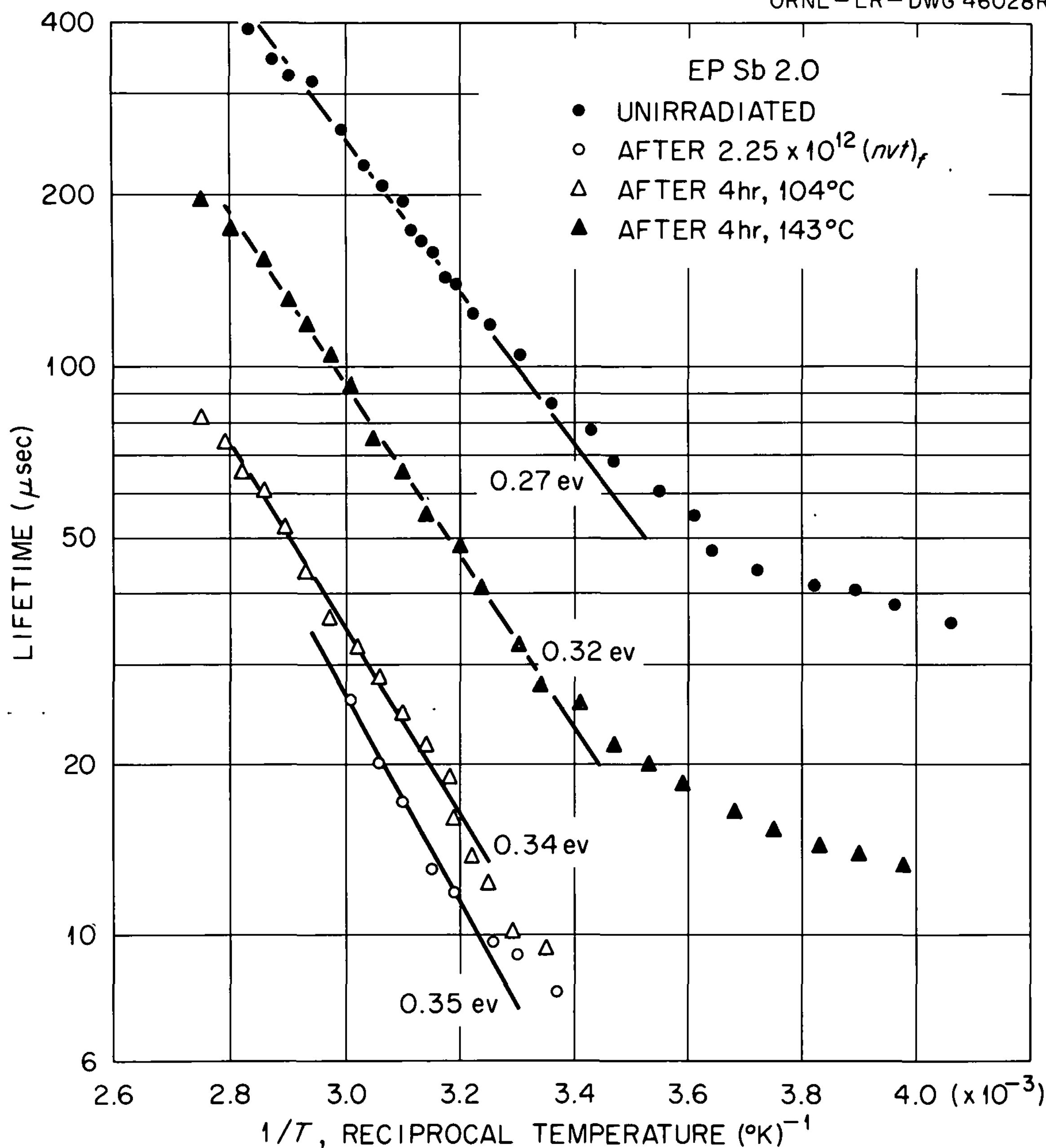

Figure 4. The Recombination Behavior of 2.0 Ohm-cm, Antimony-Doped Germanium following Irradiation by Reactor Neutrons and Successive Four-Hour Anneals.

observed.[3] The steeper slope for this lower resistivity specimen showed up very conclusively after the 104°C anneal since it was now possible to extend the measurements upward in temperature without the danger of annealing at the temperature of measurement. This slope corresponds to that observed in n-type germanium irradiated with 14-Mev neutrons.[6] Evidently, for this specimen there was no change in process due to the annealing. In contrast, the two ohm-cm, n-type sample irradiated with Co^{60} gamma rays apparently displayed a definite change in the recombination process. Figure 5 demonstrates quite strikingly the change in slope induced by the anneal at 104°C. Similar behavior is exhibited in Figs. 6 and 7 but to a lesser degree. The first is the data for the higher resistivity, n-type specimen, in which the extent of early annealing was much less pronounced. The latter is a plot for a specimen cut from the same ingot as the sample of Fig. 6, irradiated with fission neutrons.

II. DETAILED MEASUREMENTS FOR GAMMA IRRADIATION

Since the nature of gamma-ray-induced damage is expected to be simpler than for the case of neutron bombardment and since the recombination process is better understood in n- than in p-type material, emphasis has been placed on n-type germanium irradiated with Co^{60} gamma rays. Isochronal anneals were performed on antimony-doped samples with six different impurity concentrations, arsenic-doped samples with three different impurity concentrations, and one p-type, indium-doped sample. One-hour anneals for as many as eleven different temperatures, equally

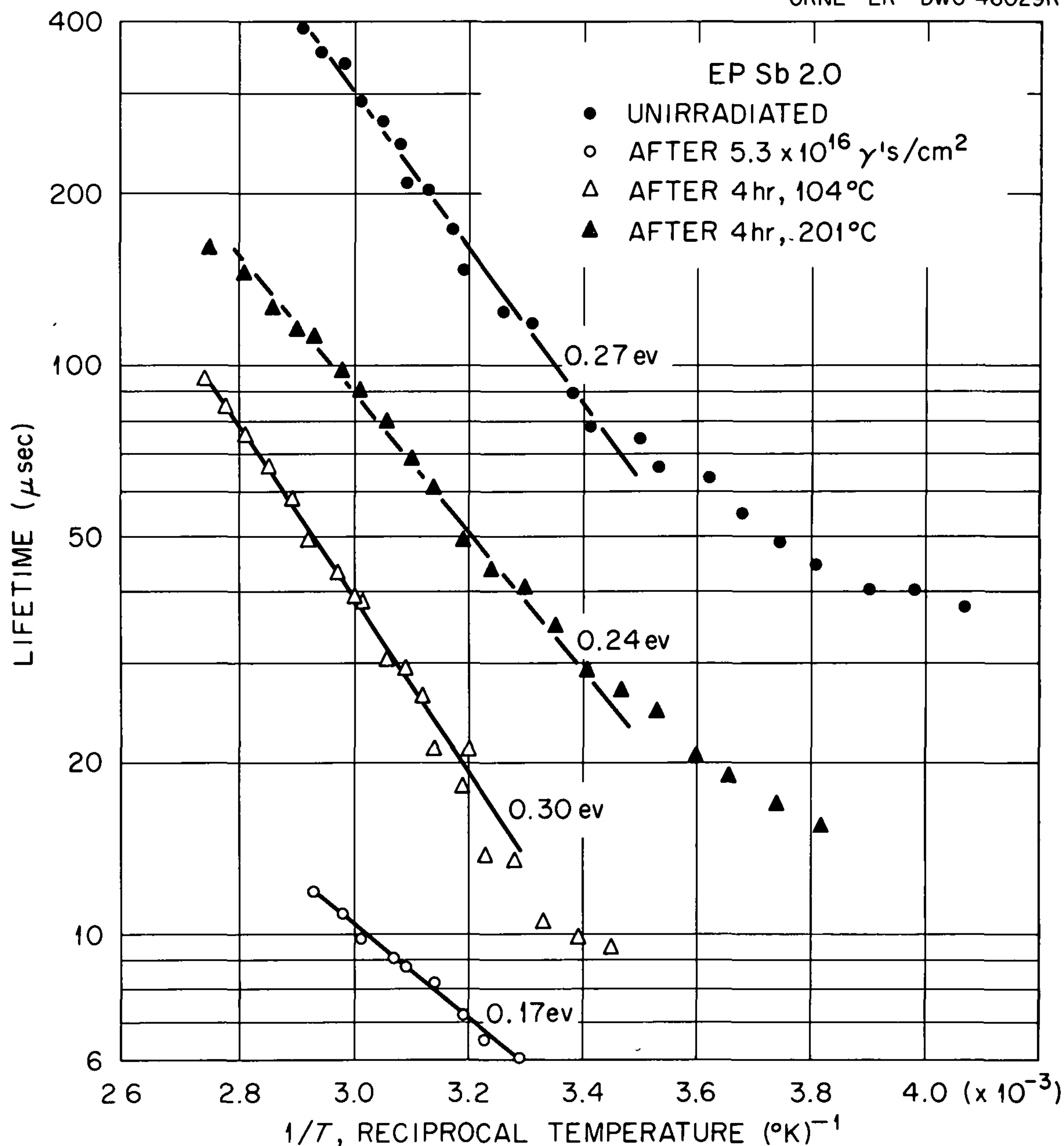

Figure 5. The Recombination Behavior of 2.0 Ohm-cm, Antimony-Doped Germanium following Irradiation by Co^{60} Gamma Rays and Successive Four-Hour Anneals.

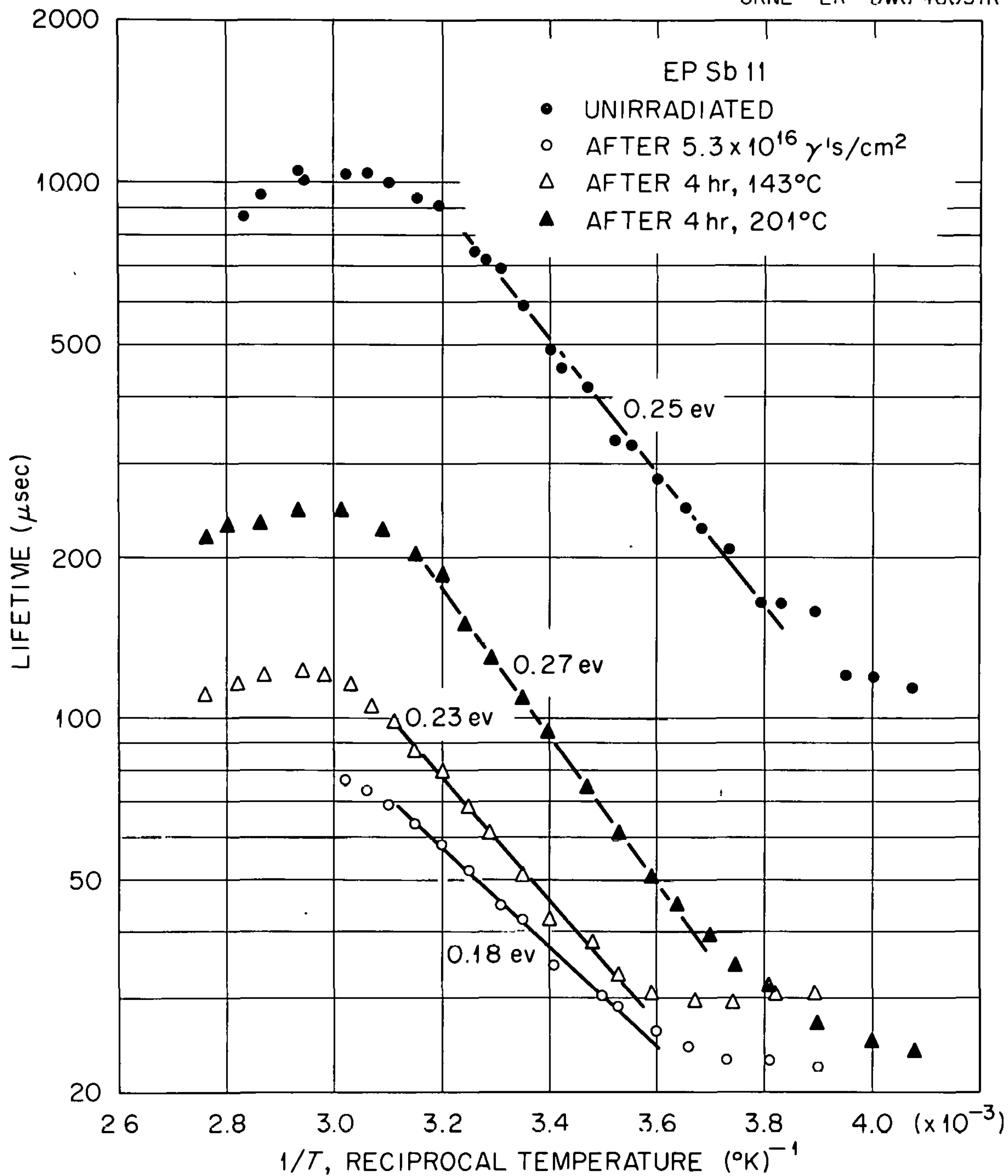

Figure 6. The Recombination Behavior of 11 Ohm-cm, Antimony-Doped Germanium following Irradiation by Co^{60} Gamma Rays and Successive Four-Hour Anneals.

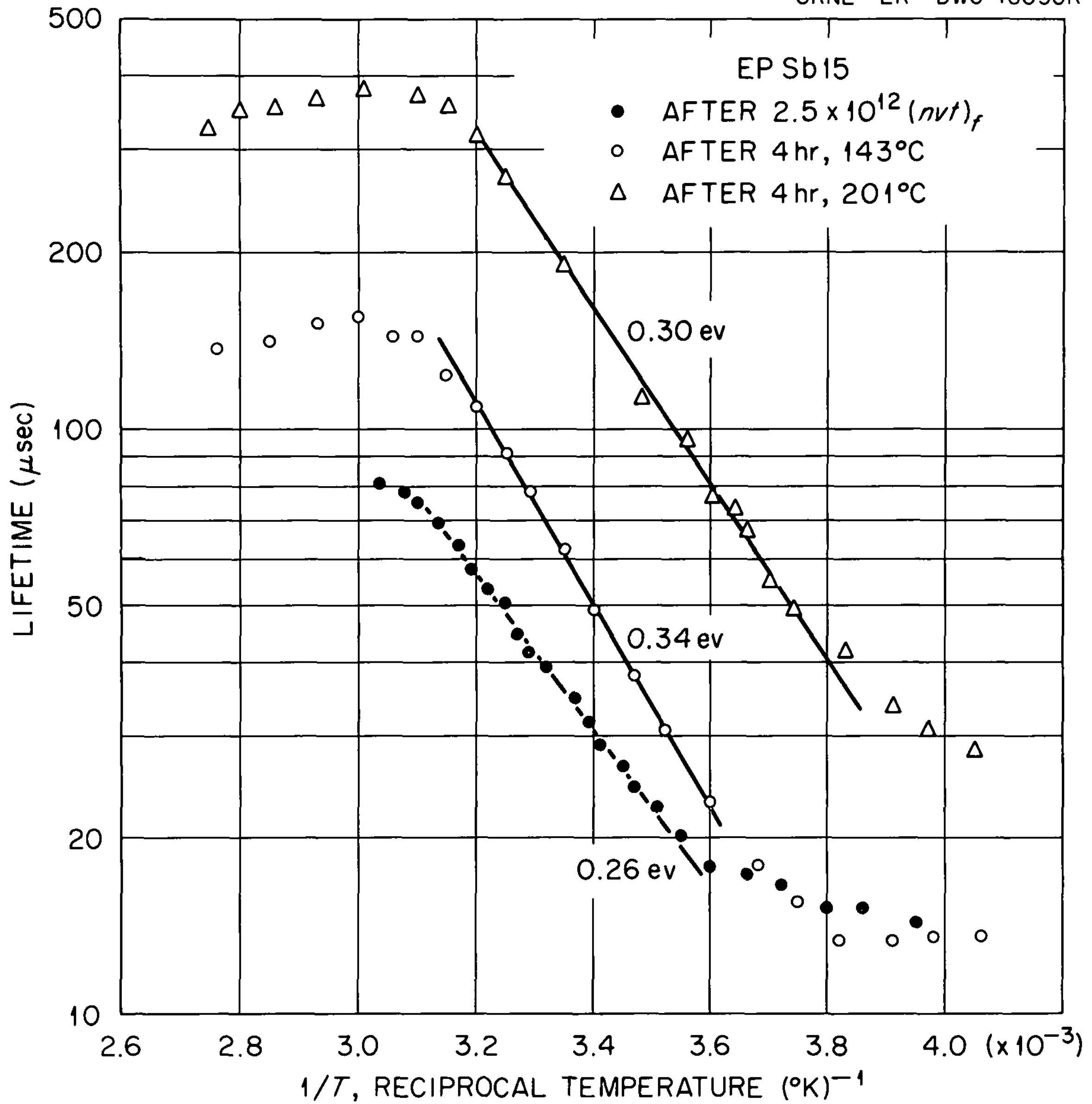

Figure 7. The Recombination Behavior of 15 Ohm-cm, Antimony-Doped Germanium following Irradiation by Reactor Neutrons and Successive Four-Hour Anneals.

spaced on the 1/T scale, were made. Figure 8 summarizes the results for antimony-doped material. Here the fraction of damage not annealed is plotted as a function of the annealing temperature. The following resistivities are represented in this plot: 15, 6.2, 3.7, 2.3, and 0.44 ohm-cm. Details, such as the amount of irradiation received prior to annealing, will be given with later figures. The important feature shown in Fig. 8 is that the annealing behavior depends markedly on the impurity concentration (as determined from conductivity) throughout the resistivity range.

The results for arsenic-doped material, shown in Fig. 9, were entirely different. Three resistivities were used in this case: 20, 5.4, and 2.6 ohm-cm. There was an early, impurity-concentration-dependent annealing whose extent ranged from about 15 to about 60 per cent in the three samples. At higher temperatures, if the curves for the two lower resistivities (higher impurity concentration) are normalized, they very nearly superimpose. The annealing behavior of NCAs 20 was actually rather similar to that for EPSb 15, which might be expected since in these higher resistivity samples the impurity concentration was rather low and might, therefore, play a less important role in the annealing process.

The results for two antimony-doped specimens were not included in Fig. 8 in order to avoid confusion. These results, as well as those for a p-type sample, are shown in Fig. 10. UMSb 1.3(A) and UMSB 1.3(B) were two samples from the same ingot. In contrast to all the other antimony-doped samples, they displayed an early reverse anneal and a

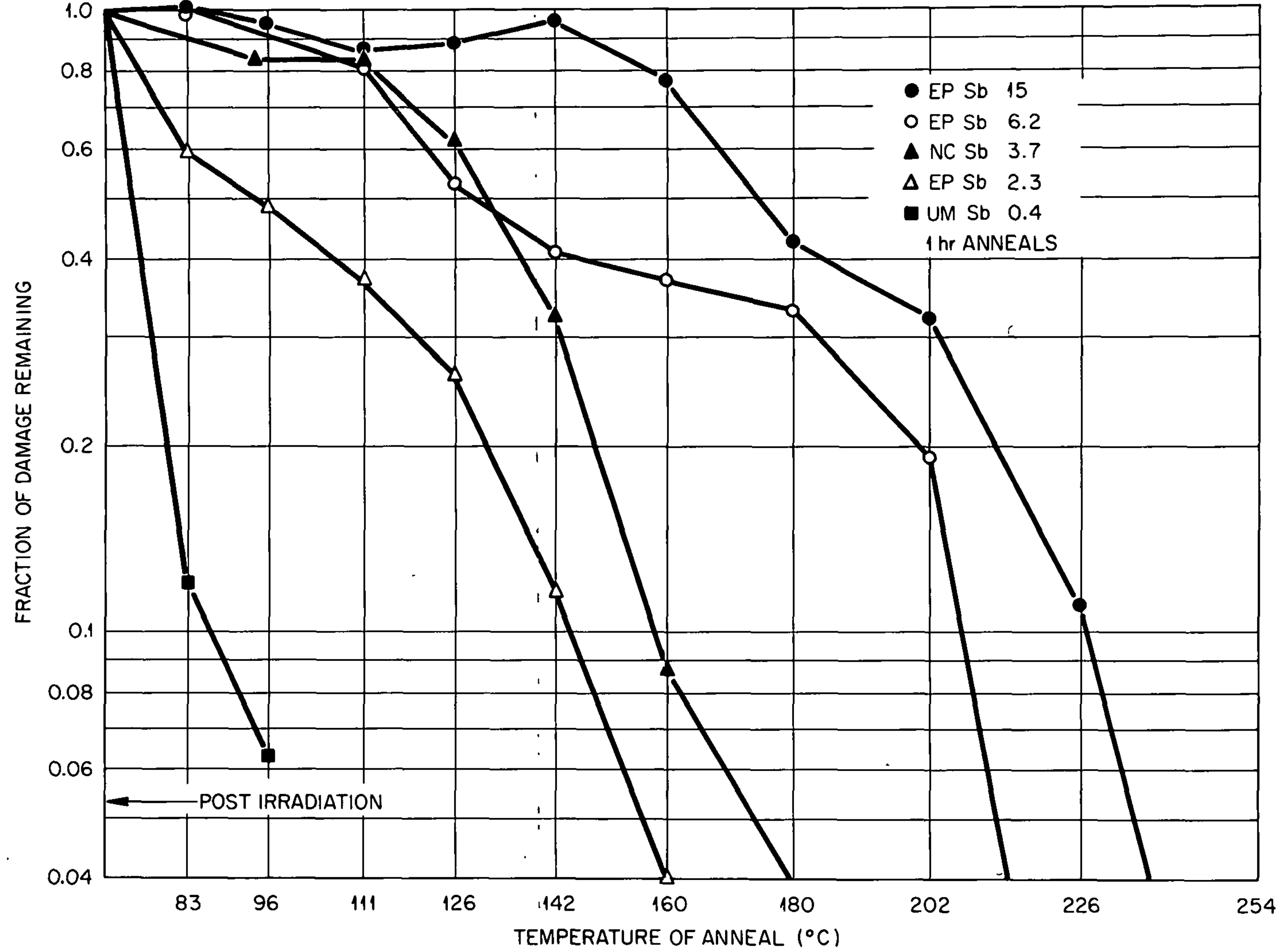

Figure 8. Fraction of Damage Remaining following Successive One-Hour Anneals, Antimony-Doped Germanium.

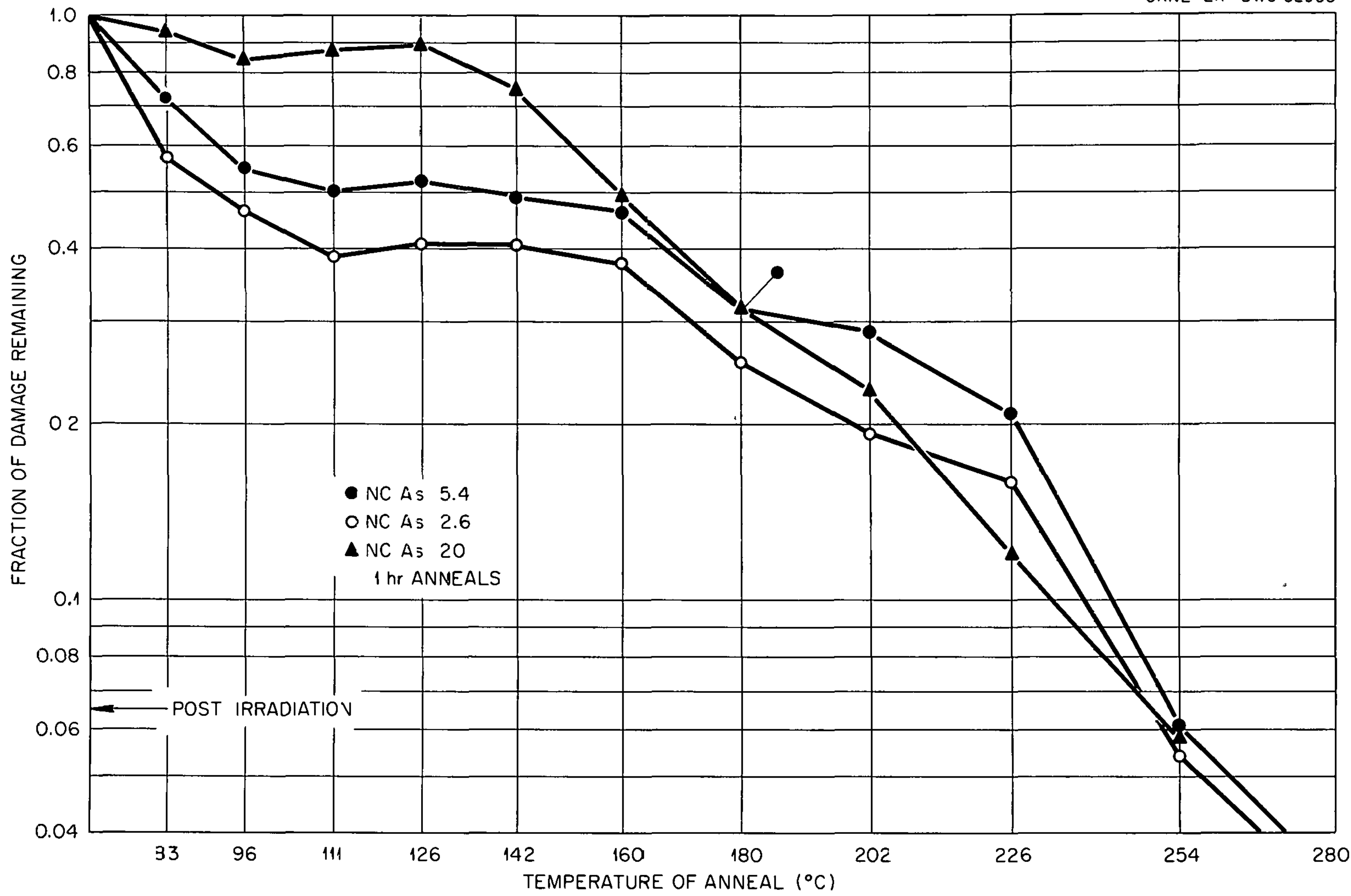

Figure 9. Fraction of Damage Remaining following Successive One-Hour Anneals, Arsenic-Doped Germanium.

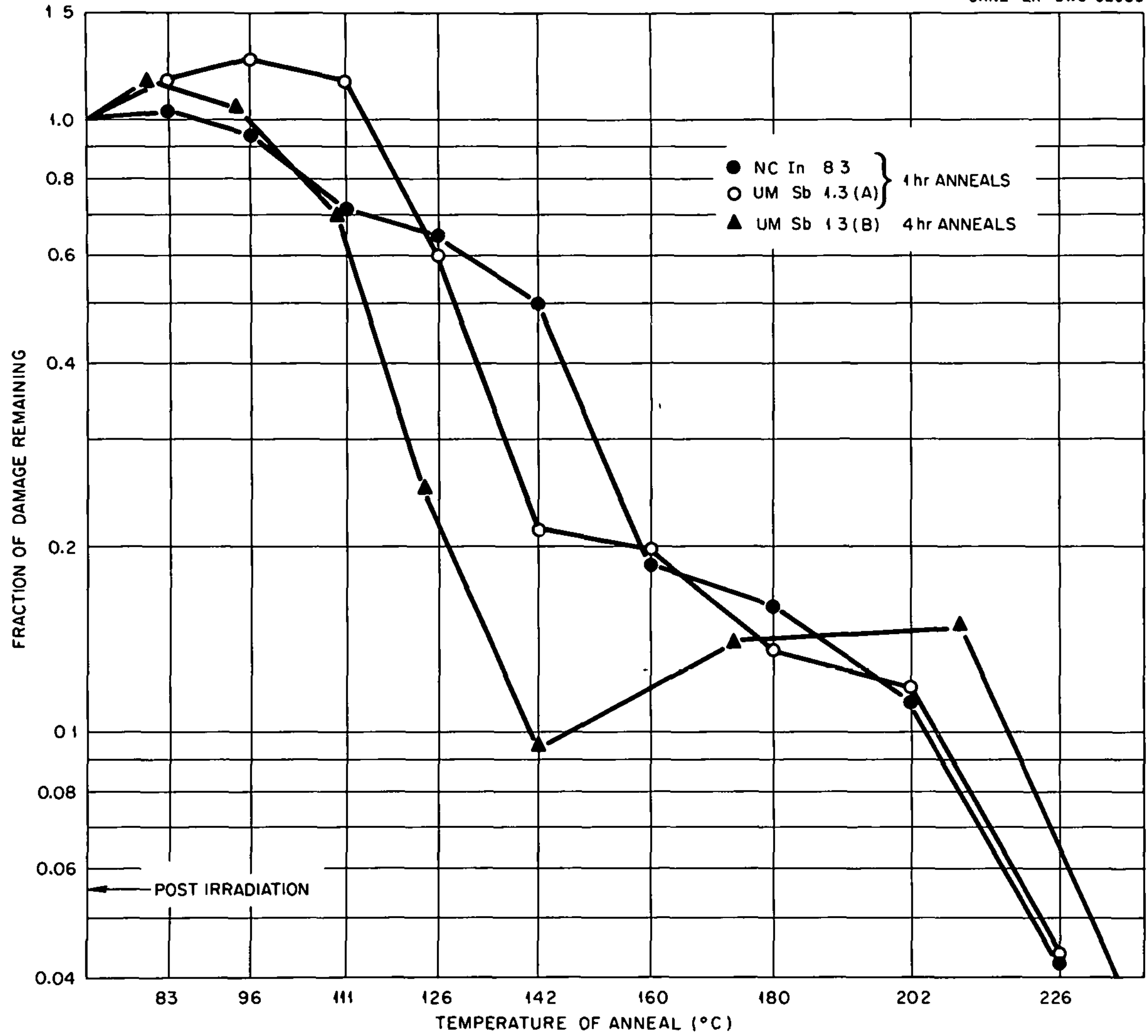

Figure 10. Fraction of Damage Remaining following Successive Anneals for One Indium- and Two Antimony-Doped Specimens.

sizeable amount of damage which remained to rather high temperatures. Note that the annealing time for UMSb 1.3(B) was four hours at each temperature, and some of the annealing temperatures were slightly different. The major fraction of the annealing occurred at a temperature which is consistent with the results shown in Fig. 8. Finally, the results for a single p-type specimen, given in Fig. 10, cannot, of course, give much information about the annealing behavior in p-type material. The similarity of its annealing behavior to that of UMSb 1.3(A) at high temperatures is probably coincidental.

As stated previously, annealing results based on lifetime measurements at a fixed temperature may not be very meaningful due to possible changes in the recombination process. In order to determine the effect of annealing upon the recombination process, lifetime measurements were made as a function of temperature. Figure 11 shows lifetime plotted logarithmically as a function of reciprocal temperature for an antimony-doped, fifteen ohm-cm specimen before and after gamma-ray exposure and after several annealing treatments. At low temperatures an increase in the lifetime is noted in the post-irradiation curves. This behavior is evidence of trapping, although the photoconductivity decays were quite exponential at these lower temperatures. Similar behavior has been observed by others[15] in high-resistivity, gamma-irradiated germanium. An analysis of this behavior in terms of

[15] S. M. Ryvkin and I. D. Yaroshetskii, Fizika Tverdogo Tela 2, 1966 (1960).

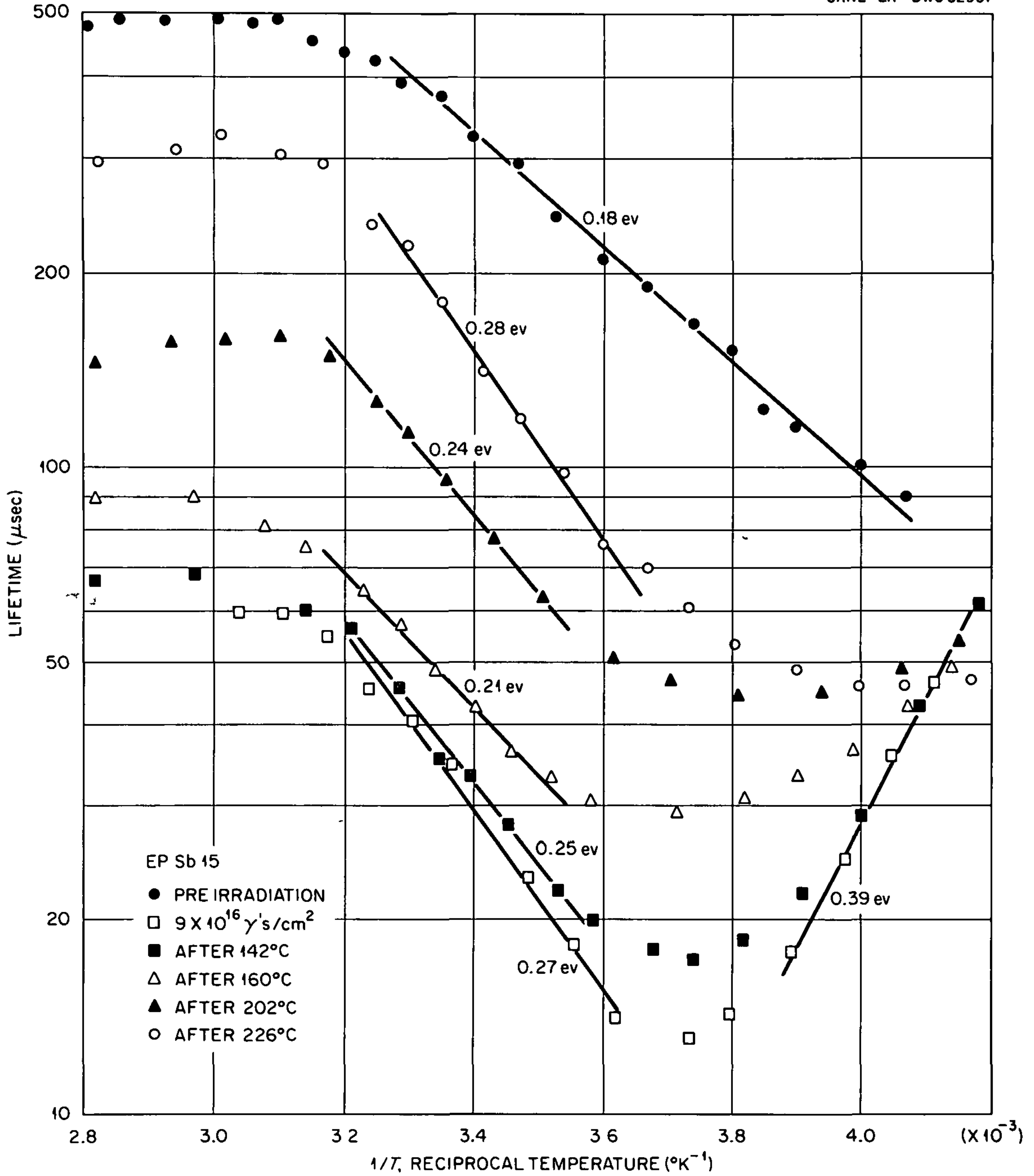

Figure 11. The Recombination Behavior of 15 Ohm-cm, Antimony-Doped Germanium following Irradiation by Co^{60} Gamma Rays and Successive One-Hour Anneals.

a trapping process will be given in the discussion. Another important point is that the slopes of the post-irradiation curves are much steeper than observed previously[3] for similar material. Sample EPSb 15 came from a different ingot than the specimens of similar resistivity used in the preliminary measurements. (See Figs. 6 and 7.)

In evaluating the quantity f, $(1/\tau - 1/\tau_0)(1/\tau_i - 1/\tau_0)^{-1}$, used in Figs. 8, 9, and 10, the value of τ taken was not generally the room-temperature value. Rather, the temperature at which the lifetime value was taken varied among the samples, depending upon the resistivity. One does not wish to use the lifetime values at high temperatures since the samples become intrinsic, complicating the recombination process. On the other hand, at low temperatures trapping processes may be important. Therefore, a moderate value of 1/T should be chosen. For EPSb 15, of Figs. 8 and 11, the value of lifetime was taken at $1/T = 3.35 \times 10^{-3}\ {}^{\circ}K^{-1}$. From Fig. 11 it is seen that there exists, therefore, a slight ambiguity in the values chosen for Fig. 8.

Figure 12 demonstrates the recombination behavior for an antimony-doped, 3.7 ohm-cm specimen following irradiation and thermal treatment. Note here the very steep slope, with no indication of trapping in the range of measurement. On the basis of simple theory, after subtracting 0.04 ev from the indicated slope (an approximate correction for the temperature variation of the density-of-states function), the position of the recombination level as measured from the valence band should be obtained.[3] The values of lifetime used to determine the data of Fig. 8 for NCSb 3.7 were taken at $1/T = 3.1 \times 10^{-3}\ {}^{\circ}K^{-1}$. For all the samples

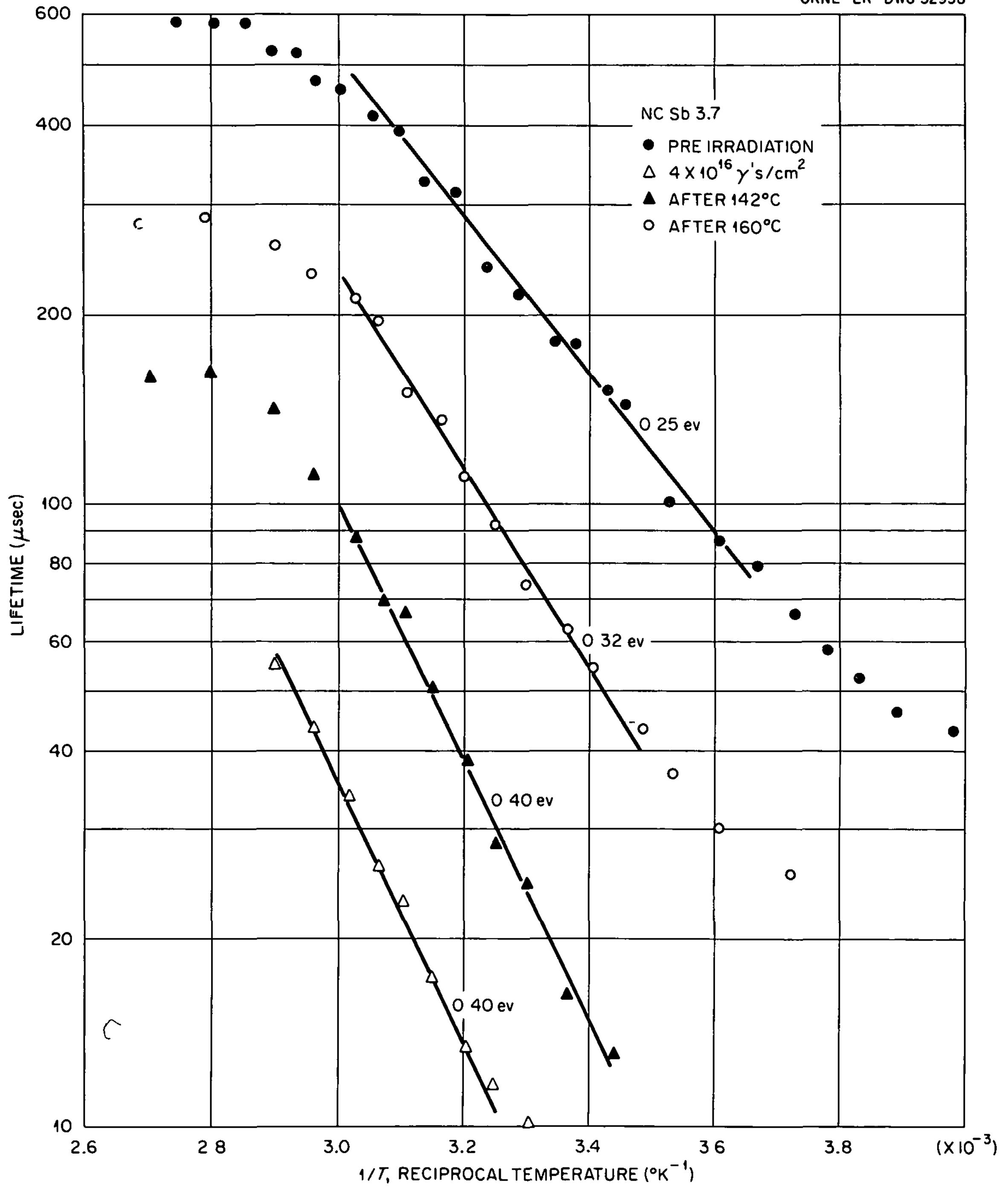

Figure 12. The Recombination Behavior of 3.7 Ohm-cm, Antimony-Doped Germanium following Irradiation by Co^{60} Gamma Rays and Successive One-Hour Anneals.

represented in Figs. 8, 9, and 10, the temperature dependence of lifetime was obtained at each of the annealing temperatures. However, for each specimen only a few of the resulting curves are shown to provide clarity. In Fig. 13, for 2.3 ohm-cm, antimony-doped material, the behavior is very similar to that displayed in Fig. 12. Again, the post-irradiation slope is quite steep and no trapping is observed. The values of lifetime used for the data of Fig. 8 were taken at the same 1/T value as in Fig. 12.

With reference to the other antimony-doped specimens, the recombination behavior of UMSb 1.3 was anomalous, as was its annealing behavior. Figure 14 illustrates this fact. The slopes here have lower values than those shown in Figs. 12 and 13. These anneals were four-hour anneals, as opposed to those given the other specimens, which were one hour each. The values of lifetime used for Fig. 10 were taken at $1/T = 3.1 \times 10^{-3}$ $^{\circ}K^{-1}$.

UMSb 0.44 was difficult to measure because of its low resistivity. The results are shown in Fig. 15. One may not be justified in drawing a straight line through any portion of the curves, but some slopes are indicated for the sake of comparison. Again, $1/T = 3.1 \times 10^{-3}$ $^{\circ}K^{-1}$ was taken as the point on the curve from which the values of lifetime for the annealing data were taken.

In Figs. 16 through 18 the results of lifetime measurements are shown for the three arsenic-doped specimens. Unfortunately, some time had elapsed between the time of irradiation and the first lifetime measurements made on these samples. During this time some room-temperature

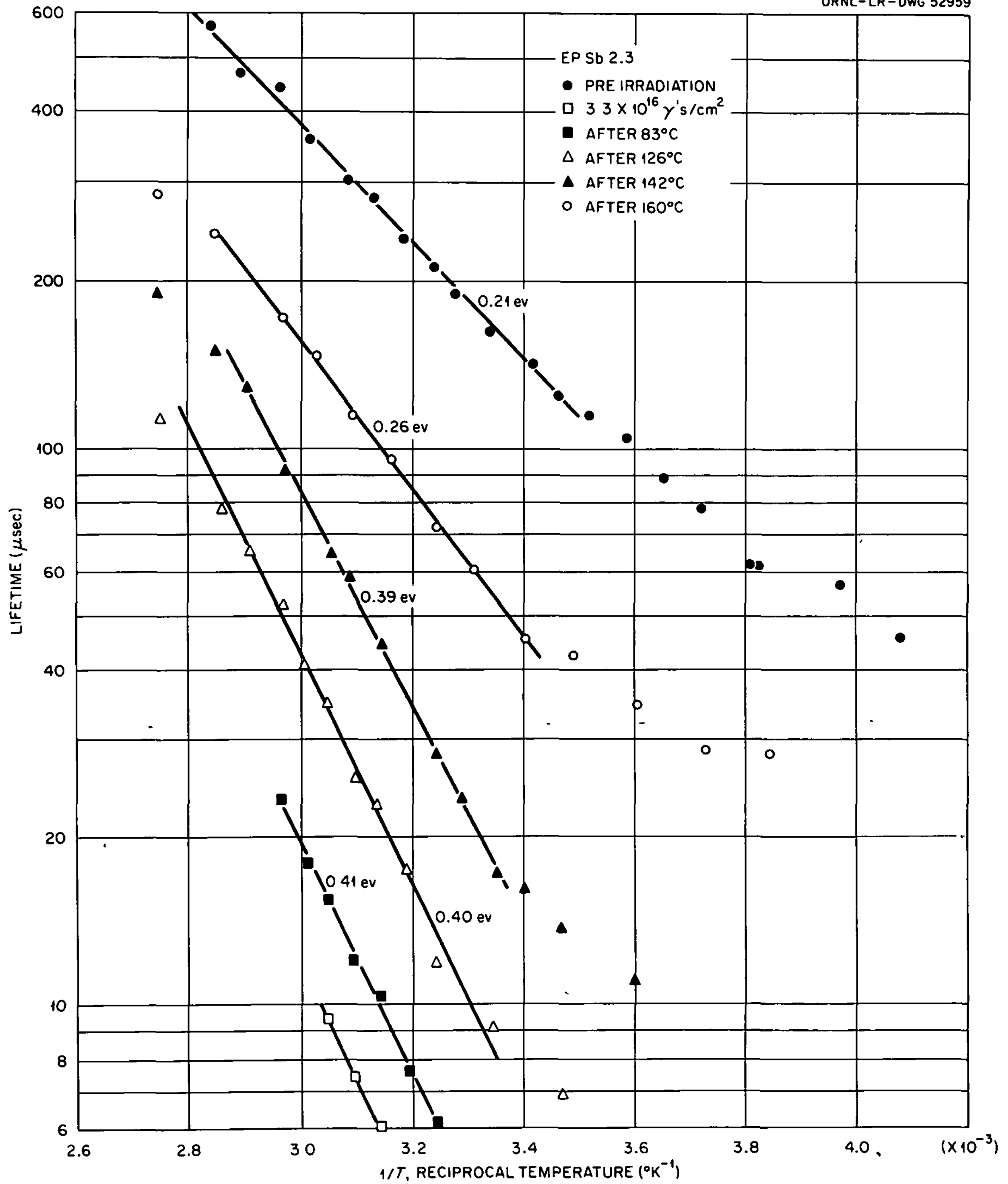

Figure 13. The Recombination Behavior of 2.3 Ohm-cm, Antimony-Doped Germanium following Irradiation by Co^{60} Gamma Rays and Successive One-Hour Anneals.

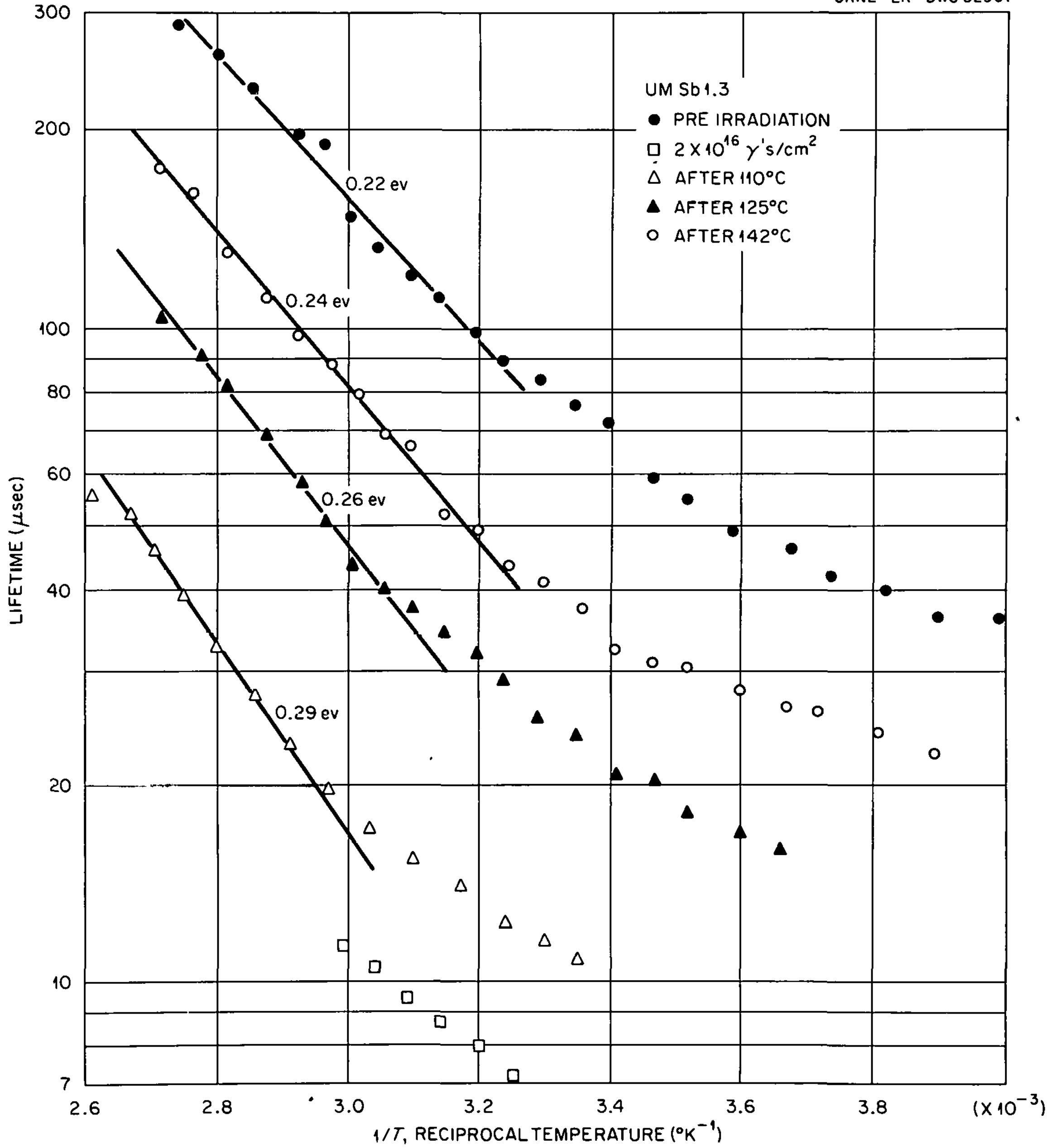

Figure 14. The Recombination Behavior of 1.3 Ohm-cm, Antimony-Doped Germanium following Irradiation by Co^{60} Gamma Rays and Successive One-Hour Anneals.

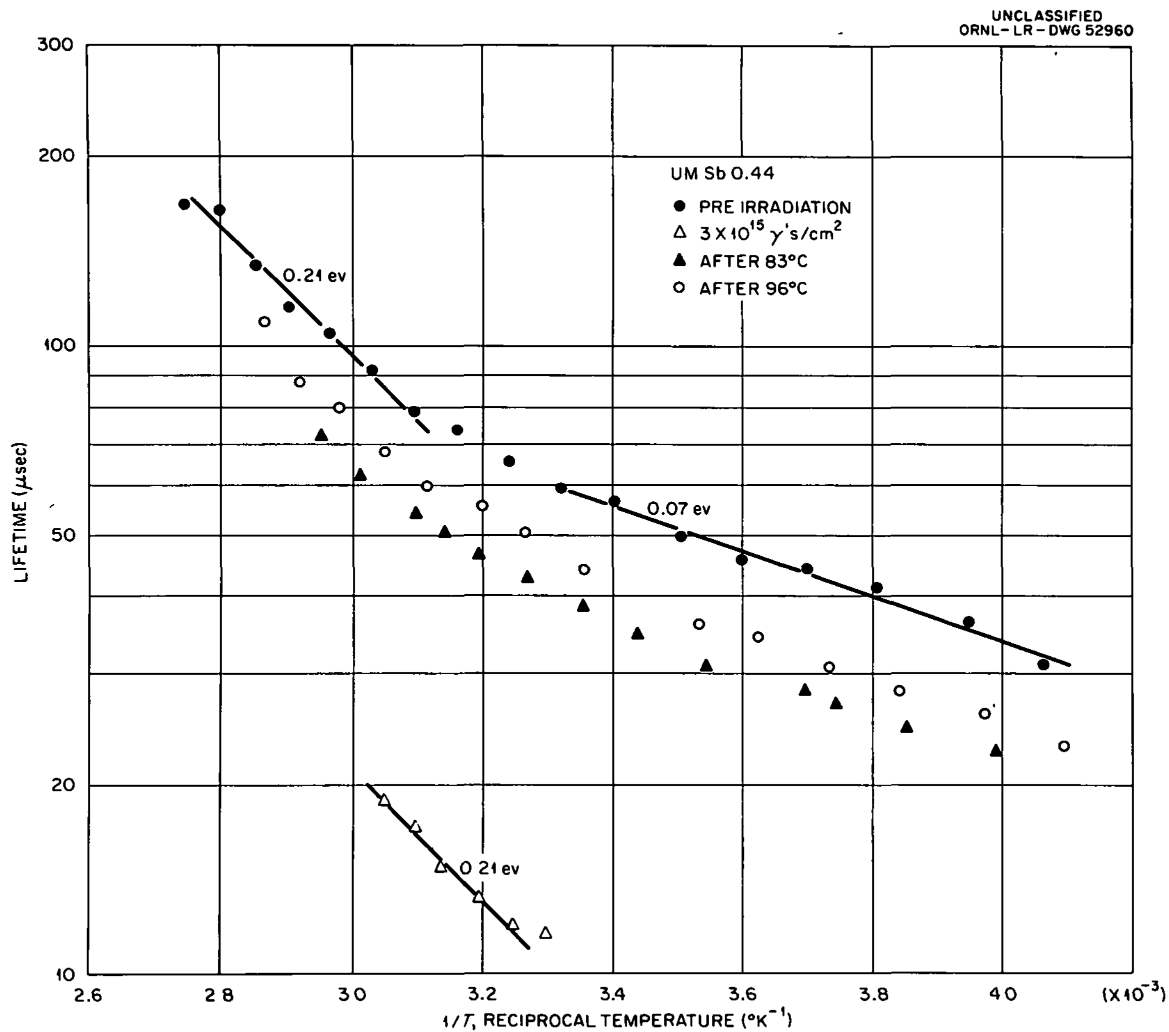

Figure 15. The Recombination Behavior of 0.44 Ohm-cm, Antimony-Doped Germanium following Irradiation by Co^{60} Gamma Rays and Successive One-Hour Anneals.

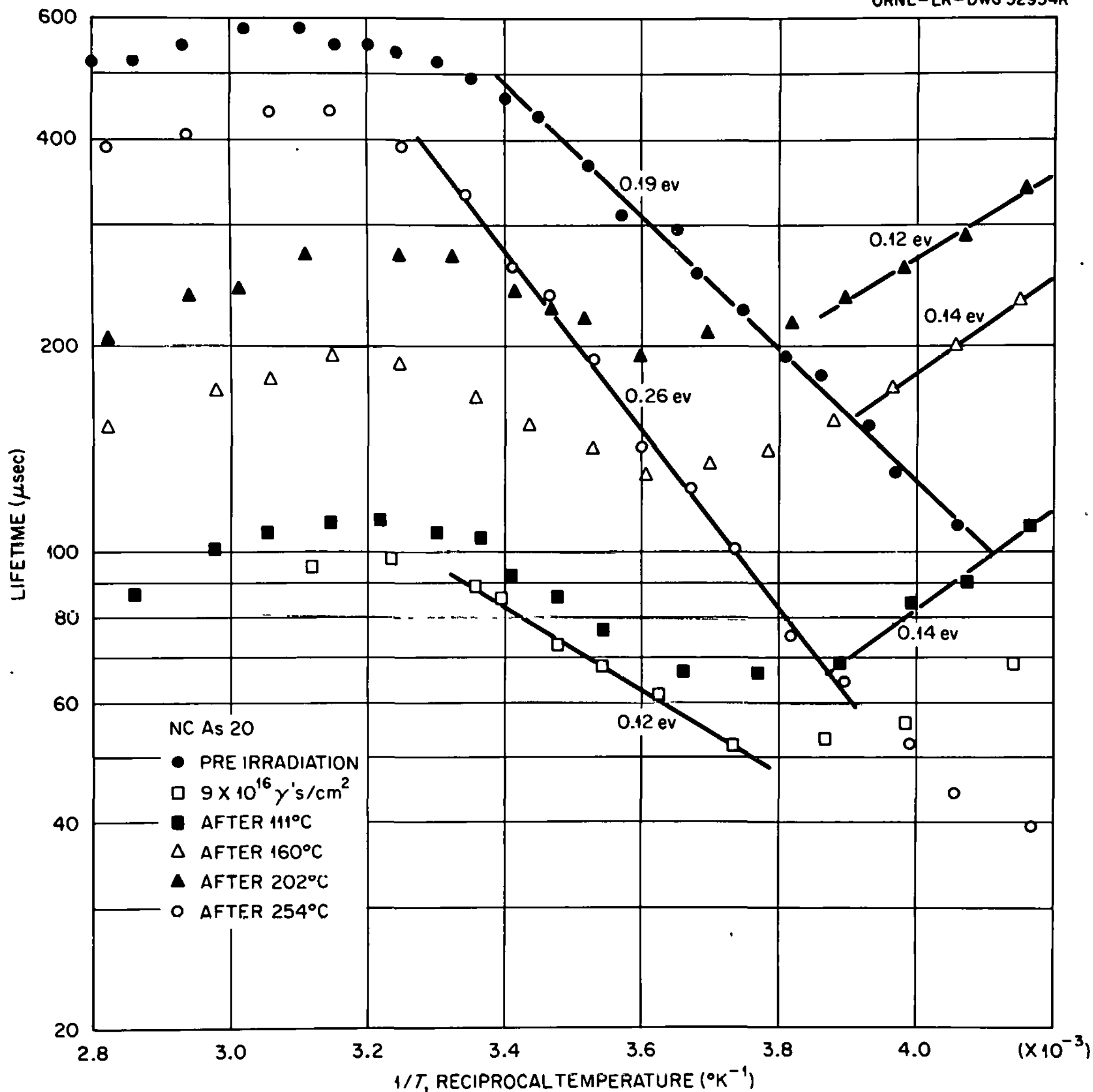

Figure 16. The Recombination Behavior of 20 Ohm-cm, Arsenic-Doped Germanium following Irradiation by Co^{60} Gamma Rays and Successive One-Hour Anneals.

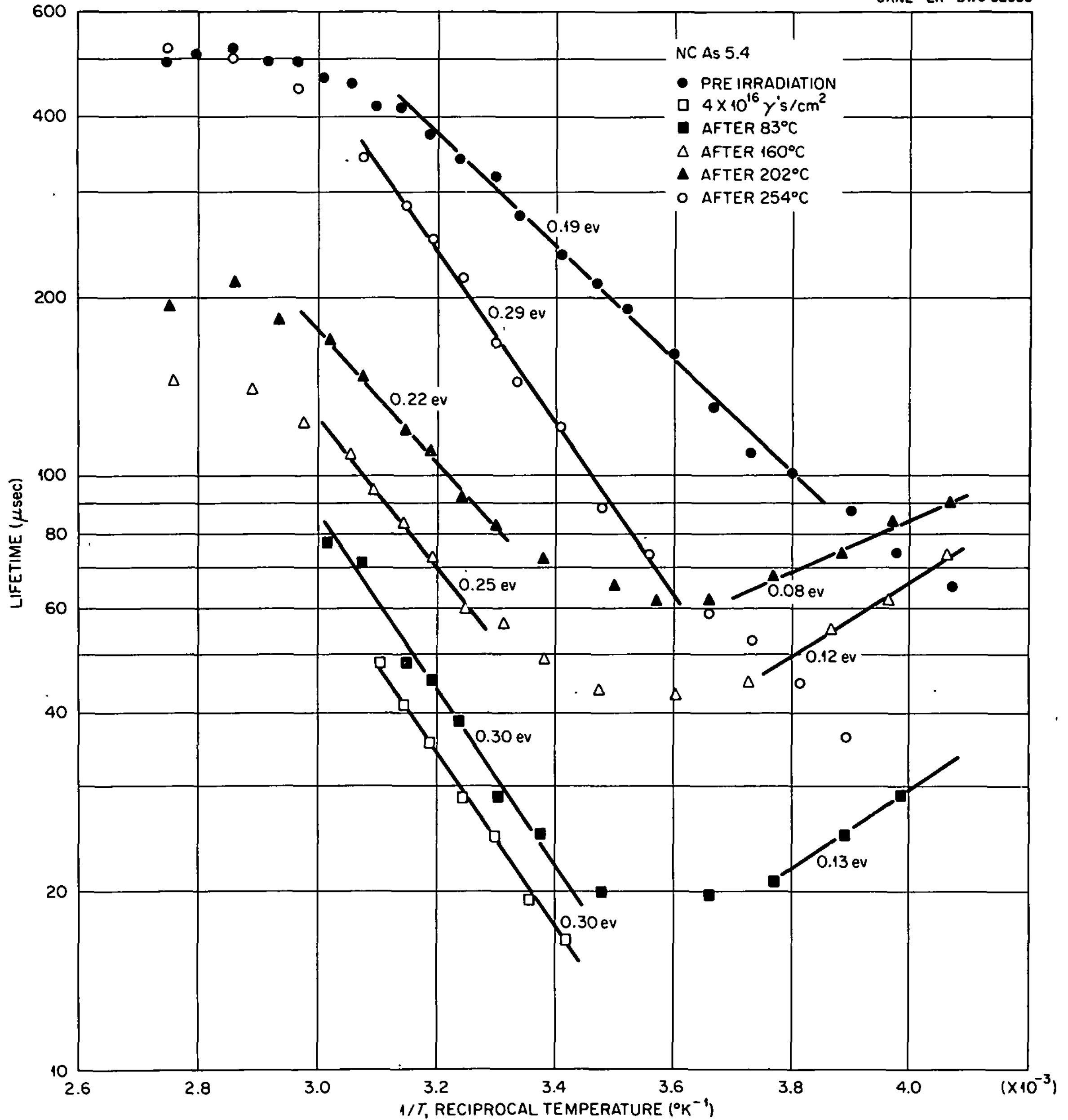

Figure 17. The Recombination Behavior of 5.4 Ohm-cm, Arsenic-Doped Germanium following Irradiation by Co^{60} Gamma Rays and Successive One-Hour Anneals.

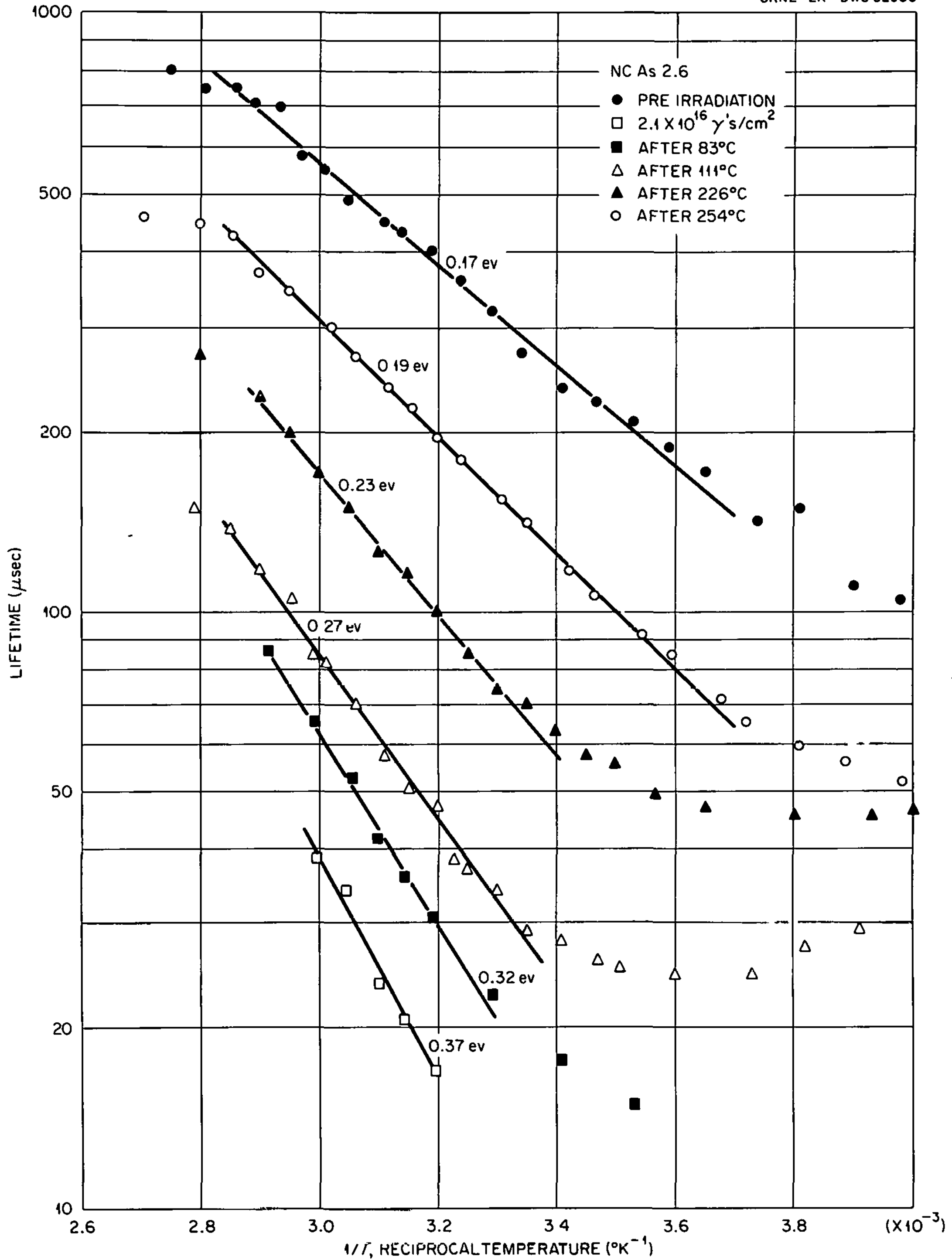

Figure 18. The Recombination Behavior of 2.6 Ohm-cm, Arsenic-Doped Germanium following Irradiation by Co^{60} Gamma Rays and Successive One-Hour Anneals.

annealing had occurred. When this fact was discovered, the measurements were repeated up to 111°C or 126°C. The new curves were normalized to the old curves at 111°C and, so, Figs. 16 through 18 are a composite of these two sets of data, the curves for annealing temperatures $\leq$ 111°C being from the second set of data. In these three figures strong trapping is observed. In fact, for the high resistivity specimen, NCAs 20, the trapping seemed to persist into the intrinsic range. Furthermore, the traps appeared to anneal at a much higher temperature than did the recombination centers. (In fact, it appeared that the trap concentration actually increased following anneal at the lowest temperature.)

The problem of interpreting the data of Fig. 16 in terms of damage was difficult because of the overlapping of the intrinsic and trapping regions. Values of lifetime used in obtaining the data of Fig. 9 were taken at $1/T = 3.0 \times 10^{-3}$ $^{\circ}K^{-1}$ and 3.45×10^{-3} $^{\circ}K^{-1}$. The fraction of damage remaining agreed reasonably well at these two values except at high annealing temperatures, where the trapping centers began to anneal. The points of Fig. 9 for NCAs 20 were taken at the lower value of reciprocal temperature for annealing temperatures of 202°C and above, while for lower annealing temperatures the values were taken at the higher value of reciprocal temperature. For NCAs 2.6 and NCAs 5.4 the values of reciprocal temperature at which the lifetime values were taken were 3.1×10^{-3} $^{\circ}K^{-1}$ and 3.2×10^{-3} $^{\circ}K^{-1}$, respectively. Figure 19 shows the recombination behavior for the p-type specimen NCIn 8.3. This behavior is somewhat similar to that observed earlier.[5] The value of $1/T$ at which the data of Fig. 10 were taken was 3.2×10^{-3} $^{\circ}K^{-1}$.

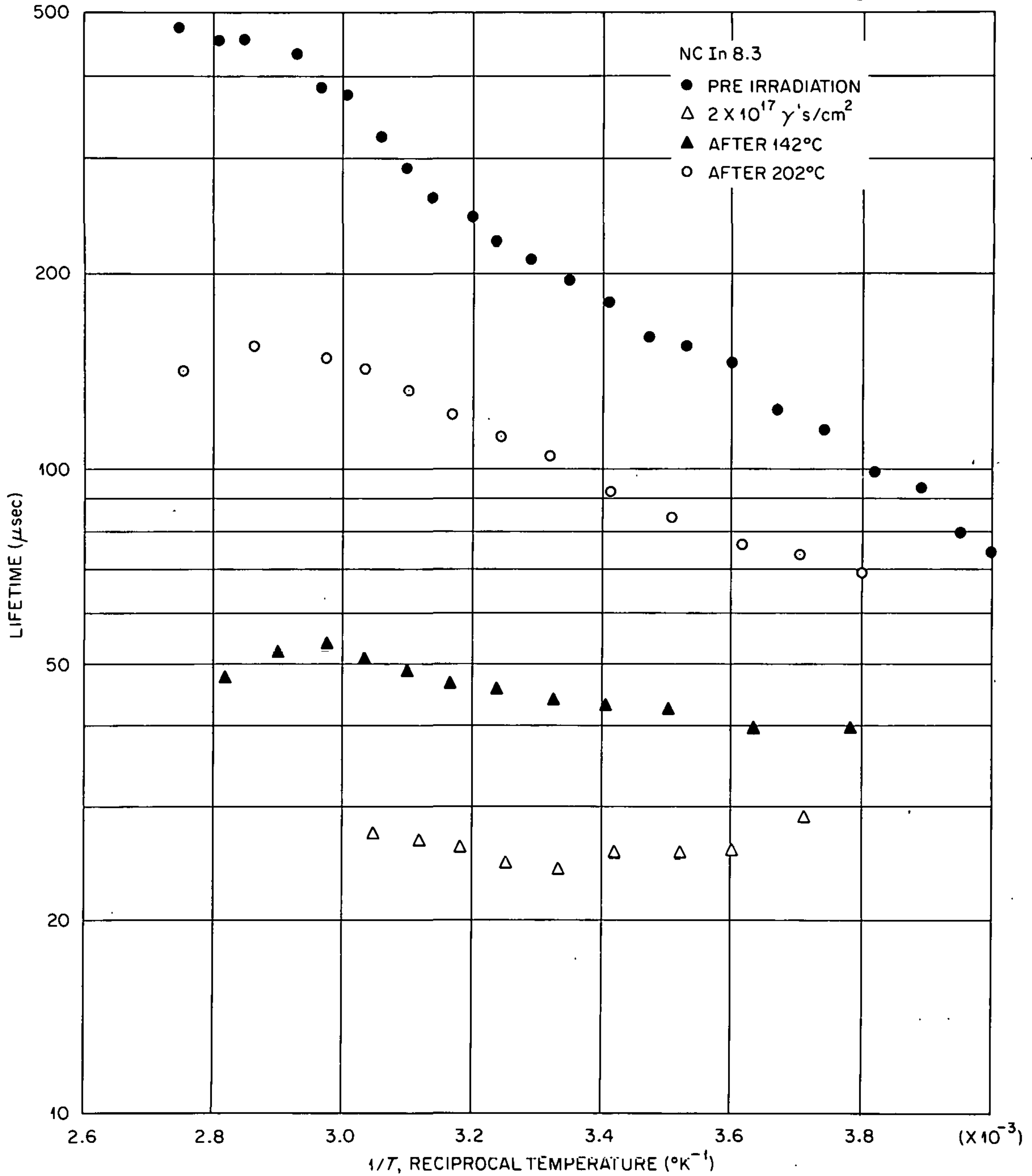

Figure 19. The Recombination Behavior of 8.3 Ohm-cm, Indium-Doped Germanium following Irradiation by Co^{60} Gamma Rays and Successive One-Hour Anneals.

In addition to these results, data were obtained from a number of isothermal anneals. These data deal with the details of the annealing process and will be presented later with the discussion of the annealing behavior.

CHAPTER IV

DISCUSSION

I. THE RECOMBINATION PROCESS

The purpose of this research program was twofold: to investigate the annealing behavior of defects produced by Co^{60} gamma irradiation in germanium and to study the recombination behavior of these defects. Before an attempt could be made to understand annealing behavior obtained through the observation of the recombination process, an understanding of the recombination process itself had to be obtained. Hole-electron pairs injected into the crystal recombine through energy levels lying in the forbidden gap. In the case under discussion these energy levels were produced by crystalline imperfections caused by bombardment. Among the quantities which one hopes to determine from the experimental measurements are the capture probabilities associated with the recombination centers of interest and the position of the energy levels responsible for recombination. These facts, combined with other experimental evidence, should help in determining the fundamental nature of the recombination centers.

The problem of recombination through a level in the forbidden gap was first treated by Hall[16] and Shockley and Read.[17] The trapping

---

[16] R. N. Hall, Phys. Rev. 87, 387 (1952).

[17] W. Shockley and W. T. Read, Phys. Rev. 87, 835 (1952).

process has been treated by Hornbeck and Haynes.[18] In earlier investigations the Hall-Shockley-Read theory has been applied to various cases of single-level recombination,[3-6] but here it appears necessary to treat the case of recombination through a recombination center in the presence of a trapping level. Wertheim[19] has extended the calculations of Hall, Shockley, and Read to this case. Ryvkin and Yaroshetskii[15] have treated the problem somewhat differently, obtaining solutions in certain limiting cases. The method of development presented here closely parallels Wertheim's.

The net capture rate for electrons at a given type of energy level, U_n, is equal to the rate with which electrons from the conduction band enter these energy levels minus the rate with which electrons are re-excited. Now the rate with which the first process occurs is given by $n'N^{O'}c_n$, where n' is the instantaneous concentration of electrons in the conduction band, $N^{O'}$ is the instantaneous concentration of energy levels unoccupied by electrons, and c_n is the electron capture probability. The rate with which electrons are re-excited is given by $g_nN^{-'}$, where g_n is the generation constant for electrons and $N^{-'}$ is the instantaneous concentration of electron-occupied levels. Therefore,

$$U_n = c_n n'N^{O'} - g_n N^{-'}. \qquad (1)$$

At equilibrium $U_n \equiv 0$ so that

---

[18] J. A. Hornbeck and J. R. Haynes, Phys. Rev. 97, 311 (1955).

[19] G. K. Wertheim, Phys. Rev. 109, 1086 (1958).

$$g_n = \frac{c_n n N^o}{N^-} \,, \tag{2}$$

where n, N^o, and N^- are the equilibrium values of n', $N^{o}{}'$, and $N^{-}{}'$, respectively. If the Fermi level lies at the same position as the energy level, the probability of occupancy of energy levels is then one-half* so that $N^- = N^o$. The equilibrium electron concentration for such a condition is called n_1. Then

$$g_n = c_n n_1 . \tag{3}$$

If δn is the change in electron concentration due to a non-equilibrium condition (such as that occurring following a pulse of light) and δN is the corresponding change in the occupancy of energy levels by electrons, then $n' = n + \delta n$, $N^{-}{}' = N^- + \delta N$, and $N^{o}{}' = N^o - \delta N$; thus,

$$U_n = c_n(n + \delta n)(N^o - \delta N) - c_n n_1(N^- + \delta N). \tag{4}$$

Upon collecting terms,

$$U_n = c_n \left[N^o \delta n - (n + n_1 + \delta n)\, \delta N + nN^o - n_1 N^- \right]. \tag{5}$$

---

*Because of the statistical weight associated with the localized state, this statement is not exactly correct. The distribution function (probability that the ith state is occupied by an electron) is

$$f_n = \left(1 + \gamma_i e^{(E_i - \zeta)/kT}\right)^{-1} ,$$

where ζ is the Fermi level, E_i is the energy of the state, and γ_i is the ratio of the statistical weight of the empty state to that of the filled state. Thus, the probability of occupancy when the Fermi level is at the recombination level is one-half only if $\gamma_i = 1$. However, for electronic states γ_i is generally either two or one-half due to spin degeneracy.

Substituting Eq. (3) into Eq. (2), it is seen that $nN^{o} = n_1 N^{-}$. Therefore,

$$U_n = c_n\left[N^{o}\delta n - (n + n_1 + \delta n)\delta N\right]. \tag{6a}$$

In exactly the same way the corresponding equation for U_p, the net hole capture rate, may be obtained:

$$U_p = c_p\left[N^{-}\delta p + (p + p_1 + \delta p)\delta N\right]. \tag{6b}$$

The case of interest is that of n-type material ($n >> p$), with the Fermi level well above the energy level ($n >> n_1$, $p_1 >> p$). Furthermore, $N^{-} \simeq N$, the total number of levels; and the excitation is controlled so that $\delta n << n$. Under these conditions Eqs. (6a) and (6b) reduce to

$$\begin{aligned} U_n &= c_n(N^{o}\delta n - n\delta N), \\ U_p &= c_p\left[N\delta p + (p_1 + \delta p)\delta N\right]. \end{aligned} \tag{7}$$

In the problem under consideration there are two types of levels.* One level will be referred to as a recombination level and one as a trapping level. The following expressions may then be written:

---

*The solution of the problem in the case of a single level can be obtained in exactly the same manner as is used here for the more complicated case, resulting in the standard Hall[16] Shockley-Read[17] equation, which may be written:

$$\tau = \frac{\frac{1}{c_n}(p + p_1) + \frac{1}{c_p}(n + n_1)}{N_r(n + p)}.$$

$$\left(\frac{d}{dt}\right)\delta n = -U_{nr} - U_{nt},$$
$$\left(\frac{d}{dt}\right)\delta p = -U_{pr} - U_{pt},$$
$$\left(\frac{d}{dt}\right)\delta N_r = U_{nr} - U_{pr}, \tag{8}$$
$$\left(\frac{d}{dt}\right)\delta N_t = U_{nt} - U_{pt},$$

where the subscript r denotes the recombination level and the subscript t the trapping level. The requirement for charge neutrality is

$$\delta N_r + \delta N_t + \delta n = \delta p. \tag{9}$$

If one level is a hole trap, the electron-capture probability at this level is very small compared with the hole-capture probability. Under the assumption that c_{nt} is negligibly small, Eq. (8) becomes:

$$\left(\frac{d}{dt}\right)\delta n = -U_{nr},$$
$$\left(\frac{d}{dt}\right)\delta p = -U_{pr} - U_{pt},$$
$$\left(\frac{d}{dt}\right)\delta N_r = U_{nr} - U_{pr}, \tag{10}$$
$$\left(\frac{d}{dt}\right)\delta N_t = -U_{pt}.$$

Using Eq. (9) to eliminate δN_r from Eq. (10), a system of three, coupled, non-linear differential equations is obtained. It is useful to write down the three non-linear equations before substituting for δN_r since the approximations involved in obtaining a linear set of equations are more easily justified:

$$\left(\frac{d}{dt}\right)\delta n = -\, c_{nr}(N_r^0 \delta n - n \delta N_r),$$

$$\left(\frac{d}{dt}\right)\delta p = -\, c_{pr}\left[N_r \delta p + (p_{1r} + \delta p)\delta N_r\right] - c_{pt}\left[N_t \delta p + (p_{1t} + \delta p)\delta N_t\right],$$

$$\left(\frac{d}{dt}\right)\delta N_t = -\, c_{pt}\left[N_t \delta p + (p_{1t} + \delta p)\delta N_t\right]. \qquad (11)$$

N_r^0 cannot be dropped, even though it is very small, since δN_r might also be very small. Only the second two equations are non-linear. These may be made linear and the problem solved, providing the following assumptions are made:

$$\delta N_r \delta p << p_{1r} \delta N_r + N_r \delta p,$$
$$\delta N_t \delta p << p_{1t} \delta N_t + N_t \delta p. \qquad (12)$$

These assumptions are reasonable since the injection level is quite low. Equation 12 is satisfied if either $\delta p << p_1$ or $\delta N << N$; so for low injection levels the approximations given in Eq. (12) are almost certainly justified. Using these approximations and eliminating δN_r through Eq. (9), the following set of linear differential equations is obtained, where use is now made of the symbolic operator, D:

$$D \delta n = -\, (c_{nr}N_r^0 + c_{nr}n)\delta n + c_{nr}n \delta p - c_{nr}n \delta N_t,$$

$$D \delta p = c_{pr}p_{1r}\delta n - (c_{pr}N_r + c_{pt}N_t + c_{pr}p_{1r})\delta p + (c_{pr}p_{1r} - c_{pt}p_{1t})\delta N_t,$$

$$D \delta N_t = 0 \delta n - c_{pt}N_t \delta p - c_{pt}p_{1t}\delta N_t. \qquad (13)$$

Equation (13) may be written in the following way:

$$(D + a_{11})\delta n + a_{12}\delta p + a_{13}\delta N_t = 0,$$
$$a_{21}\delta n + (D + a_{22})\delta p + a_{23}\delta N_t = 0, \qquad (14)$$
$$0 + a_{32}\delta p + (D + a_{33})\delta N_t = 0,$$

where the a_{ij}'s are the negative values of the coefficients appearing in Eq. (13). Upon eliminating δN_t and δp from Eq. (14), the following expression is obtained:

$$(D^3 + pD^2 + qD + r)\delta n = 0, \qquad (15)$$

where

$$p = (a_{11} + a_{22} + a_{33}),$$
$$q = (a_{11}a_{22} + a_{11}a_{33} + a_{22}a_{33} - a_{23}a_{32} - a_{12}a_{21}), \qquad (16)$$
$$r = (a_{11}a_{22}a_{33} - a_{11}a_{23}a_{32} + a_{12}a_{21}a_{33} + a_{13}a_{21}a_{32}).$$

The solution is:

$$\delta n = Ae^{-m_1 t} + Be^{-m_2 t} + Ce^{-m_3 t}, \qquad (17)$$

where m_1, m_2, m_3 are the negative values of the roots of the characteristic equation so that

$$(D + m_1)(D + m_2)(D + m_3) = 0, \qquad (18a)$$

or

$$D^3 + (m_1 + m_2 + m_3)D^2 + (m_1m_2 + m_1m_3 + m_2m_3)D + m_1m_2m_3 = 0. \qquad (18b)$$

Experimentally, only the longest time constant is observed; thus, only the smallest root of the equation is important. Since exponential decays are experimentally observed, the time constants should be well

separated. If m_1 is the smallest root, $m_1 << m_2, m_3$. Comparing Eqs. (15) and (18),

$$m_1m_2 + m_1m_3 + m_2m_3 = q; \tag{19}$$

or, under the assumption mentioned, $m_2m_3 \approx q$; but $m_1m_2m_3 = r$. Therefore,

$$m_1 \approx \frac{r}{q}; \tag{20}$$

and the solution to the problem is given approximately by

$$\delta n = Ae^{-\frac{r}{q}t}. \tag{21}$$

The lifetime is given approximately by q/r. Inserting q and r from Eq. (16) and substituting the values for the a_{ij}'s, the following expression is obtained:

$$\tau = \frac{\frac{1}{c_{pt}}(N_r^oN_r + N_r^op_{1r} + nN_r) + \frac{1}{c_{pr}}(N_r^oN_t + nN_t + N_r^op_{1t} + np_{1t}) + \frac{1}{c_{nr}}(N_rp_{1t} + p_{1r}p_{1t} + p_{1r}N_t)}{(N_r^oN_rp_{1t} + N_r^op_{1r}p_{1t} + nN_rp_{1t} + N_r^op_{1r}N_t)}. \tag{22}$$

On the basis of the assumptions already made, $nN_r >> N_r^oN_r + N_r^op_{1r}$, $nN_t + np_{1t} >> N_r^oN_t + N_r^op_{1t}$, which gives the final result:

$$\tau = \frac{p_{1r}}{c_{nr}nN_r} + \frac{1}{c_{nr}n} + \frac{N_tp_{1r}}{c_{nr}nN_rp_{1t}} + \frac{N_t}{c_{pr}N_rp_{1t}} + \frac{1}{c_{pt}p_{1t}} + \frac{1}{c_{pr}N_r}. \tag{23}$$

This result is obtainable directly from Wertheim's solution[19] when suitable assumptions* are applied.

---

*These assumptions (besides the requirements of a low density of recombination centers and small fractional filling of traps) are:

Figure 20 illustrates the temperature dependence of the terms in Eq. (23). The relative magnitudes of the terms in the figure are not meant to be significant. For this figure the recombination and trapping levels were assumed to lie at 0.36 ev and 0.17 ev above the valence band, respectively (A correction in slope due to the $T^{3/2}$ term in p_1, which amounts to 0.04 ev in the temperature range considered, has been applied.), and it was assumed that there was no intrinsic contribution to the carrier concentration. The results of Eq. (23) may be applied in a very straightforward manner to the experimental data. In Fig. 21 an attempt has been made to synthesize representative temperature dependence of lifetime by adding three terms of Eq. (23) which affect the recombination behavior in arsenic-doped material. Here the effect of the temperature dependence of the intrinsic carrier concentration has been included by replacing n by n + p where both n and p include the intrinsic contribution. This correction can only be approximate due to the assumption made in obtaining Eq. (23) that n is very large compared with p. The position of the energy levels assumed for Fig. 21 was the same as for Fig. 20. The points shown in Fig. 21 are the result of adding the three terms indicated in the figure.

Inspection of Fig. 21 makes the results for arsenic-doped material quite understandable. For instance, the curve representing an

---

(1) the recombination levels lie below the Fermi level; (2) the trapping levels lie below the recombination levels. In the derivation presented here, the only restriction on the position of the trapping levels is that they lie below the Fermi level (not necessarily below the recombination level).

UNCLASSIFIED
ORNL-LR-DWG 53591

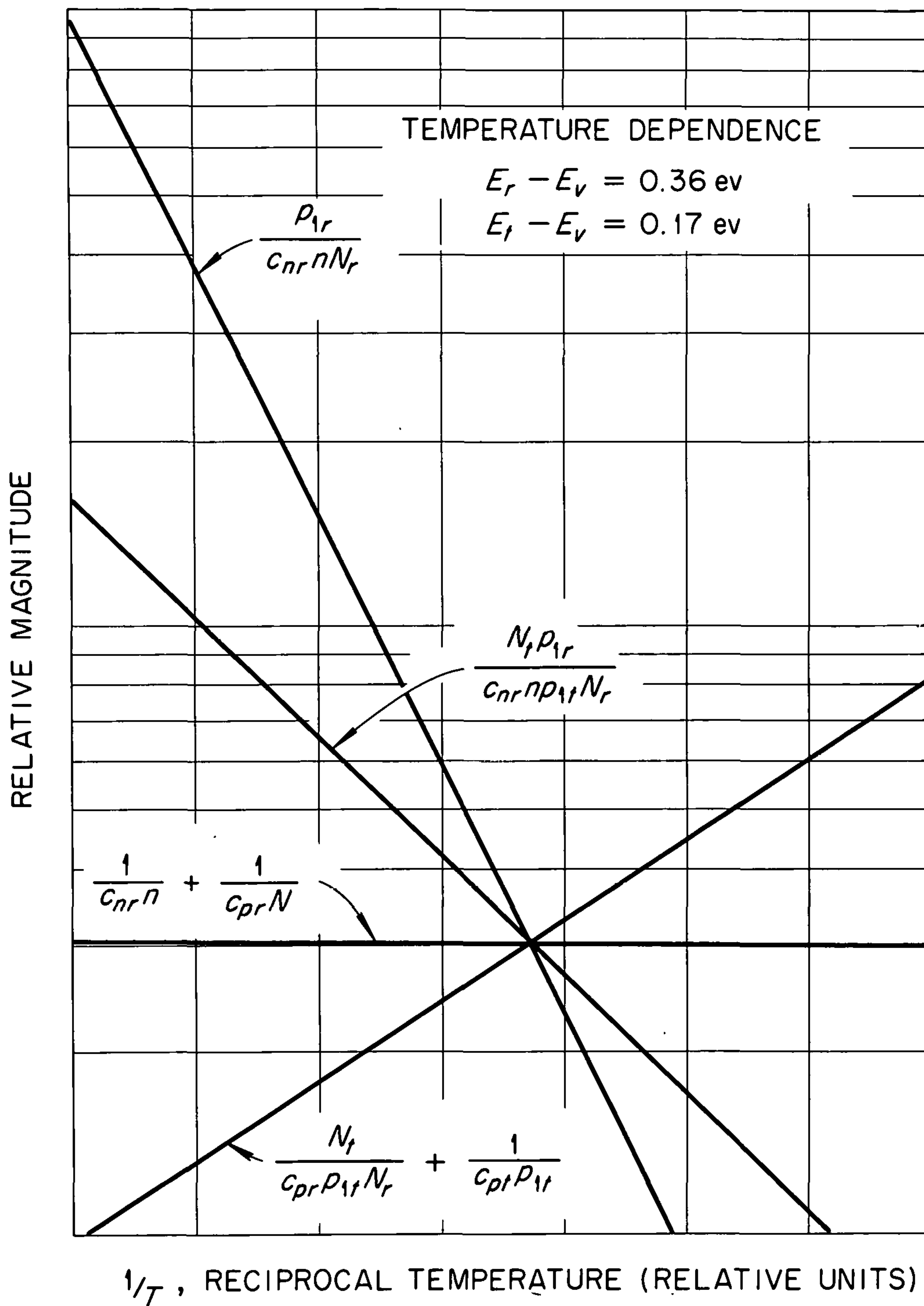

Figure 20. The Temperature Dependence of the Terms Involved in the Recombination Equation.

UNCLASSIFIED
ORNL-LR-DWG 53590

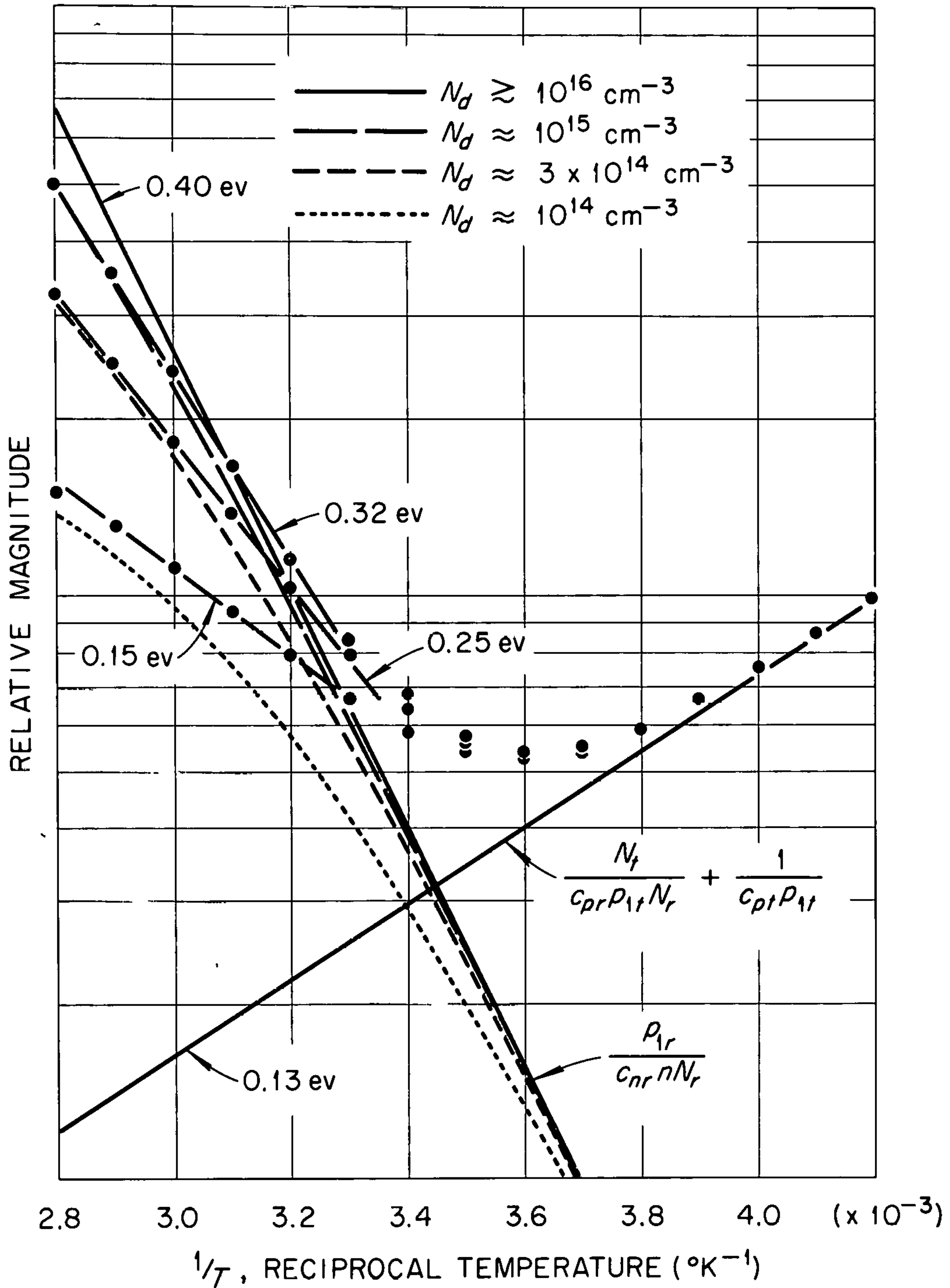

Figure 21. The Result of Adding Three Terms of the Recombination Equation, Including the Effect of Intrinsic Carriers.

arsenic concentration, N_d, of 3×10^{14} cm^{-3}* corresponds to a sample resistivity of about five ohm-cm and the shape of this curve is very similar to the lower four curves of Fig. 18. The data of Figs. 17 and 19 are also well explained on the basis of Fig. 21. At high temperature some of the experimental lifetime values are lower than predicted; this fact is undoubtedly due to the approximations made in accounting for the contribution to recombination of intrinsic carriers. If p becomes comparable with n, then the recombination equation will change completely, becoming more complicated than Eq. (23). For samples in which trapping centers affect the recombination to such high temperatures as demonstrated in Fig. 21, it is not possible to obtain the position of the recombination level with any accuracy due to the complexity of the recombination behavior. Fortunately, the antimony-doped specimens did not display such behavior.

In Fig. 11 a rather steep slope in the trapping portion of the lower curves for this highest resistivity antimony-doped specimen is seen. Evidently, the trapping level in this specimen is much higher than in the case of arsenic-doped material. However, there may be a contribution to the slope due to the fact that the carrier concentration is decreasing with decreasing temperature in this range. The Hall curves for n-type material indicate a freezing out of carriers at an energy level 0.20 ev below the conduction band.[20] These levels are

---

*N_d, the concentration of chemical donors, is equal to the extrinsic electron concentration, n.

[20] J. W. Cleland, J. H. Crawford, Jr., and D. K. Holmes, Phys. Rev. 102, 722 (1956).

introduced at a rate[21] of $\sim 5 \times 10^{-4}$/gamma cm^{-2} so the change in carrier concentration resulting from the filling of these levels would be $\sim 4 \times 10^{13}$ in this case, or about one-half of the room-temperature value. The position obtained by Ryvkin and Yaroshetskii[15] for the trapping level in near-intrinsic germanium was $E_t - E_v = 0.24$ ev. Although Figs. 12 and 13 do not display trapping behavior similar to that of Fig. 11, the reason that points are not included for lower temperatures in the case of the curves following anneal at 160°C is that the photoconductivity decay curves became nonexponential, evidently due to the fact that trapping was beginning to occur. Since Eq. (23) was derived on the basis of a single time constant, it cannot be applied to these low temperatures. However, the trapping does not appear to be important in the higher temperature range. Assuming no dependence of capture probability on temperature, the recombination center lies ~ 0.36 ev above the valence band. Even though arsenic-doped material displays the presence of trapping levels not present in antimony-doped material, there is no reason to assume a difference in the position of the recombination level. Although it cannot be proved that the same recombination center is effective in arsenic- and antimony-doped material, the analysis shown in Fig. 21 indicates that this is a reasonable assumption.

The behavior of UMSb 1.3 and UMSb 0.44 shown in Figs. 14 and 15 is anomalous as compared with the other antimony-doped specimens. It

---

[21] J. W. Cleland, unpublished data.

cannot be stated with certainty whether this difference is due to the higher impurity concentration or to a difference due to the method of manufacture. In the latter case the difference may have been due to compensating impurities, dislocations, or lack thereof. If the recombination level were at the same position as for the other antimony-doped samples, which seems to be the most reasonable assumption, then the temperature dependence demonstrated in Fig. 21 does not account for their behavior. Figure 22 shows the effect of including a different temperature-dependent term, $N_t p_{1r}/c_{nr} n N_r p_{1t}$. The temperature dependence here corresponds to a difference in position between the recombination and trapping levels, and this term becomes important for a relatively high density of trapping levels. As can be seen, Fig. 22 duplicates fairly well the behavior of Fig. 14. The pre-irradiation and post-irradiation curves in Fig. 14 are similar. Thus, the observed behavior would be explained if a large number of trapping levels were present in the unirradiated specimen. The following expression for lifetime would then hold:

$$\tau = \frac{p_{1r}}{c_{nr} n N_r} \left[1 + \frac{N_t}{p_{1t}} \right]. \qquad (24)$$

For a high concentration of trapping levels, $N_t \gg p_{1t}$, the observed results would be obtained. There are other combinations of terms with which one could approximate the behavior of Figs. 14 and 15. In fact, at sufficiently high carrier concentrations, the term in the recombination equation, $1/c_{pr} N$, must become important; but Eq. (24) demonstrates the simplest model. The value of $E_r - E_t$ chosen for Fig. 22 was 0.07 ev.

UNCLASSIFIED
ORNL-LR-DWG 53589

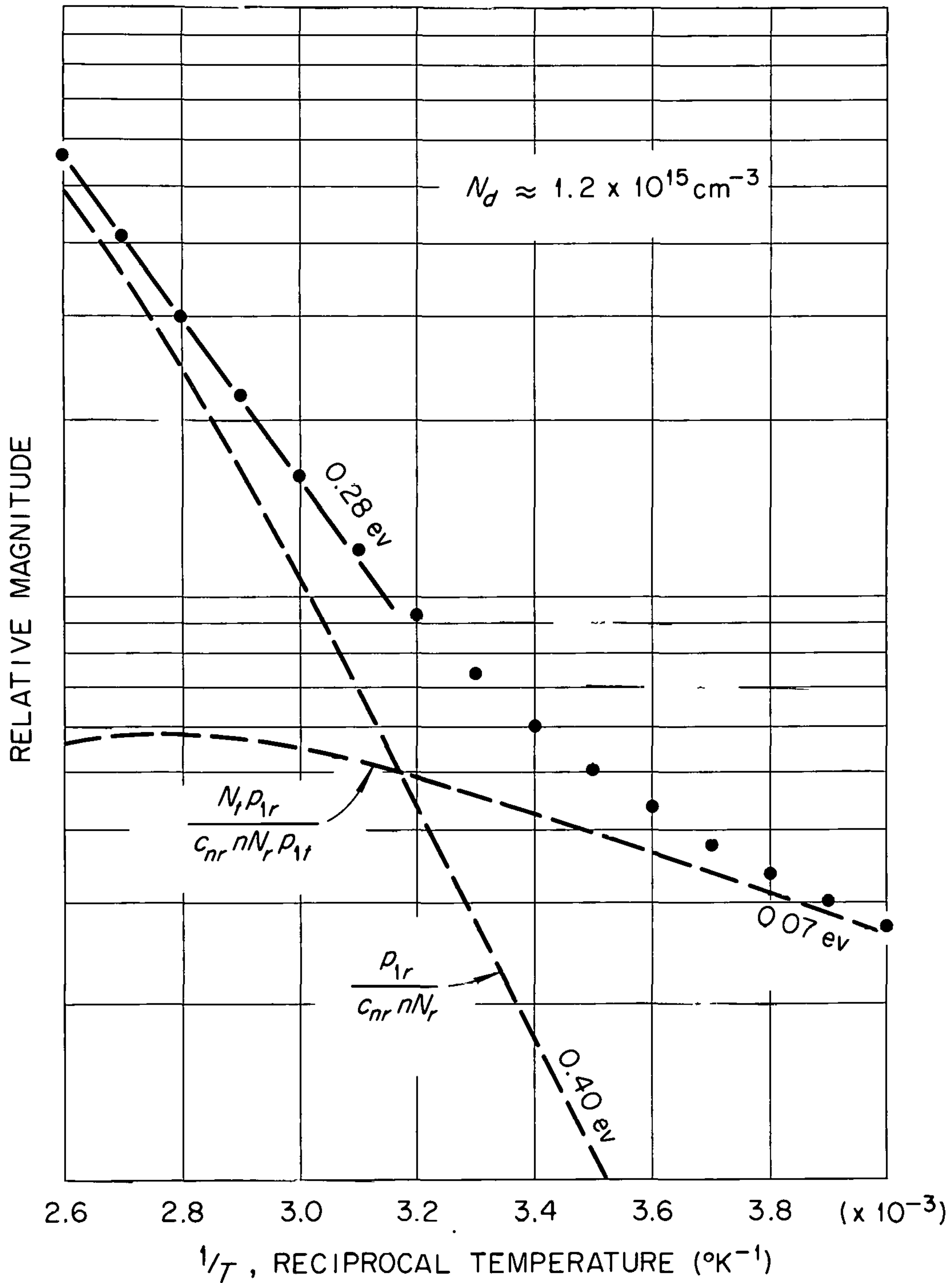

Figure 22. A Different Combination of Terms from the Recombination Equation.

Briefly, the behavior of UMSb 1.3 and UMSb 0.44 can be explained on the basis of recombination centers introduced at $\approx$ 0.36 ev from the valence band and trapping centers present in the unirradiated crystal at $\sim$0.29 ev above the valence band. None of the well-studied[22] deep-level impurities seem to fit these data. Copper and cobalt have energy levels 0.33 ev and 0.25 ev above the valence band, respectively; but these levels presumably would not be available for trapping since higher, occupied levels exist in each case.

It should be noted that the model proposed here is quite different from that used to explain recombination behavior in previous papers[3-5] in which the effect of trapping centers was neglected. On the basis of the few studies then available, it was postulated[3] that recombination occurs through an energy level located $\sim$0.20 ev below the conduction band; the hole capture probability limits the recombination and is temperature dependent.* The post-irradiation data of Figs. 5 and 6 are similar to those used to draw the above conclusion. The bottom curve of Fig. 5 was reported earlier[3] and was the only sample reported with resistivity lower than ten ohm-cm. The data of Fig. 6, as well as for other samples of similar resistivity, are easily explained on the basis of the present model. For these samples $N_d \approx 10^{14}$ and the corresponding curve in Fig. 21 agrees well with the

---

[22] W. W. Tyler, J. Phys. Chem. Solids 8, 59 (1959).

*Ryvkin and Yaroshetskii[15] also concluded that the recombination center was at $E_c - E_r = 0.20$ ev even though they considered trapping. However, the samples which they used were all near intrinsic at room temperature.

data. However, it is surprising that the data of Fig. 6 for ~ eleven ohm-cm material are so different from the data of Fig. 11. The answer undoubtedly lies in the fact that these are rather high resistivity samples, and compensating impurities are very likely present.

The discrepancy between data for the 2.0 ohm-cm sample (antimony-doped) shown in Fig. 5 and the data of Fig. 13 will now be considered. For the lowest curves in these two figures, the ranges of measurement were rather small; the lifetimes were rather low and, thus, difficult to measure, especially in such low resistivity samples. Thus, the discrepancy with the present results could be experimental. It may also be that the behavior shown in Fig. 5 was governed by Eq. (24), but in this case it would be required that a large number of traps originally in the sample be removed with heat treatment.

The present model also adequately accounts for the results for reactor and 14-Mev-neutron irradiation.[3,5,6] Figure 23, taken from Ref. 6, shows the result of irradiating three antimony-doped samples of different resistivity with 14-Mev neutrons. Evidently, the rate of introduction of traps relative to the rate of production of recombination centers by 14-Mev neutrons is considerably less than in the case of gamma irradiation. Also, there is some indication that the position of the recombination center is slightly lower in the forbidden gap, 0.32 ev above the valence band.* Figures 4 and 7 demonstrate results for n-type germanium irradiated with reactor neutrons. Other

---

*This is the position obtained previously[6] for this case, without considering trapping effects.

UNCLASSIFIED
ORNL-LR-DWG 35051R

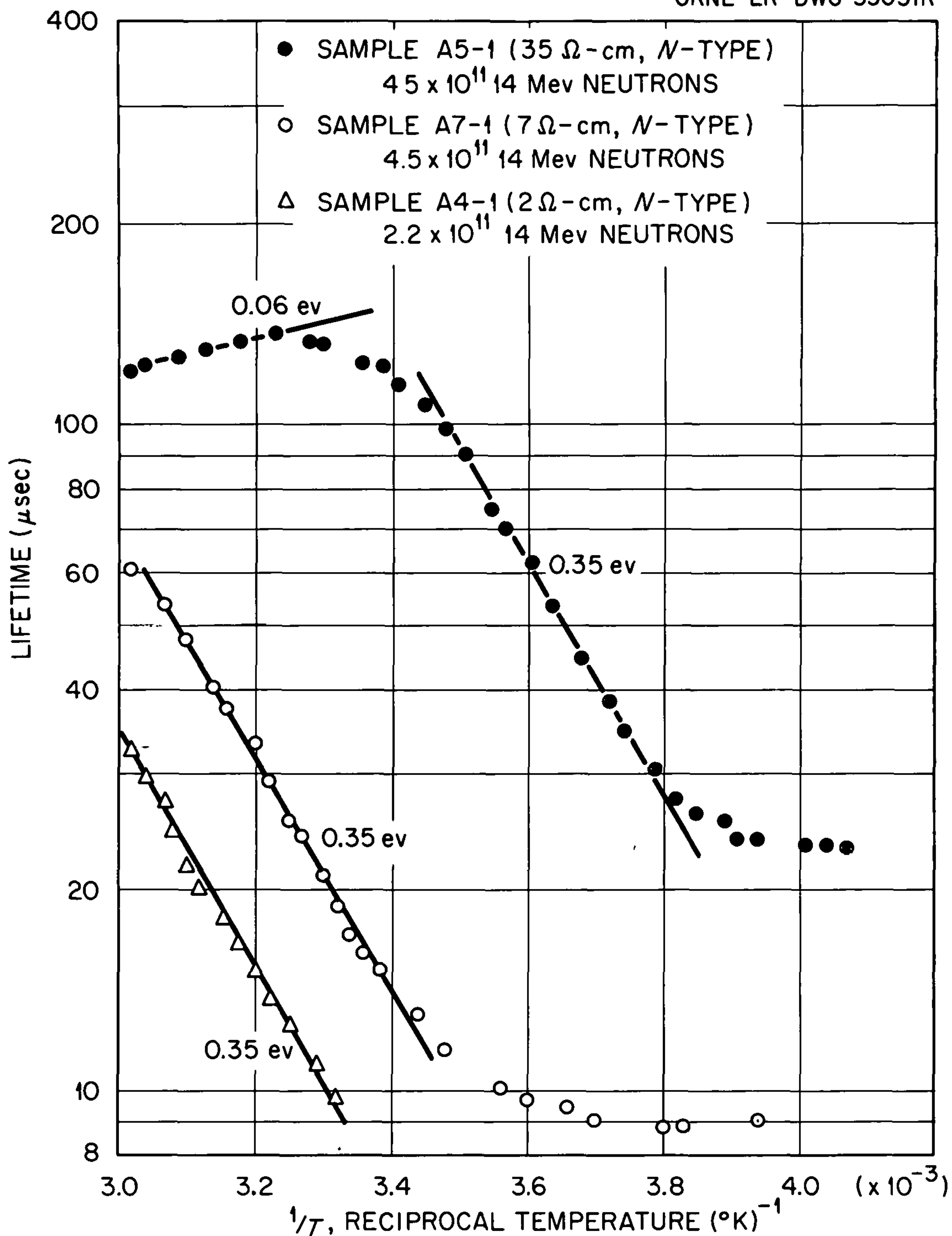

Figure 23. The Recombination Behavior of Antimony-Doped Germanium following Irradiation by 14-Mev Neutrons. From Reference 6.

data,[3-5] mostly on $\sim$ 15 ohm-cm material, indicate a slope for the recombination curves of $\sim$ 0.24 ev. The data were, quite logically, interpreted on the basis of recombination at a level known to be present in neutron-irradiated germanium $\sim$ 0.20 ev below the conduction band. On the basis of present data, however, the explanation is that reactor-neutron irradiation represents an intermediate condition in which the traps are more important than in the case of 14-Mev-neutron irradiation but less important than for gamma-ray irradiation. The position of the recombination level in this case is estimated to be $\sim$0.33 ev above the valence band.

Comparing the experimental data with Eq. (23), certain conclusions may be drawn concerning the relative magnitude of the terms in the recombination equation. Specifically, $p_{1r}/c_{nr}nN_r >> 1/c_{pr}N_r$ in the higher temperature range. Therefore, $p_{1r}/c_{nr}n >> 1/c_{pr}$; but $n >> p_{1r}$. Therefore, $c_{pr} >> c_{nr}$. A lower limit to the ratio c_{pr}/c_{nr} may be determined from Fig. 13. If the leveling out of the lifetime curves is due to the term $1/c_{pr}N_r$ becoming dominant, then $p_{1r}/c_{nr}nN_r \approx 1/c_{pr}N_r$ at $1/T \approx 3.6 \times 10^{-3}$ $^{o}K^{-1}$. Since there may be a contribution due to trapping effects, only a maximum value of the term $1/c_{pr}N_r$ may be determined. Thus, $c_{pr}/c_{nr} \gtrsim n/p_{1r}$, where n, the concentration of electrons in EPSb 2.3, is approximately 10^{15} cm^{-3} and p_{1r} at the stated temperature is 1.3×10^{12} cm^{-3}, or $c_{pr}/c_{nr} \gtrsim 800$. The value for capture probability which is obtained from experiment is in reality an average since the probability for a given transition depends on both the initial and final energy states. The capture probability is equal to the capture

cross section times the particle velocity so that the experimentally determined capture probability is equal to $\langle \sigma v \rangle$, where the cross section, σ, must be included in the average since it is, in general, velocity dependent. In order to obtain values for capture cross sections, the following approximation is generally made: $\langle \sigma v \rangle \approx \sigma \langle v \rangle$, where the cross section is specified for a given temperature and $\langle v \rangle$ is the mean thermal velocity at that temperature. $\langle v \rangle = \sqrt{8kT/\pi m^*}$, where m^* is the effective mass used for transport properties[23] in the case of electrons,

$$m_e^* = \left(\frac{1}{m_1} + \frac{1}{m_2} + \frac{1}{m_3}\right)^{-1} . \tag{25}$$

m_1, m_2, and m_3 are the effective electronic masses in the three principal directions in the crystal, given[24] by 1.58 m, 0.082 m, and 0.082 m, m being the electronic mass; or $m_e^* = 0.040$ m. The expression yielding m_h^* for holes is more complicated.[25] The value obtained is $m_h^* = 0.25$ m. Now, $\langle v_e \rangle / \langle v_h \rangle = (m_h^*/m_e^*)^{1/2} = 2.5$. Therefore, $\sigma_{pr}/\sigma_{nr} = 2.5\ c_{pr}/c_{nr} \gtrsim 2{,}000$. A similar calculation, based on the data of Fig. 23, for the case of 14-Mev-neutron irradiation, gives a corresponding ratio of about 1,000, in qualitative agreement with the above value.

Since the electron-capture process is rate limiting, it can be argued that the recombination center responsible for recombination in

---

[23] C. Herring, Bell System Tech. J. 34, 237 (1955).

[24] G. Dresselhaus, A. F. Kip, and C. Kittel, Phys. Rev. 98, 368 (1955).

[25] B. Lax and J. G. Mavroides, Phys. Rev. 100, 1650 (1955).

n-type germanium would be highly ineffective in p-type material. Actually, the rate at which the lifetime is degraded by irradiation in p-type germanium is lower than in n-type material[5] but large enough to indicate the action of a different recombination center. In spite of this fact, it is of interest to see if an analysis such as that carried out for n-type material might be of assistance in understanding the recombination center in p-type germanium. Figures 24, 25, and 26, taken from Refs. 3 and 5, demonstrate the results of irradiating p-type material with Co^{60} gamma rays, reactor neutrons, and 14-Mev neutrons. These were all gallium-doped specimens. The results for the single indium-doped sample (Fig. 19) were somewhat different. Since the recombination data for gallium-doped material are more extensive, discussion will be devoted primarily to them. There is no reason a priori to assume that behavior such as given by Eq. (23) holds for p-type material. That is, it is not known if a trapping level is effective in the temperature range of interest. However, attempts to treat the behavior in p-type material on the basis of a single recombination level have not been successful. For conditions of small N_r and low injection level, the Hall-[16]Shockley-Read[17] recombination equation may be written for p-type material ($p >> n$):

$$\tau = \frac{n_{1r}}{c_{pr} p N_r} + \frac{1}{c_{nr} N_r}\left(1 + \frac{p_{1r}}{p}\right). \qquad (26)$$

If the recombination center in question lies well above the Fermi level, $p_{1r}/p << 1$; and Eq. (26) reduces to:

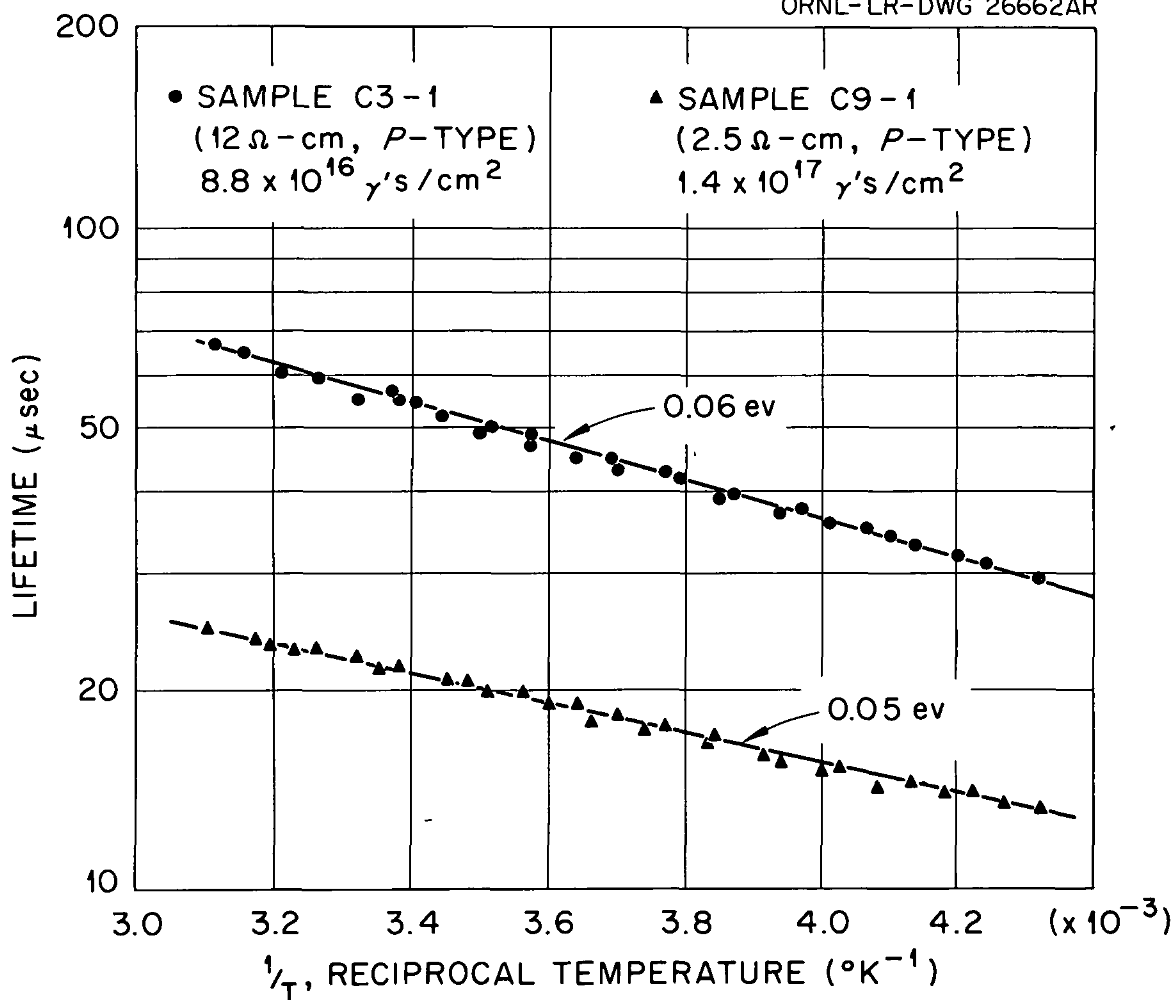

Figure 24. The Recombination Behavior of Gallium-Doped Germanium following Irradiation by Co^{60} Gamma Rays. From Reference 5.

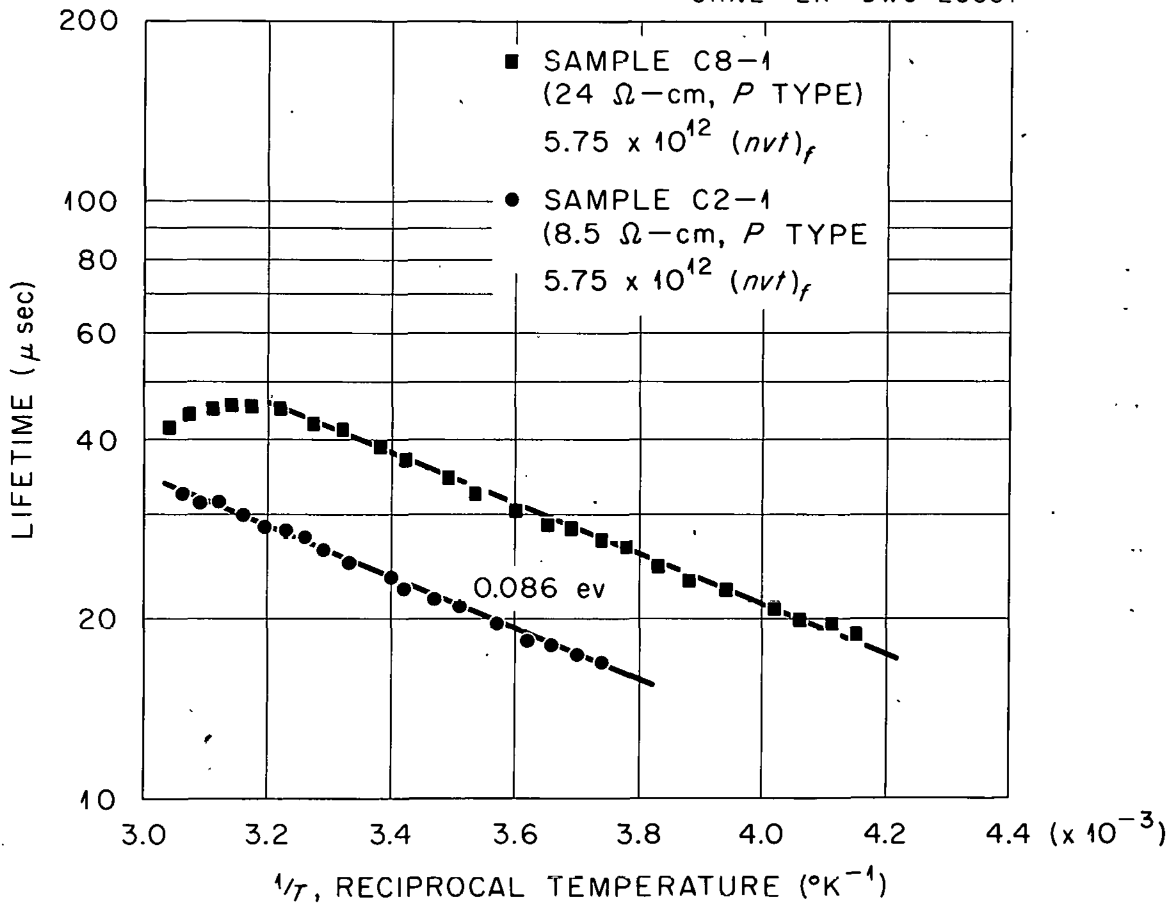

Figure 25. The Recombination Behavior of Gallium-Doped Germanium following Irradiation by Reactor Neutrons. From Reference 5.

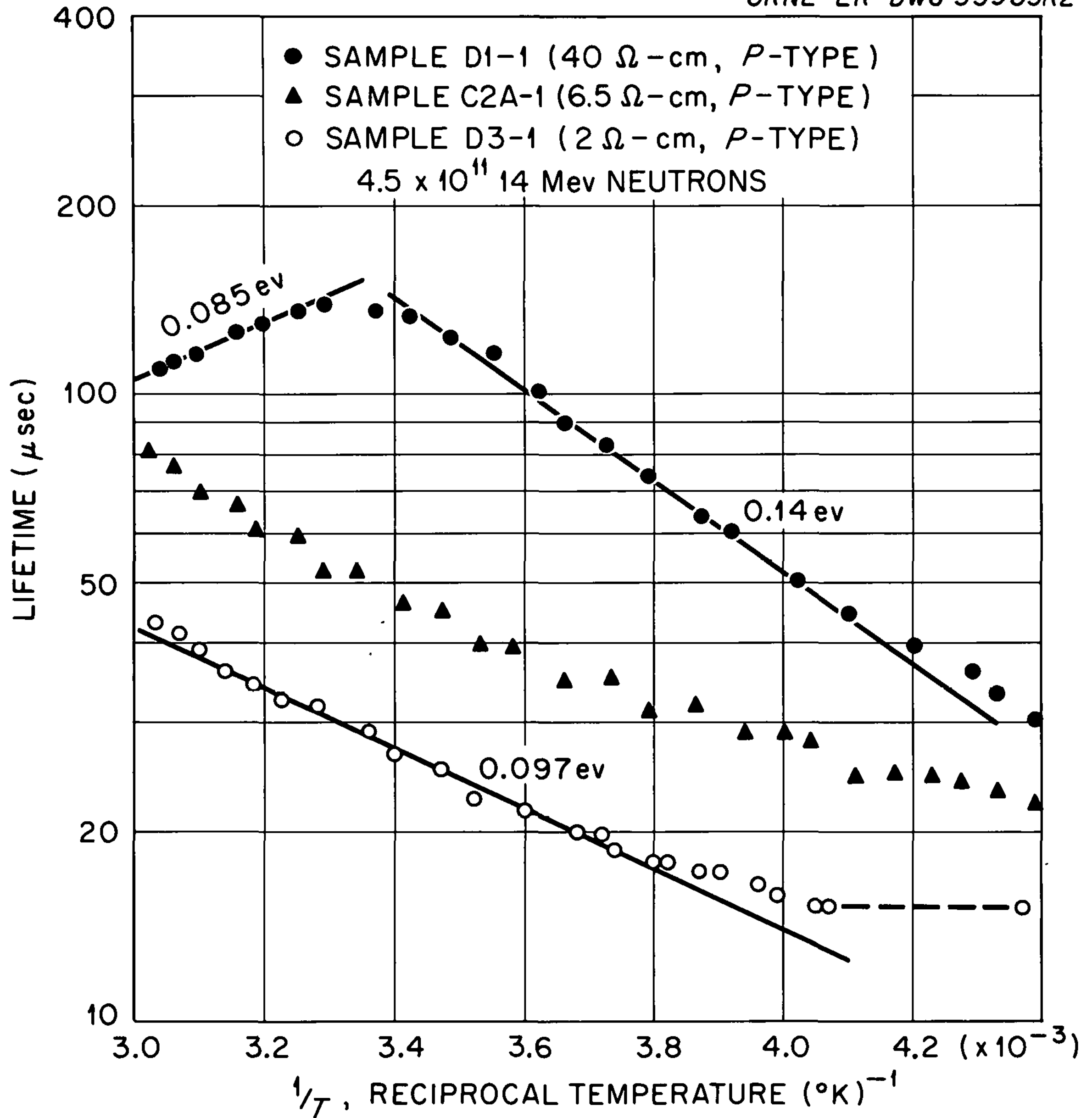

Figure 26. The Recombination Behavior of Gallium-Doped Germanium following Irradiation by 14-Mev Neutrons. From Reference 6.

$$\tau = \frac{n_{1r}}{c_{pr}pN_r} + \frac{1}{c_{nr}N_r}. \qquad (27)$$

This equation follows directly from the equation for p-type material corresponding to Eq. (23), when the effects of trapping centers are neglected. On the other hand, if the center lies below the middle of the gap, the term containing n_{1r} becomes extremely small; and

$$\tau = \frac{1}{c_{nr}N_r}\left(1 + \frac{p_{1r}}{p}\right). \qquad (28)$$

It has been noted that levels near the center of the band gap are most effective. If such recombination centers are operative in p-type specimens, Eq. (27) would be expected to hold. Then the log τ versus $1/T$ curve should have a slope at high temperatures similar to that for n-type material, if hole capture is rate limiting, or should display no temperature dependence, if electron capture is rate limiting. Inspection of Figs. 24 through 26, however, reveals a small slope, ≈ 0.09 ev in the case of reactor-neutron exposure and ≈ 0.06 ev for gamma-irradiated specimens, with a somewhat higher value for 14-Mev-neutron irradiation. It is, therefore, tempting to conclude that the recombination center lies near a band edge and either Eq. (27) or (28) is applicable, depending on whether the level lies near the conduction band or near the valence band. However, due to the fact that the temperature-dependent terms contain either n_{1r} or p_{1r}, a level at the position indicated would be $\sim 10^{-4}$ as effective as a level near the center of the band gap (for the same capture cross sections). This would tend to make such an explanation doubtful. It might be that the

second term in Eq. (27) is dominant and the temperature variation observed is due to temperature dependence of electron capture probability.

Wertheim and Pearson[26] have attributed similar behavior in plastically deformed germanium to temperature dependence of capture probability. For recombination at a charged center, a variation in capture probability with temperature might be expected. However, the data of Figs. 24 through 26 cannot be explained simply on the basis of a temperature variation of capture probability. Note that the temperature behavior is approximately the same in Figs. 24 and 25 for the two p-type samples of different resistivity, yet the values of the lifetime at the same temperature are quite different. This would indicate that a temperature dependence of c_{nr} cannot be responsible for the temperature dependence of lifetime since electron capture does not appear to be the limiting process. (The term in question, $1/c_{nr}N_r$, is carrier-concentration independent.) The behavior apparently cannot be ascribed to variations in c_{pr} since the term in Eq. (26) involving c_{pr} also involves n_{1r}. The behavior can be explained,[5] but with some difficulty, on the basis of coupled levels. However, it might be more satisfactory to use an explanation involving recombination in the presence of traps. Equation (23) was derived for n-type material, but it is easily seen that the solution is completely symmetrical for p-type material with the trapping and recombination levels above the Fermi level. In this case the proper expression is

---

[26] G. K. Wertheim and G. L. Pearson, Phys. Rev. 107, 694 (1957).

$$\tau = \frac{n_{1r}}{c_{pr}pN_r} + \frac{1}{c_{pr}p} + \frac{N_t n_{1r}}{c_{pr}pN_r n_{1t}} + \frac{N_t}{c_{nr}N_r n_{1t}} + \frac{1}{c_{nt}n_{1t}} + \frac{1}{c_{nr}N_r} . \qquad (29)$$

This relation introduces a new type of temperature dependence, not predicted by the simple theory. The experimental results are not inconsistent with the premise that the lifetime in gallium-doped, p-type material irradiated with Co^{60} gamma rays and reactor neutrons obeys the following relation:

$$\tau = \frac{N_t n_{1r}}{c_{pr}pN_r n_{1t}} ; \qquad (30)$$

and the temperature dependence shown in Figs. 24 and 25 would correspond to the difference in position between the recombination and trapping levels. The difference in the case of 14-Mev-neutron irradiation is presumably due to other terms from the recombination equation becoming important. For Eq. (30) to hold, the number of traps must be large compared with the number of recombination centers; and the recombination process must be hole-capture limiting ($c_{nr} >> c_{pr}$). Since the pre-irradiation recombination behavior is not unlike the post-irradiation case, the trapping centers entering Eq. (29) apparently would be present in the unirradiated material. As is true for the case of n-type material, the position of the recombination level appears to be nearer the center of the gap in the case of neutron irradiation. Again this is probably due to the extensive local perturbation produced by neutrons, which would cause a spreading out of the energy levels. The energy levels nearest the center of the band gap, being most effective, would dominate the recombination process. Thus, it is possible to explain

recombination behavior in p-type germanium by assuming a high concentration of trapping centers in unirradiated material. Although this argument explains the observed behavior, it is only tentative. Evidently, the trapping centers postulated in the case of the gallium-doped material used in obtaining the data of Figs. 24 and 25 are different from any that might be present in the indium-doped sample reported in Fig. 19, as evidenced from the difference in temperature behavior.

Figure 27 displays the energy-level structure proposed to explain the recombination behavior of n-type germanium exposed to various kinds of irradiation. It is not possible from the present data to locate these levels for p-type material. In n-type germanium the energy level responsible for recombination apparently is shifted slightly downward in the case of neutron irradiation. The important difference in the three types of irradiation would appear to be that the number of recombination levels introduced relative to trapping levels is largest in the case of 14-Mev-neutron irradiation and smallest for Co^{60} gamma irradiation. This, coupled with the fact that the lifetime change compared with carrier removal is greater for reactor-neutron irradiation than for Co^{60} gamma irradiation and still greater for 14-Mev-neutron irradiation,[3-6] indicates that the levels which remove electrons but do not act as recombination centers act as traps. The difference in rate of lifetime change compared with carrier removal was previously explained[3] on the basis of a difference in capture probabilities for the different types of irradiation.

Unfortunately, it is impossible to determine capture probabilities and cross sections for recombination simply on the basis of the results

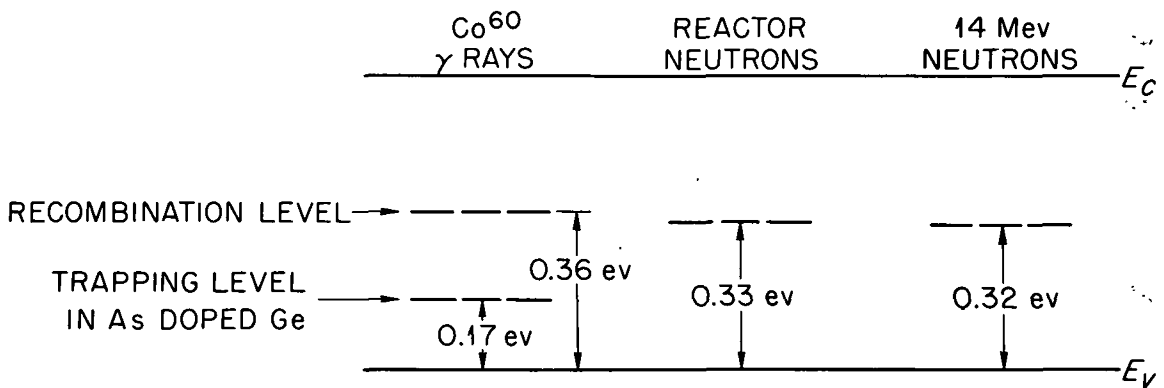

Figure 27. The Energy-Level Structure Proposed to Explain the Recombination Behavior of n-Type Germanium Exposed to Various Kinds of Irradiation.

presented here. The reason for this is that the number of recombination centers cannot be determined since their introduction rate is not known. (Before,[3-5] when the energy level at 0.20 ev below the conduction band was thought to be responsible for recombination, the rate of introduction of this level as obtained from changes in carrier concentration was assumed to be identical with the rate of recombination-center introduction.) Furthermore, the addition of a trapping term to the recombination expression complicates any determination of capture probabilities even if the number of centers were known. However, upon examining the annealing behavior, it will be seen that under certain assumptions the values of the electron-capture probability and cross section can be obtained for the recombination centers.

The dependence of the stability of recombination centers upon impurity concentration, together with the complications imposed by the trapping process, indicates that any analysis of recombination behavior based solely on the variation of lifetime with carrier concentration is invalid. It had previously been stated,[5] on the basis of the temperature behavior, that such an analysis for p-type material could not be made. Nonetheless, recent work has been based on such a method.[27]

---

[27] See, for instance, J. J. Loferski and P. Rappaport, J. Appl. Phys. 30, 1181 (1959).

II. THE ANNEALING BEHAVIOR

Figures 3 and 8 through 10 demonstrate that the annealing process by which lifetime recovers from the effect of irradiation is complicated. Furthermore, the presence of trapping levels complicates the analysis of the lifetime data since there are two types of centers present. In Eq. (23) there are two terms, $N_t/c_{pr}N_rp_{1t}$ and $1/c_{pt}p_{1t}$, which display the same temperature dependence. The first term depends on N_t; the second does not. Thus, it does not seem possible to determine the annealing kinetics of trapping levels from the present measurements. Figures 3 and 8 through 10 display approximately the annealing of recombination centers. However, in the case of arsenic-doped material, annealing of the traps probably introduces some inaccuracies. Further complications, apparently caused by high concentrations of traps in unirradiated material, occur in the two lowest resistivity, antimony-doped samples. It seems apparent that the information to be obtained from the annealing data will be largely of a qualitative nature. Several conclusions can be drawn from the results of the exploratory measurements shown in Fig. 3. The annealing behavior depends markedly both on the type of irradiation and the type and resistivity of the material. (The n-type specimens were antimony doped; the p-type specimens were indium doped.) Two ohm-cm, n-type material annealed more readily than fifteen ohm-cm, n-type material regardless of the irradiation used. (The fifteen ohm-cm value is nominal. Although the three specimens were from the same ingot, the values ranged from eleven to fifteen ohm-cm.) The most striking difference between types of irradiation was demonstrated by the

p-type material. Here the annealing behavior for material irradiated by Co^{60} gamma rays was quite different from the two specimens irradiated by neutrons throughout the annealing range.

Figure 3 is of use primarily in demonstrating the difference in annealing behavior between various types of irradiation since Figs. 8 through 10 deal with the difference in impurity concentration in much greater detail. Figure 8 displays the dependence of annealing behavior upon antimony doping. Although there are complications in the structure of the curves which may depend on other factors, the overall annealing depends principally upon the impurity concentration. That is, gross annealing occurs at lower temperatures for higher impurity concentrations throughout the impurity-concentration range considered here. There is also, for the arsenic-doped samples, a partial anneal in the low-temperature range which is impurity-concentration dependent, as seen in Fig. 9. After this early anneal the curves for NCAs 2.6 and NCAs 5.4 would very nearly superimpose if normalized, so this higher temperature anneal is at least approximately impurity-concentration independent. Figure 10 displays results for two additional antimony-doped samples and a single p-type sample. As mentioned in the preceding section, these two antimony-doped specimens from the same ingot displayed different recombination behavior from the other antimony-doped samples. The annealing behavior was also somewhat different. Although the bulk of the annealing occurred in the temperature range expected on the basis of the data of Fig. 8, there was an initial "negative" annealing and a residual damage which did not anneal until higher

temperatures. It is interesting to note from Figs. 3 and 5 that EPSb 2.0 also retained a sizeable fraction of its damage until higher temperatures, in contrast to EPSb 2.3 of Figs. 8 and 13. There may be some connection between this fact and the difference in temperature dependence of lifetime discussed earlier. Figure 10 reiterates the fact that annealing in p-type material is different from that in n-type material. The annealing seemed to occur in several steps, indicating that no unique process was responsible.

Some of the behavior that has been mentioned can be explained using the postulate that the recombination center consists of an interstitial or vacancy associated with an impurity atom (antimony or arsenic). This would account for the fact that more energetic irradiation produces relatively larger numbers of the centers since a displaced atom would have a higher probability of coming under the influence of an impurity atom if it had higher recoil energy. However, annealing behavior would seem difficult to explain on such a basis.

Helpful information can be obtained from isothermal anneals as to the nature of the annealing process. One of the best clues to determine the nature of the annealing process is the order of the annealing reaction. If q is the concentration of the entity undergoing anneal and the process is first order, with k' the rate constant,

$$\frac{dq}{dt} = -k'q; \tag{31}$$

so that

$$q(t) = q_o e^{-k't}. \tag{32}$$

To test whether a reaction is first order, q is plotted logarithmically as a function of time. For a first-order process a straight line results, and

$$k' = 1/t \ \ln q_o/q. \tag{33}$$

If the annealing of q depends upon the simultaneous "using-up" of a second entity whose concentration is given by q', then the process is second order. For a second-order reaction it is more convenient to express the process in terms of $x = q_o - q$. Then

$$\frac{dx}{dt} = k'(q_o - x)(q_o' - x) \tag{34}$$

and

$$k' = \frac{1}{t(q_o - q_o')} \ln \frac{q_o'(q_o - x)}{q_o(q_o' - x)} \tag{35}$$

unless $q_o = q_o'$, in which case

$$k' = \frac{1}{t} \left(\frac{1}{q_o - x} - \frac{1}{q_o}\right). \tag{36}$$

If. Eq. (35) holds, plotting $(q - x)/(q' - x)$ logarithmically as a function of time yields a straight line while, if Eq. (36) holds, $(q_o - x)^{-1}$ is a linear function of time. If $q' >> q$, then the kinetics are again first order. Regardless of whether the process is first or second order, the activation energy can be determined from

$$k' = Ae^{-E/kT}, \tag{37}$$

where E is the activation energy, determined by measuring k' at several temperatures.

The above conclusions pertain to processes limited by a potential barrier. They do not apply, in general, to diffusion-limited

processes. The problem of diffusion-controlled reactions has been treated and applied to annealing problems by Waite[10] and by Reiss.[28] One result is that, in certain cases, diffusion-controlled processes also display first-order kinetics. However, in this case the activation energy, E, is the energy of motion of the diffusing entity.

It is seen that first-order annealing processes can arise in various ways. First, if the rate-limiting step is the breaking up of a complex, the process will be first order and the activation energy will correspond to the potential barrier to dissociation of the complex. Second, if the rate-determining process is the annihilation of the defect in question at the site of a second entity whose concentration is not altered appreciably by the annealing process (either the second entity is not used up, or its concentration is very large compared with the defect concentration), first-order kinetics apply and the activation energy corresponds to the potential barrier to annihilation. Third, if the annihilation of defects is limited by the rate of diffusion of those defects and the annihilation process is first order, then the annealing kinetics may be first order[28] and the activation energy involved is the energy of motion of the defect.

In the first case above, the rate constant will depend only upon the height of the potential barrier and a frequency factor characteristic of the dissociating complex. In the second case, the activation energy for annihilation and a frequency factor will be involved; but the rate

---

[28]Howard Reiss, J. Appl. Phys. 30, 1141 (1959).

constant will also be proportional to q', the concentration of annihilating centers, which is assumed to be constant. In the third case, instead of a linear dependence on q', the rate constant should be proportional to $q'^{2/3}$. (The rate constant would be expected to vary inversely as the mean time required to reach an annihilation site. For a random-walk process this time varies as the square of the mean distance between sites, which, in turn, is dependent upon $q'^{-1/3}$.)

Isothermal anneals were made on several specimens. The case in which it might be hoped to gain the most information is the antimony-doped, low-resistivity material where the annealing appears to be nearly a single-step process. Figure 28, which is a semi-logarithmic plot of the fraction of damage remaining as a function of time, demonstrates the result of four isothermal anneals on NCSb 3.7. The curves appear to follow Eq. (32) fairly well; thus, first-order rate constants k' have been assigned to them. If a second-order effect is present, increasing the amount of irradiation should increase the apparent value of k'. As observed for a difference of a factor of three in the amount of irradiation, only a small difference in k' is observed, which is in the opposite sense to that expected for a second-order contribution. Figure 29 shows somewhat more complicated behavior for UMSb 1.3(A) and UMSb 1.3(B). However, Fig. 10 indicates that these samples retained residual damage following a large amount of annealing at fairly low temperature. This amount should be subtracted from the data of Fig. 29. For UMSb 1.3(A) the correction was about one-tenth, and for UMSb 1.3(B) the correction was about two-tenths. These values were subtracted from the results of

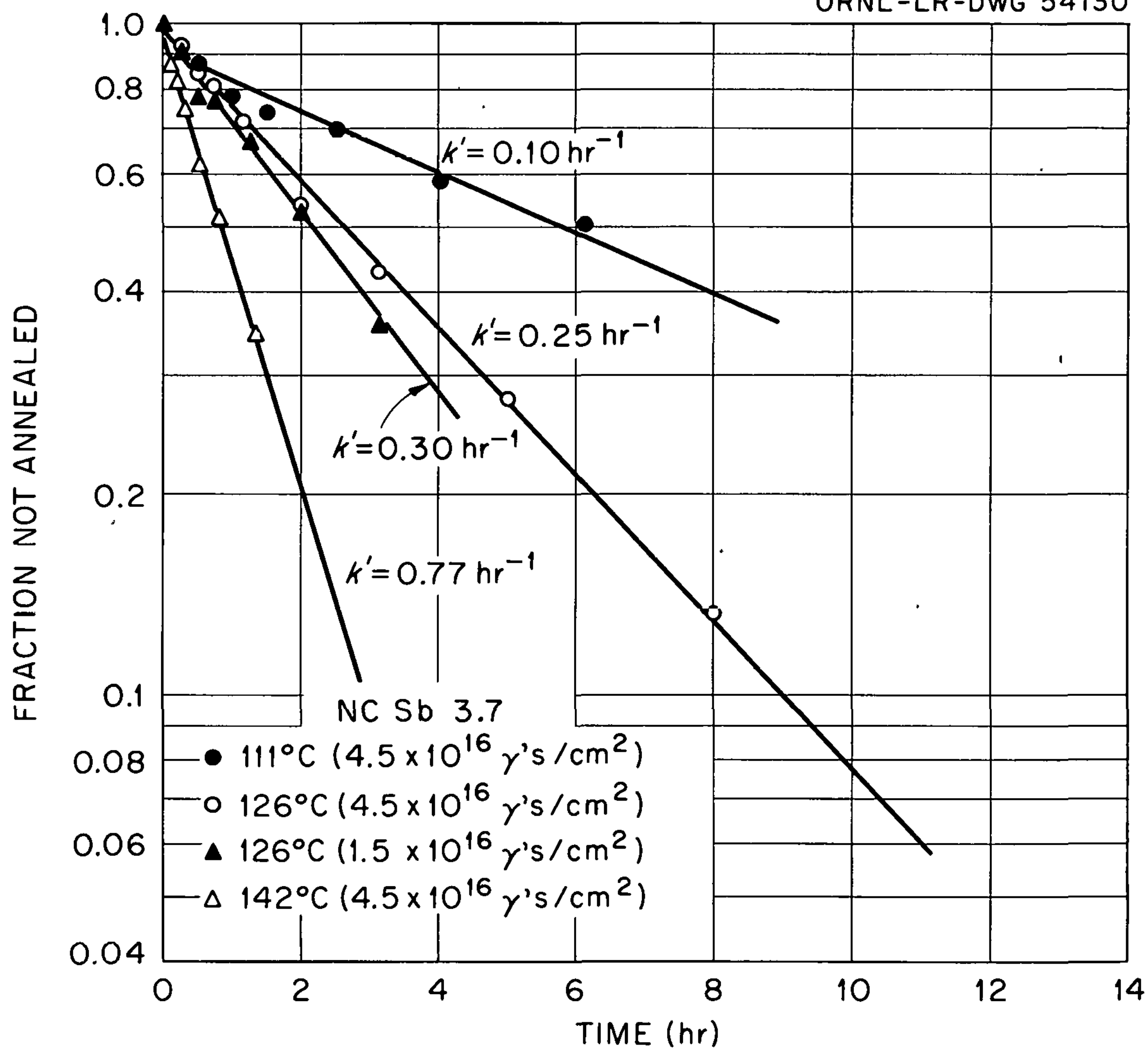

Figure 28. Isothermal Annealing Curves for 3.7 Ohm-cm, Antimony-Doped Germanium following Co^{60} Gamma Irradiation.

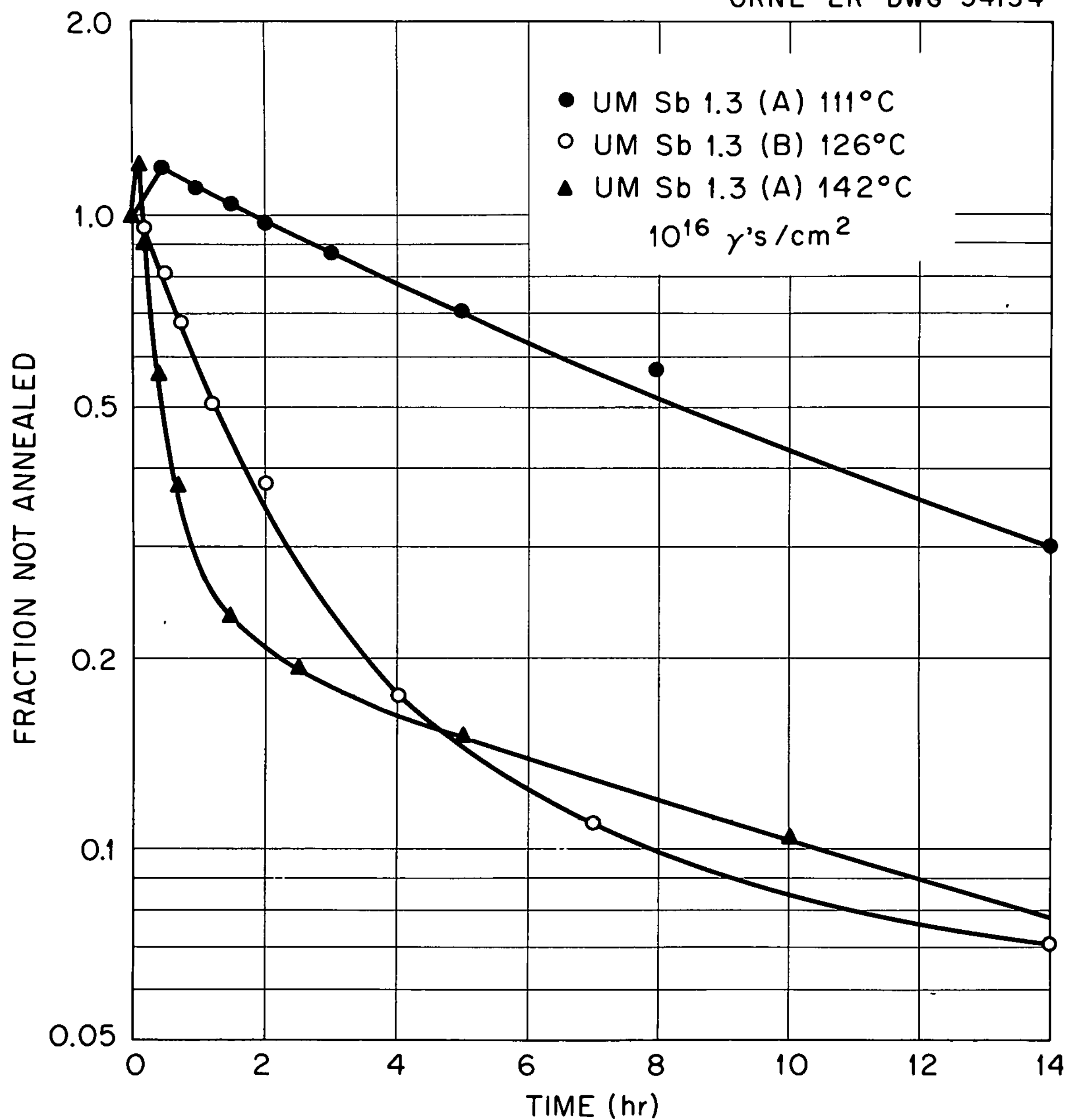

Figure 29. Isothermal Annealing Curves for 1.3 Ohm-cm, Antimony-Doped Germanium following Co^{60} Gamma Irradiation.

Fig. 29 to give the data of Fig. 30. Again, except for the anomalous early increase in damage associated with these samples, the behavior fits Eq. (32) remarkably well. As before, first-order rate constants have been assigned. Figure 31 is the result of checking to see that k' is independent of damage concentration. k' is constant within experimental error. The reason for the curves being shifted with respect to each other is the occurrence of different amounts of early "negative" annealing. Since this process occurs so quickly at 126°C, it would probably be sensitive to the amount of time spent at room temperature.

The primary annealing process in antimony-doped material thus appears to be a first-order process. Figure 32 shows the result of obtaining the activation energy on the basis of Eq. (37). The values for activation energy obtained for the two samples are somewhat different, possibly indicating that this means of determining the activation energy is not correct. However, the experimental difficulties in obtaining Fig. 32 must not be overlooked. For the UMSb 1.3 specimens a correction was applied which was quite approximate in nature and could affect the results somewhat. Actually, this correction should have been time dependent since the residual damage must anneal at a finite rate. Furthermore, the reverse-annealing process occurring early on the curves might be affecting the results at later times. In the case of NCSb 3.4 the point at 111°C has a high degree of uncertainty; thus, the activation energy determined from this sample depends on only two points, the relative uncertainty of which may be demonstrated by

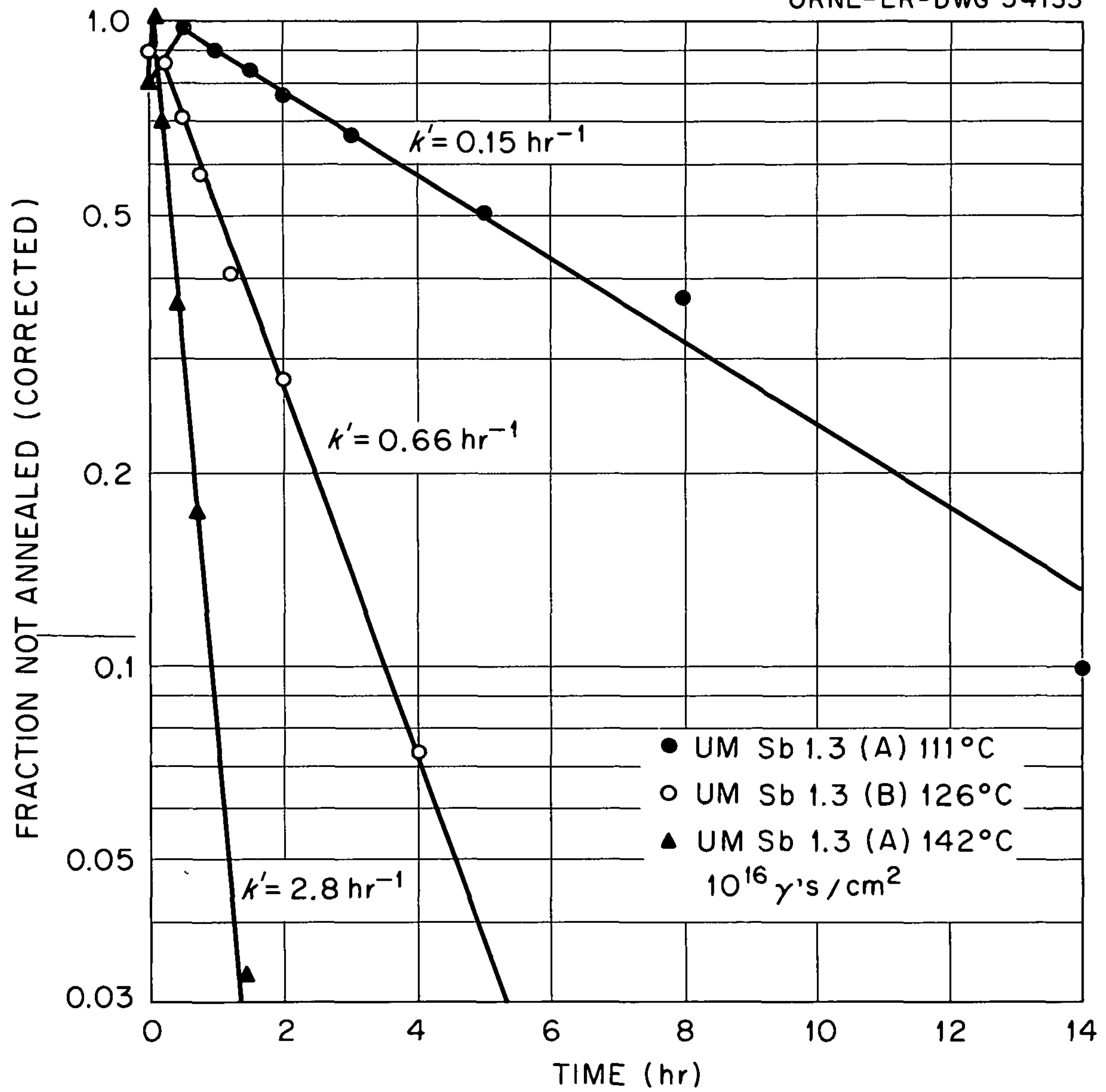

Figure 30. Corrected Isothermal Annealing Curves. Data of Figure 29.

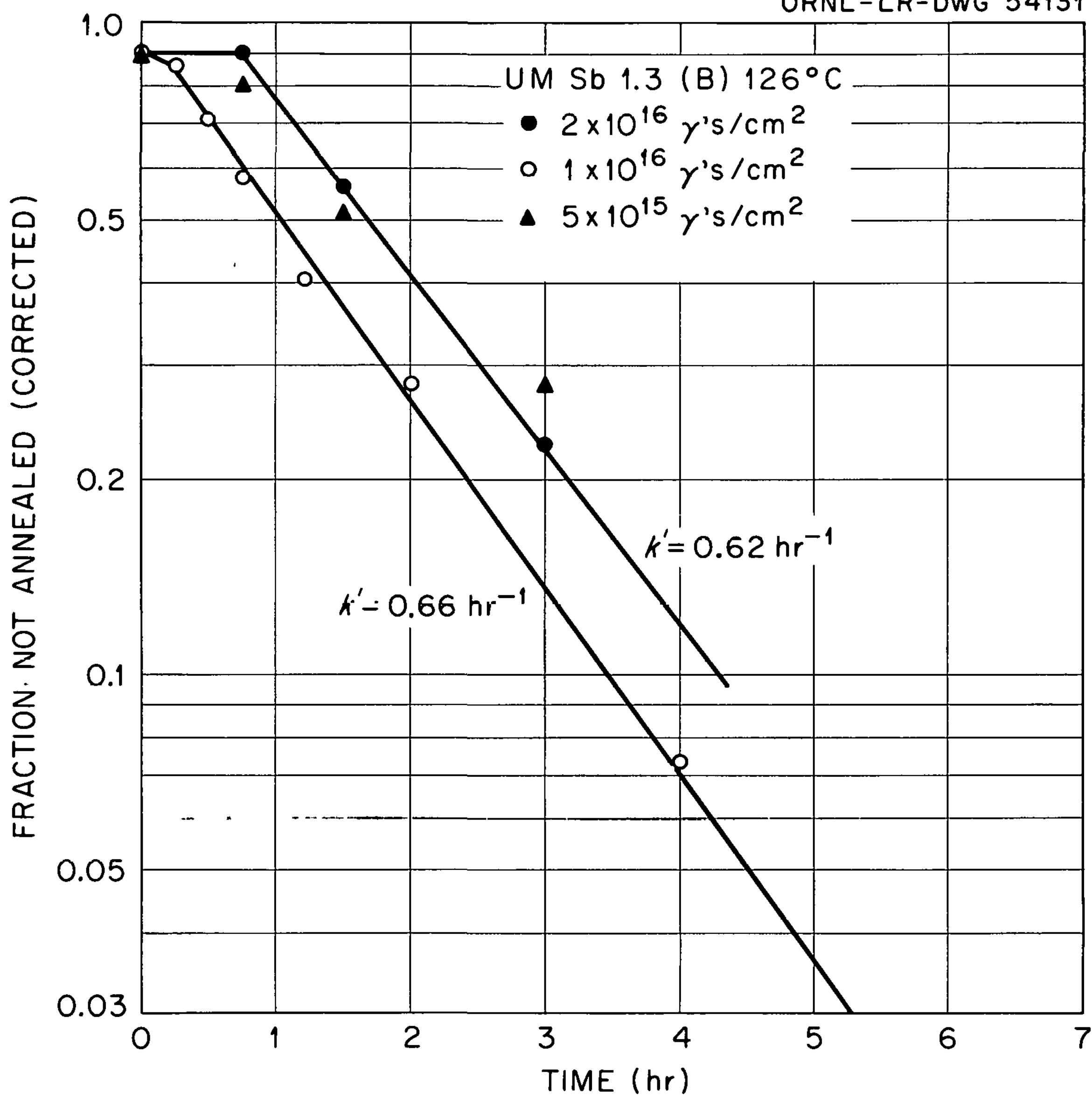

Figure 31. Corrected Isothermal Annealing Curves for 1.3 Ohm-cm, Antimony-Doped Germanium following Various Co^{60} Gamma Irradiations.

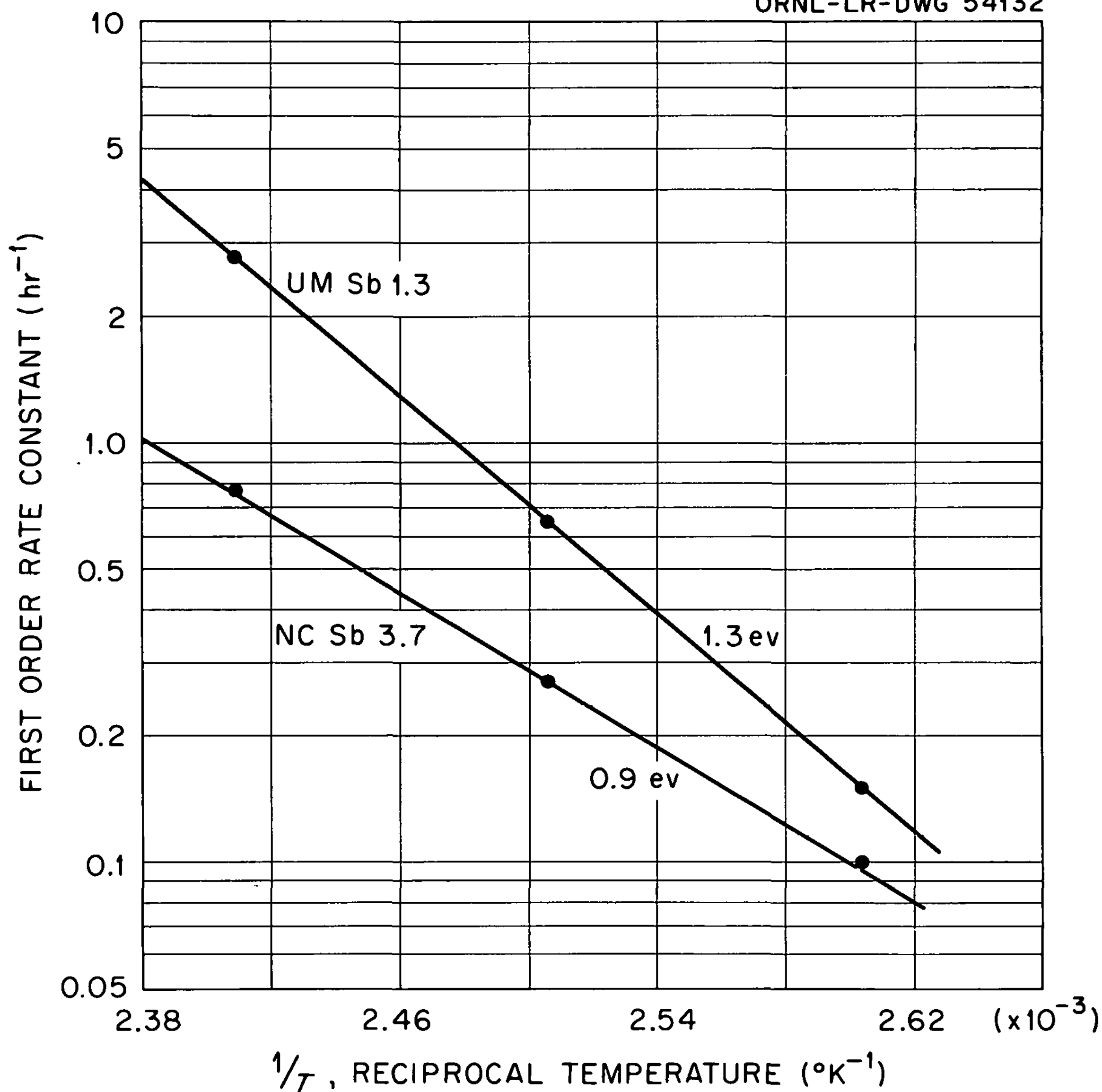

Figure 32. The First-Order Rate Constants as Obtained from Isothermal Anneals for 1.3 and 3.7 Ohm-cm, Antimony-Doped Germanium Plotted Logarithmically as a Function of Reciprocal Temperature.

the difference in k' values obtained at 126°C for two different irradiations. For these results it is considered possible that the apparent difference in activation energies is experimental.

The observed activation energy of approximately 1.1 ev could correspond either to a potential barrier at the site of the impurity atom or to the activation energy of motion for the recombination center. It is interesting to note that self-diffusion measurements[29] in germanium have resulted in a value for the activation energy of motion of a vacancy of about one electron volt. The same value has been obtained in measurements[30] of the mobility of radiation-induced defects in germanium. It is tempting to suppose that the same defect (namely, the vacancy) was observed in the three experiments: annealing, self-diffusion, and mobility.

The following speculative hypothesis is offered to explain the experimental results. A displaced germanium atom has a nearby interstitial position which is stable, and less energy is required to displace an atom to this position than to produce completely separated vacancies and interstitials. This might be reasonable on the basis that the strains produced by a vacancy and an interstitial would partly compensate if the interstitial remained close to the vacancy; and, furthermore, there might be an electrostatic interaction between

---

[29] H. Letaw, Jr., W. M. Portnoy, and L. Slifkin, Phys. Rev. 102, 636 (1956).

[30] P. Baruch, J. Appl. Phys., to be published.

Furthermore, the recombination center has the proper activation energy for motion to be a vacancy, as mentioned earlier. On the basis of these arguments, the recombination centers should be vacancies.

If the above conclusion is correct, the annealing of the arsenic-doped samples should be impurity-concentration independent and should be the same as for antimony-doped samples with sufficiently low antimony concentration. This is approximately true except for the initial concentration-dependent anneal observed in arsenic-doped specimens. This early anneal has not been explained. Possibly there was a small number of interstitial arsenic atoms which recombined with part of the vacancies, or a small fraction of the arsenic atoms might have had interstitials associated with them with which the vacancies could recombine. These possibilities would be difficult to prove.

Due to the complexity of the annealing behavior in arsenic-doped material, one cannot perform an analysis such as was carried out for the case of antimony doping. However, the early anneal is well separated from the remaining portion. Therefore, by first allowing the early anneal to occur, one may investigate the anneal occurring at higher temperatures. Such an attempt is demonstrated in Fig. 33. These isothermal annealing curves were taken following irradiation and heat treatment for one hour at 126°C. On the basis of Fig. 9, nearly all of the early anneal, but almost none of the later anneal, would have occurred. It is clear from the shape of the curves that the behavior cannot be described by a unique activation energy. Rather, there seems to be a distribution of activation energies. The processes

interstitial associated with the impurity or through forming a complex with the impurity. Thus, the annealing behavior of antimony-doped material can be explained. However, this does not account for the more complicated behavior in arsenic-doped germanium.

The difference in atomic radii between antimony and arsenic might reasonably be expected to be somehow responsible for the difference in observed annealing behavior. The covalent radii of germanium, antimony, and arsenic are 1.22 Å, 1.41 Å, and 1.21 Å, respectively.[32] However, the antimony and arsenic atoms carry unit positive charge, decreasing their size. On the basis of arguments given by Pauling,[33] the covalent radii for the antimony and arsenic atoms in the germanium lattice are approximately 1.39 Å and 1.19 Å, respectively. Thus, it would seem that there is a positive lattice strain produced by the antimony atom which is not present in the case of arsenic. An interstitial would avoid an antimony atom because its presence would add to the strain present in the region of the antimony atom. However, a vacancy would find it energetically favorable to be in the region of the large antimony atom. Furthermore, a vacancy is expected to be negatively charged and, thus, would be attracted to the antimony atom. This negative charge agrees with the fact that electron capture is the limiting process in recombination, as seen from the fact that c_{nr} is the important capture probability in the recombination equation.

---

[32] Linus Pauling, The Nature of the Chemical Bond (Cornell University Press, Ithaca, New York, 1948), p. 165.

[33] Ibid, p. 169.

the two. Wertheim[31] has obtained evidence that such close-spaced pairs occur in silicon. The energy level primarily responsible for carrier removal is associated with the coupled defect and the recombination center is either an isolated vacancy or interstitial. First, this hypothesis accounts for the difference in relative rate of introduction of recombination centers between gamma and neutron irradiation. In the case of Co^{60} gamma irradiation, most of the Compton and photoelectric electrons which create displacements have only enough energy to produce coupled pairs and relatively few isolated defects are produced. On the other hand, with 14-Mev neutrons the average energy imparted to the germanium atoms is large and, so, relatively few germanium atoms would receive just enough energy to form a coupled pair. The case of reactor-neutron irradiation would, of course, be intermediate. The difference in trapping which also depends on the natu: of the irradiation would indicate that a trapping level below the center of the gap is introduced by these close-spaced pairs. On the basis of the measurements of Ryvkin and Yaroshetskii,[15] this level lies 0.25 ev above the valence band.

In order to explain the annealing data, the defect responsible for recombination is postulated to become mobile in the temperature range in which annealing occurs. Upon coming under the influence of an impurity atom, the isolated defect responsible for recombination becomes ineffective either through recombining with a vacancy or

---

[31]G. K. Wertheim, Phys. Rev. 111, 1500 (1958).

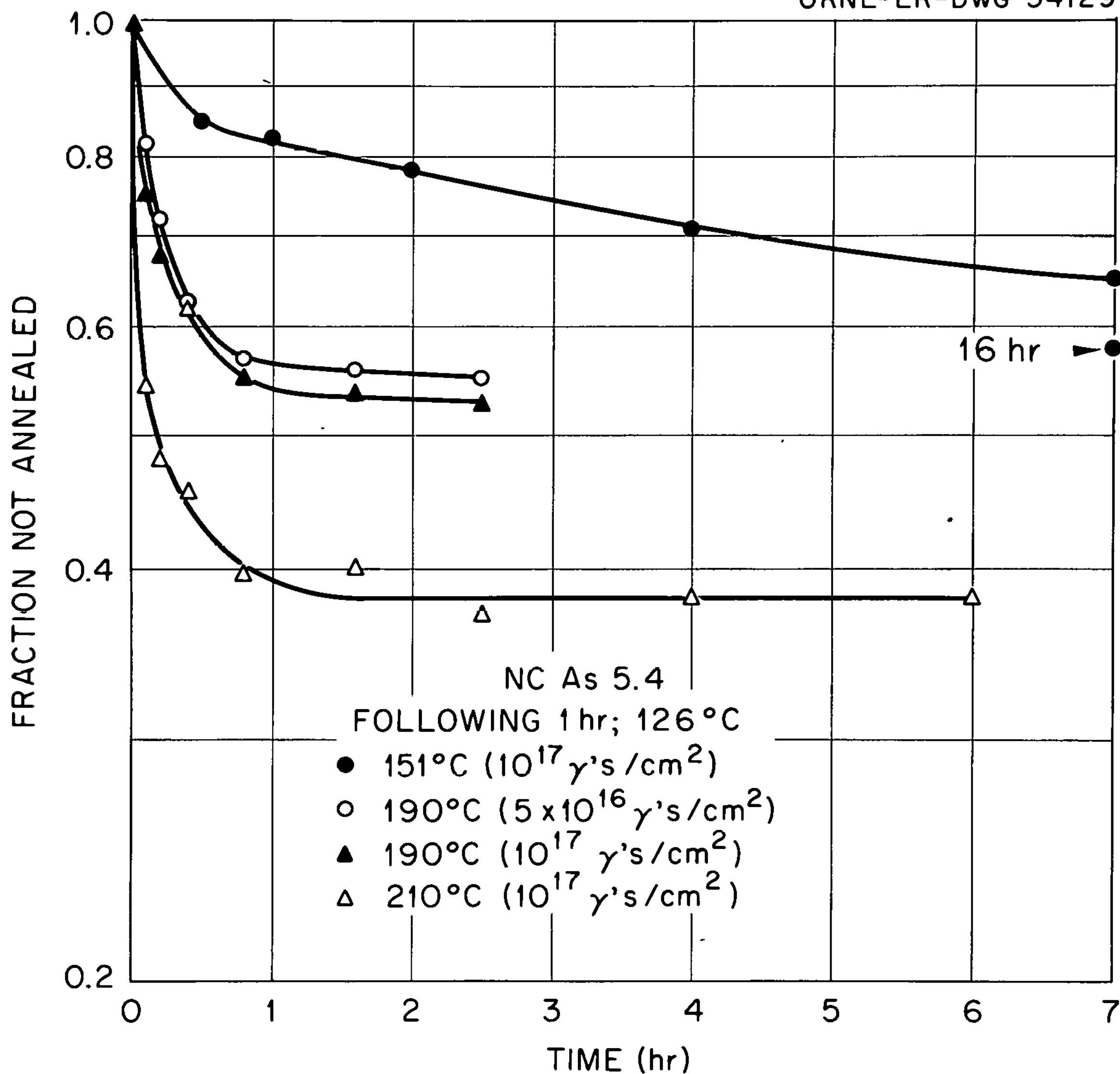

Figure 33. Isothermal Annealing Curves for 5.4 Ohm-cm, Arsenic-Doped Germanium following Co^{60} Gamma Irradiation and One Hour at 126°C.

apparently are very nearly first order, as evidenced by the two sets of data taken at 190°C for different damage concentrations. It would seem unwise to speculate on the nature of this annealing because of the small amount of information available. However, since this anneal does not depend on the defect or impurity concentration, it is evidently not direct vacancy-interstitial recombination; and it must take place at some location other than an impurity center.

A brief statement regarding the nature of the trapping centers should be included. While trapping occurs near room temperature in arsenic-doped germanium, it does not in antimony-doped material. A logical explanation would be that the trapping level in arsenic-doped germanium is due to an impurity-imperfection complex. This could be, for instance, an interstitial-arsenic pair. An interstitial-antimony pair would not be expected to occur due to the large size of the antimony atom. The trapping level was assigned the position of 0.17 ev above the valence band, but this estimate involves a greater uncertainty than that involved in the determination of the position of the recombination center.

III. COMPARISON WITH OTHER RESULTS

The main purpose of this section is to compare the work herein reported with that of Brown, Augustyniak, and Waite.[8] In their article they surveyed much of the earlier work and formulated their conclusions with that earlier work in mind. BAW were the first to notice that impurity atoms play an important role in the annealing of electron-induced damage. The nature of the damage produced by electrons should

be very similar to damage produced by gamma rays. Brown, Fletcher, and Wright[9] performed annealing experiments on electron-irradiated germanium in which they observed the restoration of conductivity due to annealing in the temperature range 160 to 300°C. These data were re-analyzed by Waite,[10] who included some more accurate data of Augustyniak. Augustyniak's measurements were made on arsenic-doped material, as were probably Brown, Fletcher, and Wright's.[34] BAW present some of these data in Fig. 2 of their paper. It was found that these data agree surprisingly well with lifetime data for arsenic-doped material shown in Fig. 33. Figure 34 contains the data given in Fig. 33 as well as data of Brown, Fletcher, and Wright and of Augustyniak. The data are plotted in the manner used by BAW. Considering the different properties employed for indices of annealing, the agreement between the conductivity and lifetime data is remarkable. The resistivity of the samples from which the conductivity data were obtained was[10,34] 0.7 ohm-cm (before irradiation), as compared with the 5.4 ohm-cm specimen used for lifetime measurements. The results agree with the observation previously made that this annealing process is not dependent upon impurity concentration. NCAs 5.4 had a pre-anneal treatment of one hour at 126°C. In the case of the conductivity samples with much higher impurity concentrations, the early, lower temperature anneal would probably have occurred in a relatively short time at room temperature and would not

[34] W. M. Augustyniak, private communication.

UNCLASSIFIED
ORNL-LR-DWG 54733

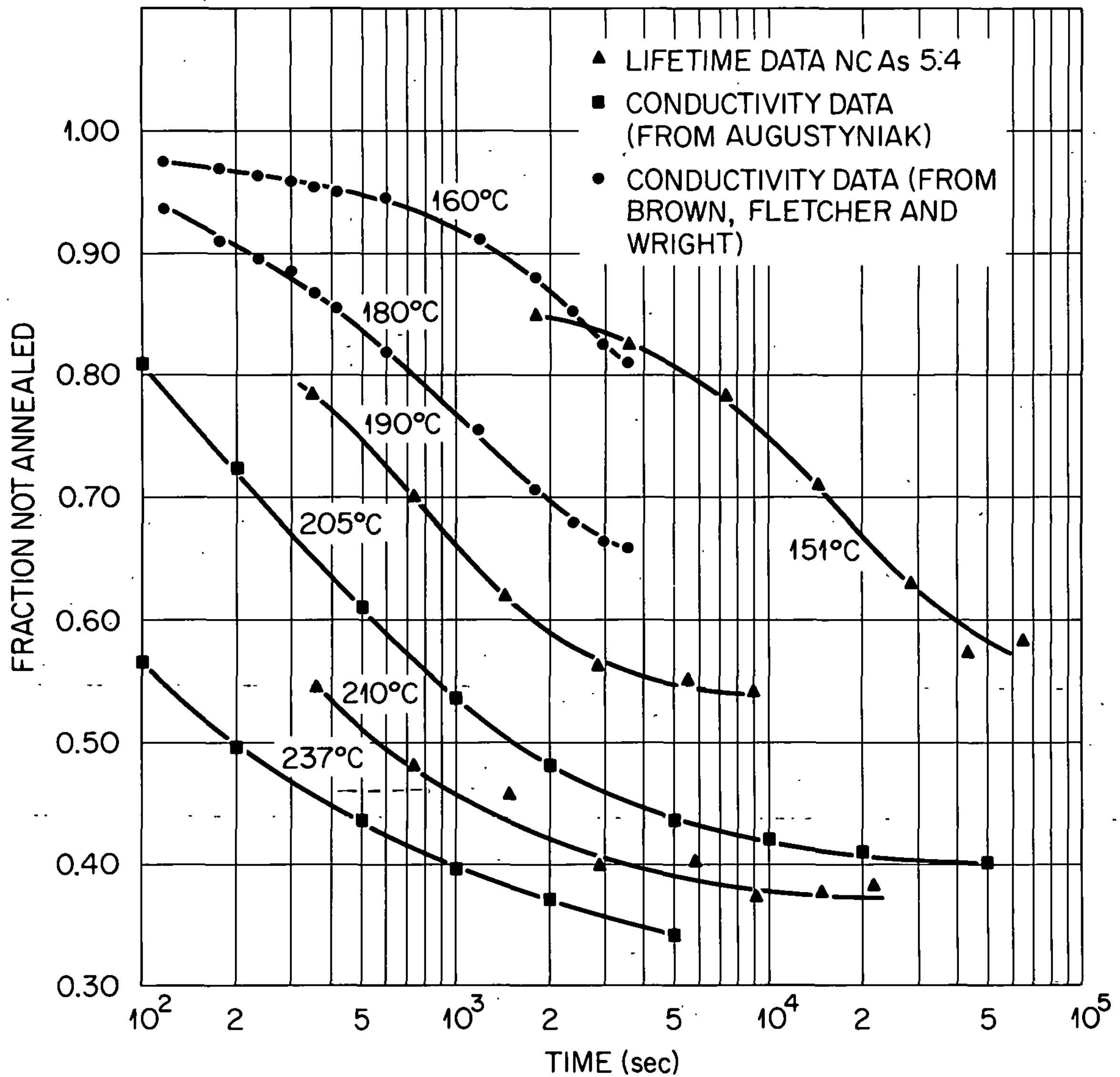

Figure 34. Comparison of Isothermal Anneals Performed on Arsenic-Doped Germanium Using Lifetime and Conductivity Data Following Co^{60} Gamma Irradiation and Electron Irradiation, Respectively. Conductivity data from References 9 and 10.

have been observed. The dose used for conductivity changes was very large compared with those used for lifetime changes. Their initial concentration of bombardment-induced defects was[10] $\sim 10^{15}$ cm^{-3}, while the value in the present case was $\sim 2 \times 10^{13}$ cm^{-3}. The agreement between the two types of data further substantiates the fact that this anneal is defect-concentration independent.

It seems unlikely that the agreement of the data shown in Fig. 34 is fortuitous. On the basis of this agreement, the center responsible for recombination in arsenic-doped material after the early anneal had occurred is felt to be the same center responsible for carrier removal.* Therefore, it was possible to count the number of recombination levels on the basis of Hall measurements and, thus, determine the electron-capture probabality for the recombination level. Table I gives the rate of removal of carriers from arsenic-doped germanium. These data were obtained using material from the same ingots as used for lifetime measurements and were kindly supplied by H. Shulman and J. W. Cleland.[35] Note that in all cases an early anneal was observed. The rate of introduction of carriers stable to this anneal was used to determine the concentration of recombination centers on the basis that two electrons were removed for every added defect. However, there may have been only one removed per defect. It was further assumed that the recombination

---

*If the annealing occurred as a second-order process in which acceptors and recombination centers were mutually annihilated, then the annealing kinetics would not be defect-concentration independent.

[35] H. Shulman and J. W. Cleland, personal communication.

TABLE I

HALL MEASUREMENTS OF ARSENIC-DOPED MATERIAL

(Data of H. Shulman and J. W. Cleland)[a]

Sample	Irradiation (gammas/cm^2)	Carrier Concentration (cm^{-3})			$-\frac{dn}{d\phi}$ (cm^{-1})	Mobility Recovery
		Initial	Post-Irradiation	Post-Low-Temperature Anneal[b]	Post-Anneal	
NCAs 5.4-3	2.75×10^{17}	3.23×10^{14}	8.6×10^{13}	1.35×10^{14}	6.8×10^{-4}	(large)
NCAs 5.4-4	4.58×10^{17}	4.50×10^{14}	1.16×10^{14}	1.30×10^{14}	7.0×10^{-4}	~ 60 %
NCAs 2.6-1	8.75×10^{17}	1.03×10^{15}	1.2×10^{14}	3.1×10^{14}	8.2×10^{-4}	~ 80 %
NCAs 2.6-4	8.50×10^{17}	1.36×10^{15}	5.67×10^{14}	5.80×10^{14}	9.2×10^{-4}	~ 70 %

[a]See Ref. 35.

[b]For instance, several hours at 83°C. Subsequent anneal at this temperature showed no additional effects.

level lies at $E_r - E_v = 0.36$ ev and that, at $1/T = 3.2 \times 10^{-3}$ for NCAs 5.4 and at $1/T = 3.1 \times 10^{-3}$ for NCAs 2.6, the lifetime is very nearly given by

$$\tau = \frac{p_{1r}}{c_{nr} n N_r}, \tag{38}$$

since the corrections to this term nearly cancel at these temperatures. (See Fig. 21.) Correcting for the pre-irradiation lifetime,

$$c_{nr} = \frac{\left(\frac{1}{\tau} - \frac{1}{\tau_o}\right) p_{1r}}{n N_r}. \tag{39}$$

Table II illustrates the calculation of c_{nr}. The value obtained is $2.0 \pm 0.4 \times 10^{-11}$ cm^3 sec^{-1}. Any inaccuracy in the position of the recombination level would have a large effect on this value. However, the estimated error does not include any such uncertainty.

In an earlier section the relationship between capture probabilities and cross sections was discussed. The cross section is approximately equal to the capture probability divided by the mean thermal velocity, $\langle v \rangle$. Using the expressions given, the resulting value for the mean thermal velocity of electrons in germanium at 300°K is 3.1×10^7 cm sec^{-1}. Using this value, the electron capture cross section was found to be approximately 7×10^{-19} cm^2.

Figure 35 is a reproduction of data from BAW. These data[8] represent samples containing $\sim 2 \times 10^{15}$ antimony atoms per cm^3, irradiated with one-Mev electrons at 79°K. Thus, all the damage stable at 79°K is present at the beginning of the anneal. Presumably, most

TABLE II

DETERMINATION OF CAPTURE PROBABILITY AND CROSS SECTION

Sample	$\left(\frac{1}{\tau} - \frac{1}{\tau_o}\right)^a$ (sec^{-1})	$p_{1r}(cm^{-3})^b$	$n(cm^{-3})$	$N_r(cm^{-3})^c$	$c_{nr}(cm^3/sec)$	$\sigma_{nr}(cm^2)$
NCAs 5.4	1.26×10^4	7.67×10^{12}	3.4×10^{14}	1.4×10^{13}	2.0×10^{-11}	6.5×10^{-19}
NCAs 2.6	1.37×10^4	1.23×10^{13}	9×10^{14}	9.1×10^{12}	2.1×10^{-11}	6.8×10^{-19}

[a] Following anneal at 126°C, measured at $1/T = 3.2 \times 10^{-3} (°K)^{-1}$ and $1/T = 3.1 \times 10^{-3} (°K)^{-1}$ for NCAs 5.4 and NCAs 2.6, respectively.

[b] $p_{1r} = N_v e^{-\frac{0.36}{kT}}$, where N_v is the effective number of states at the temperature T in the valence band.

[c] $N_r = \frac{-\left(\frac{dn}{d\Phi}\right)\Phi}{2}$, $\frac{dn}{d\Phi} = -7.0 \times 10^{-4}$ and -8.7×10^{-4} for samples NCAs 5.4 and NCAs 2.6, respectively.

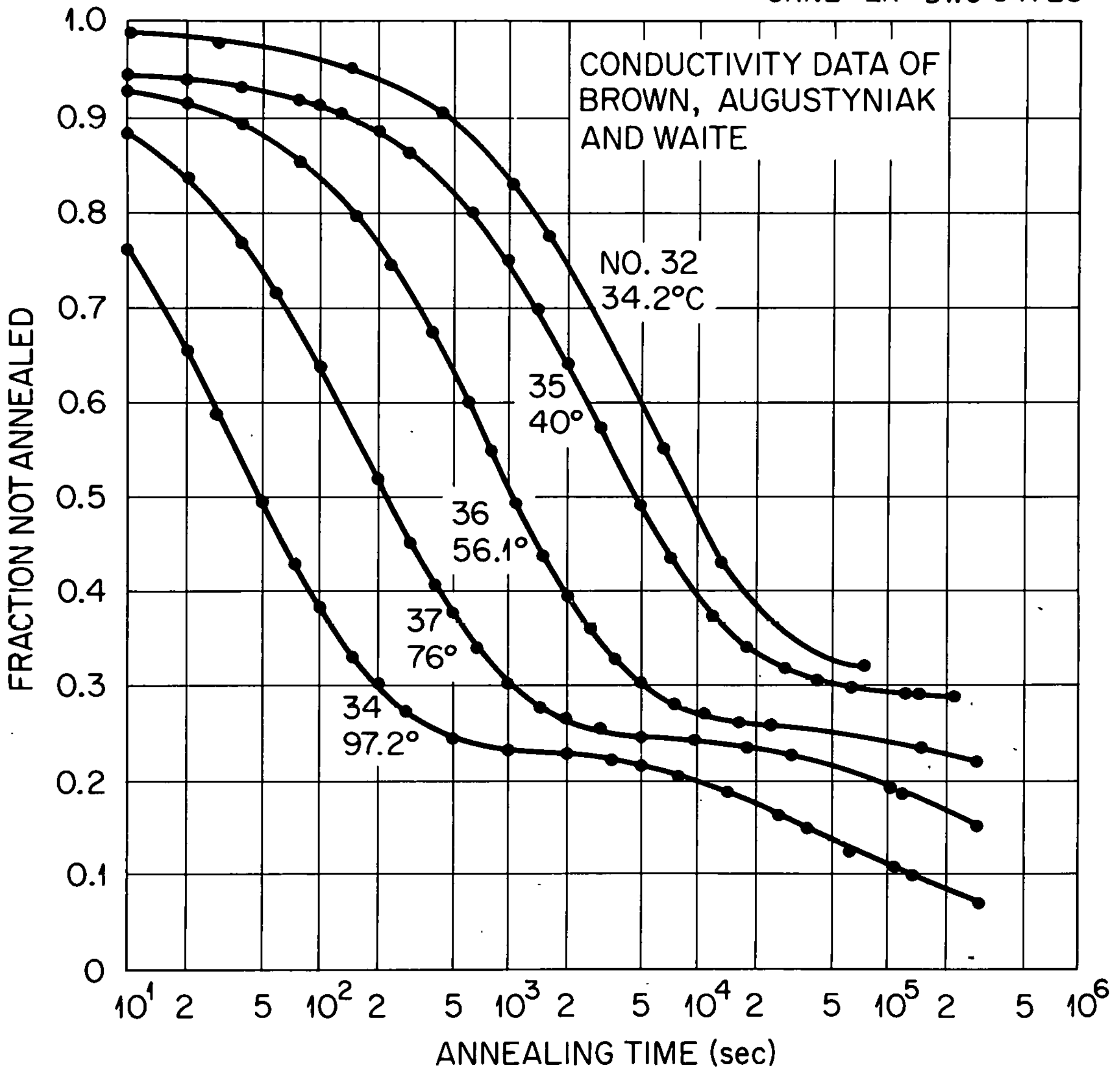

Figure 35. Isothermal Annealing Behavior in the Temperature Range just above Room Temperature of Antimony-Doped Germanium Irradiated with 1-Mev Electrons at 79°K. From Reference 8.

of the annealing shown in Fig. 35 would have already occurred in the lifetime samples before measurement. An analysis of this data is presented here which was not applied by BAW and which is of interest. (It should be emphasized that in analyzing annealing behavior there is not often a unique approach. This data of BAW can be analyzed on the basis of a diffusion-controlled, first-order process; but this fact alone does not definitely establish the actual nature of the annealing process.) Evidently, there is a sizeable fraction of the damage which does not anneal during the main process; and this fraction must be subtracted from the total in order to observe only this main process. Figure 36 demonstrates the result of subtracting a fraction from the original data such that first-order behavior is observed for long annealing times. The amount which is subtracted is fairly unique, being within $\pm$ 0.02 of the stated value, 0.32. Now, for this method of analysis to be valid, it should produce equivalent results for all annealing temperatures. Furthermore, the amount of damage annealed in the main process should be independent of the annealing temperature. That this is the case is shown in Fig. 37, where annealing curves for four temperatures are presented. The data for annealing at the lowest temperature were much less complete than for the higher temperatures; therefore, they were not included. Upon subtracting a nearly constant fraction, almost identical behavior is seen to exist for the four temperatures. In fact, up until the time that 60 per cent of the damage has been removed, both the corrected and uncorrected curves very nearly superimpose, merely by shifting the time scale. This fact indicates

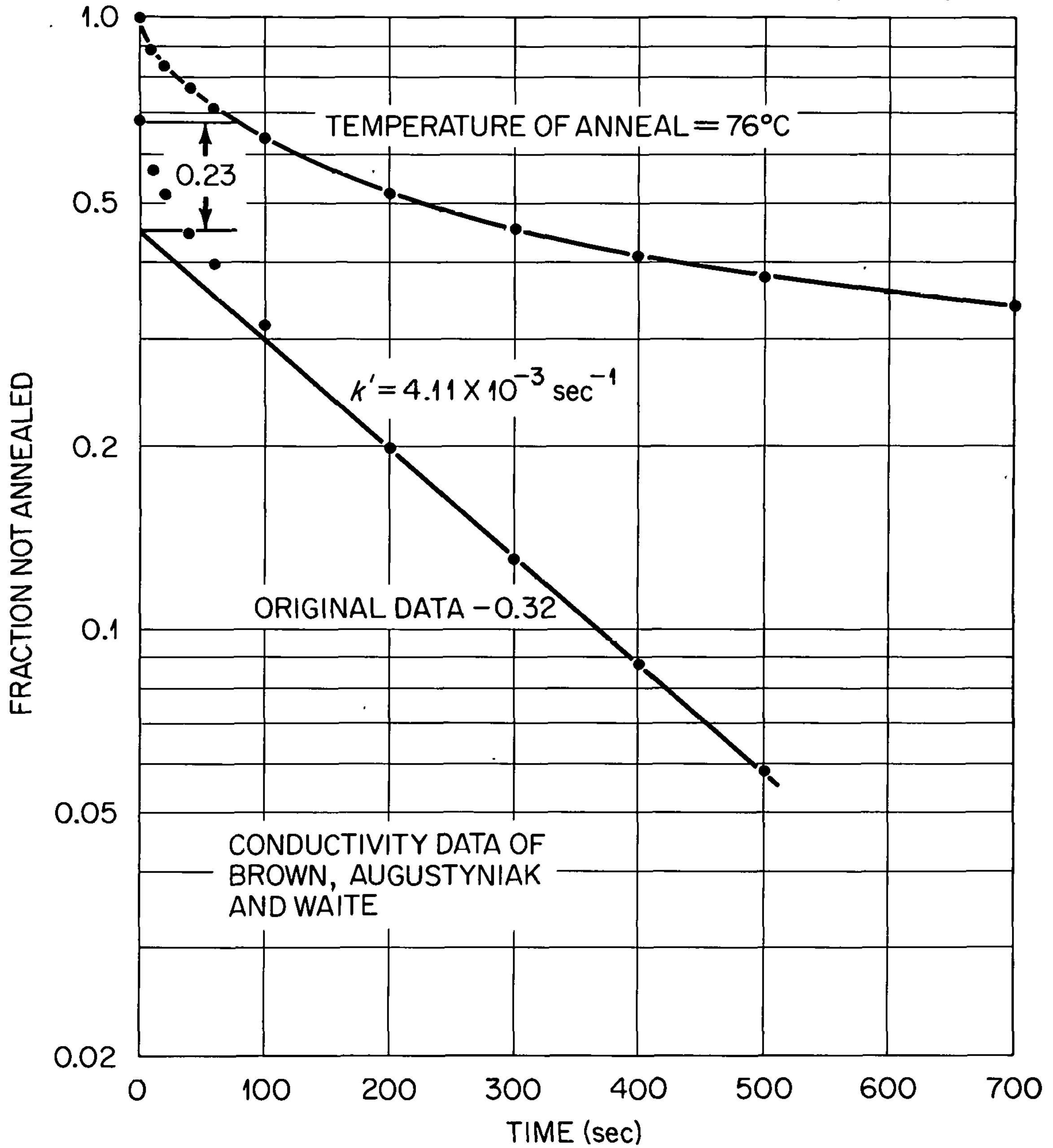

Figure 36. A Semi-Logarithmic Plot of a Portion of the Data of the Preceding Figure, before and after Subtracting the Fraction 0.32.

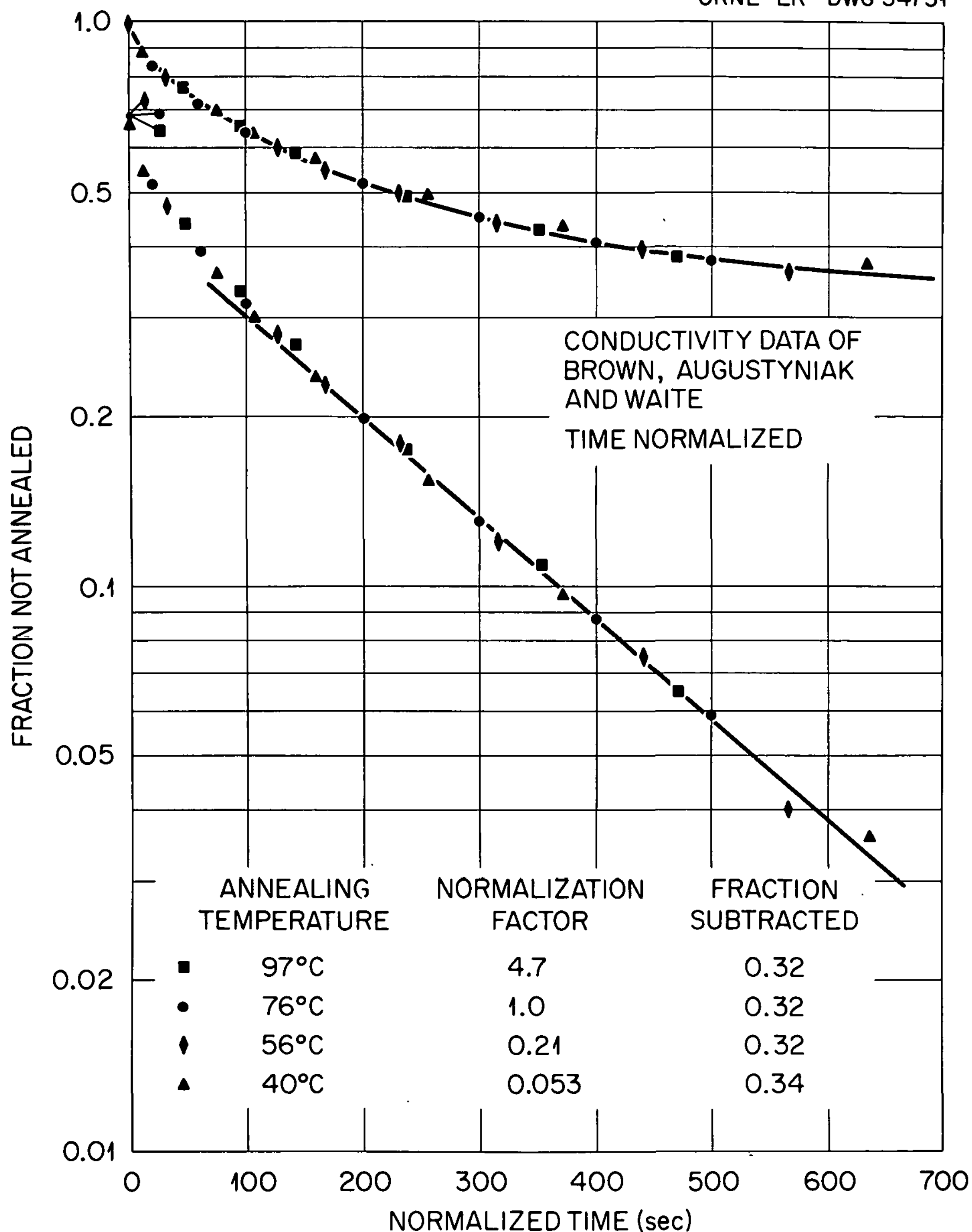

Figure 37. Four of the Isothermal Annealing Curves of Figure 35 Plotted as in Figure 36 but Time-Normalized to the Data of Figure 36.

that a single activation energy is responsible for the entire process. (The process occurring at longer times does not have any appreciable effect on these curves.) The observed behavior is consistent with a first-order, diffusion-limited process.[10,28] In effect, the first-order rate constant is time dependent, becoming constant only at long times. Figure 38 is a plot of the first-order rate constant obtained for the four temperatures plotted as a function of the reciprocal of the annealing temperatures. The data indicate an activation energy of 0.79 ev. This is practically the same value that BAW obtained merely by plotting the time required to attain one-half anneal as a function of reciprocal temperature. The reason that these two results are alike is clear from the upper curves of Fig. 37. These curves superimpose over this annealing range due to the fact that the annealing process is controlled by a single activation energy, except for processes which are completely unimportant at the time one-half of the damage has been removed.

Clearly, an understanding of any process which occurs prior to those observed in this study is important to the understanding of these results. It is of interest to note that the early anneal is dependent upon the nature of the impurity, as were also the present data for annealing at higher temperatures. Figure 39, also from BAW, displays this fact. This figure displays isothermal anneals at 56°C performed on samples which were essentially identical except for the doping agent. The antimony-doped samples show more extensive early anneal than those doped with arsenic or phosphorous. Since this

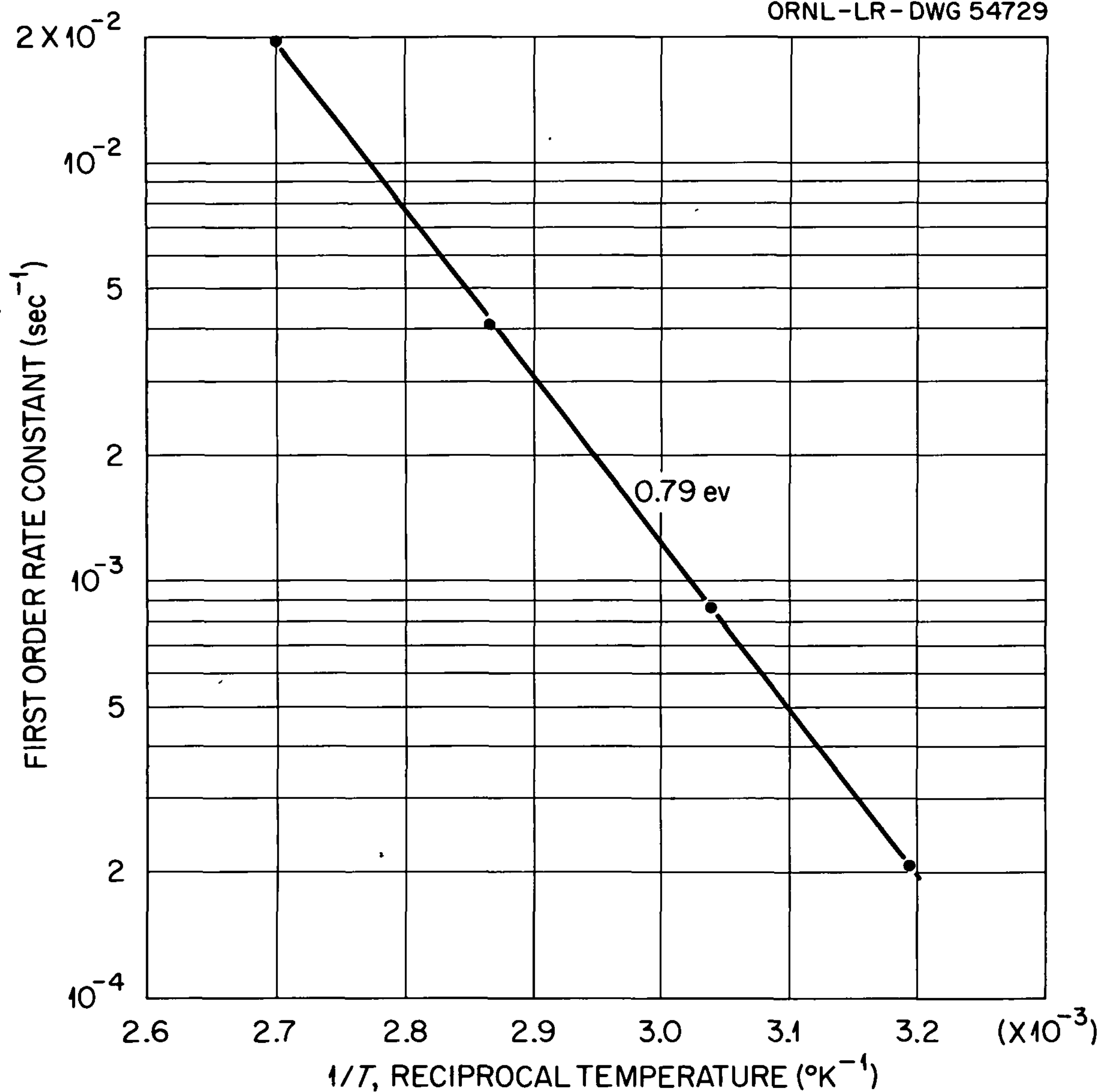

Figure 38. First-Order Rate Constant as a Function of Reciprocal Temperature from the Preceding Figure. The indicated activation energy is 0.79 ev.

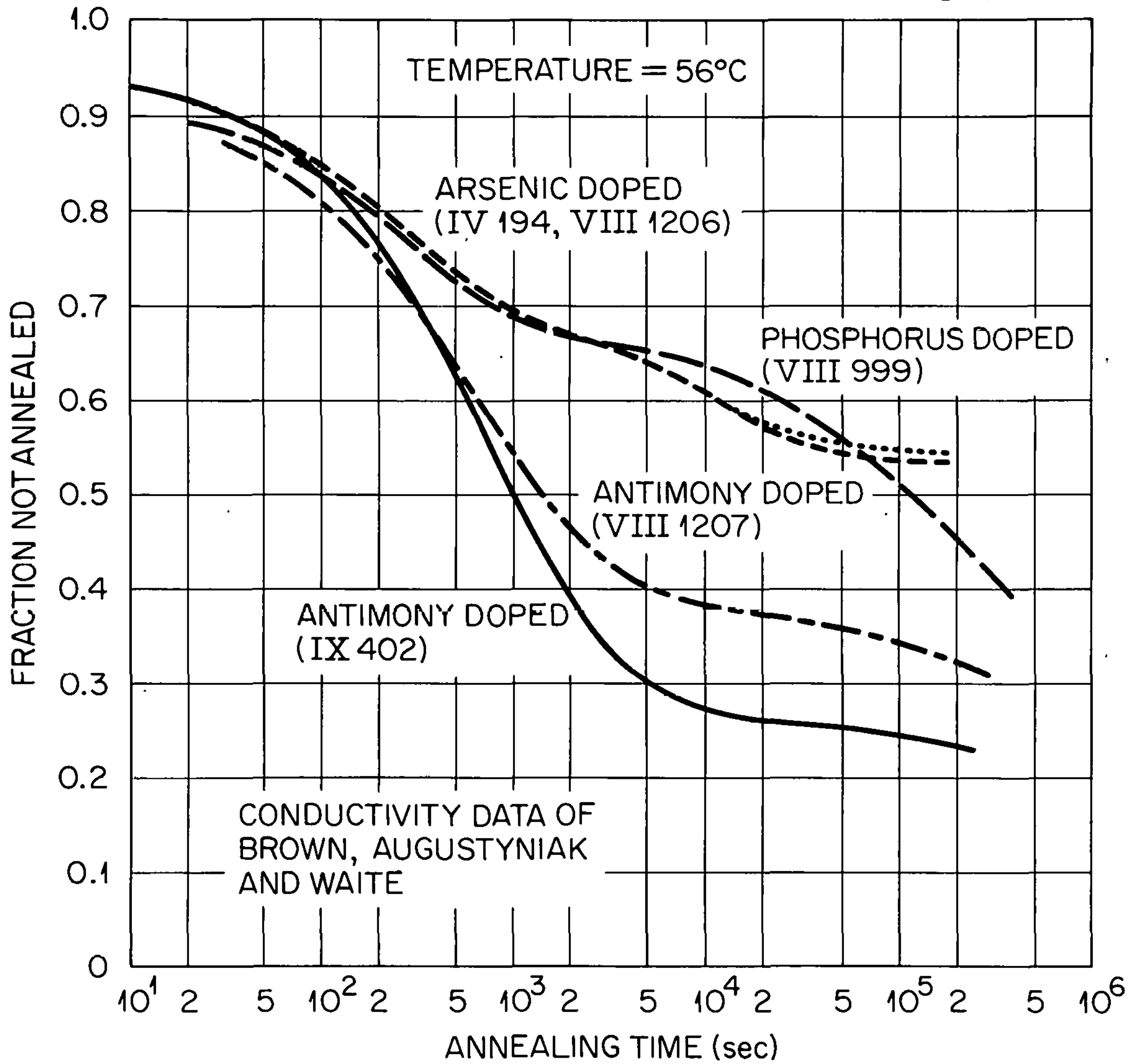

Figure 39. Isothermal Annealing Curves (56°C) Showing the Difference in Annealing Behavior among Specimens with Different Chemical Doping. From Reference 8.

annealing process is structure dependent, it cannot be due entirely to direct vacancy-interstitial recombination. Although analysis of the data of BAW in terms of a first-order process would be invalid if some direct recombination occurred, the value obtained for the activation energy would still be approximately correct.

An attempt has been made to explain the annealing at higher temperatures on the basis of the annealing of vacancies. An obvious possibility is to ascribe the early anneal to interstitial migration. The less rapid anneal and, also, the trapping levels present in the case of arsenic doping could be explained on the basis of interstitials associating themselves with arsenic atoms instead of being completely annealed. If the annealing process occurring near 50°C is, indeed, due to interstitial migration, then there may well be some vacancy-interstitial recombination. Whether or not this occurs could probably be determined by investigating the dependence of the annealing on the defect concentration. The various annealing results seem to indicate that neither the vacancy nor the interstitial is a positively charged donor. On the basis of the data of BAW and Brown, Fletcher, and Wright,[9] in no temperature range is there any significant annealing which produces a decrease in electron concentration. If the interstitial were a positively charged donor, then at the time of its anneal the magnitude of the change in carrier concentration should actually increase. As previously noted (Table I), in arsenic-doped material the early recovery in mobility is much larger than the recovery in carrier concentration. BAW, in Figs. 8 and 9 of their paper, show that for

arsenic-doped material the annealing of mobility proceeds along an entirely different path than the carrier concentration. In antimony-doped material the two properties anneal nearly together. This seems consistent with the idea that the early (approximately 50°C) anneal is associated with interstitial motion and that in the case of arsenic-doped material at least part of the interstitials associate themselves with arsenic atoms. In antimony-doped material this association would not be expected to occur because of the lattice strain an antimony-interstitial pair would produce. If the interstitial is an acceptor, it is negatively charged; and each time an interstitial associates itself with an arsenic atom two charged scattering centers are removed, thus increasing the mobility. The notion that this mobility increase for arsenic-doped material might be caused by the association of a defect with an arsenic atom was mentioned by BAW. However, they did not suggest that this defect might be an interstitial.

Although in n-type germanium defects introduced at 79°K are stable up to near room temperature, p-type material demonstrates large annealing effects in this range. This fact is demonstrated in Fig. 12 of BAW. This annealing, which occurs near 200°K in p-type material, is associated with trapping centers and is very dependent upon the charge state of the center. Thus, it is understandable that n-type material does not show annealing in this same temperature range. In fact, the annealing in p-type material near 200°K occurs only when light shining on the specimen has filled the traps with electrons.[8] In n-type material these centers are all filled with electrons at these temperatures.

Thus, these centers are probably not stable in n-type material even at 79°K. (This conclusion appears to be in agreement with the data of MacKay and Klontz,[36] who investigated the annealing behavior of electron-induced defects at lower temperatures and saw major recovery between 30°K and 70°K.) A good possibility for the nature of these defects would be that they are an unstable species of vacancy-interstitial pair. The dependence of annealing on charge state might be a further indication of this fact since the Coulomb forces associated with the charge would not be effective for very large separations.

---

[36] J. W. MacKay and E. E. Klontz, J. Appl. Phys. <u>30</u>, 1269 (1959).

CHAPTER V

SUMMARY

The most significant result of this study is felt to be the analysis of the recombination behavior by including the effect of trapping centers. Some ideas have been formulated concerning annealing behavior, but the concepts concerning recombination seem to be on a better footing. The recombination data in irradiated germanium can be explained in a more logical, consistent manner than was possible before. Figure 27 shows the energy-level structure proposed to explain the recombination data in n-type germanium. Evidence from the annealing data, together with recombination data, points to the isolated vacancy as the recombination center. The position of the energy level associated with the recombination center is located approximately 0.36 ev above the valence band in gamma-irradiated material. The capture probability associated with this center cannot be given with certainty due to the difficulty in determining the number of recombination centers. However, on the basis of some reasonable assumptions, a value has been obtained, $c_n = (2.0 \pm 0.4) \times 10^{-11}$ cm^3 sec^{-1}. From this value an estimate of the electron-capture cross section has been made, yielding the value $\sigma_n \sim 7 \times 10^{-19}$ cm^2. The number of isolated vacancies appears to be fairly small as compared with the number of coupled, vacancy-interstitial pairs in the case of Co^{60} gamma irradiation. These coupled pairs may be responsible for the energy level located 0.20 ev below the conduction band commonly observed[1,20] through Hall

measurements. It is even more likely that they are responsible for a trapping level about 0.25 ev above the valence band. The behavior in p-type germanium which previously was not explained can be accounted for quite reasonably on the basis that a high concentration of trapping centers initially present in the material is effective in the room-temperature range. Differences in the recombination behavior among types of irradiation can be explained on the basis that particles which impart higher energy to the germanium atom produce larger numbers of isolated vacancies as compared with the number of vacancy-interstitial pairs. There is apparently a small shift in the position of the energy level for the free vacancy in the case of neutron irradiation. This is probably due to the heavy, localized damage produced by neutron irradiation.

The annealing behavior is rather complicated and it was not possible to obtain a unique analysis of the observed behavior. However, some ideas were presented concerning the annealing process. The annealing behavior in germanium, as demonstrated by the lifetime measurements presented and conductivity measurements of others,[8,9,36] is not inconsistent with the following model. Irradiation produces three major types of defects: vacancies, interstitials, and vacancy-interstitial pairs. Some of these vacancy-interstitial pairs (possibly corresponding to the case in which the displaced atom occupies the nearest interstitial position) are unstable at rather low temperatures provided the associated energy level is occupied by an electron. In n-type germanium these centers are unstable below 79°K, while in p-type

material annealing of these close pairs is observed at higher temperatures (approximately 200°K), this annealing proceeding at a much higher rate when light is shown on the specimen, filling the trapping levels with electrons. Progressing to higher temperatures, the next defect to anneal seems to be the interstitial. It becomes mobile at about 50°C and has an activation energy for motion of approximately 0.8 ev. In arsenic-doped material many of these interstitials may associate themselves with arsenic atoms, with the resultant combination being stable up to about 225°C. The interstitial atoms would not form complexes with antimony atoms because of the large size of the antimony atom. According to this model, vacancies become mobile at about 100°C, their activation energy for motion being approximately 1.1 ev. Evidently, the vacancies show an affinity for antimony atoms, probably forming complexes which anneal at higher temperatures. However, this type of defect (vacancy-antimony pair), if it exists, does not affect the recombination. The idea of the vacancy and interstitial both forming complexes with donor atoms (interstitials in the case of arsenic atoms, vacancies in the case of antimony atoms), is reasonable in view of the fact that both vacancies and interstitials appear to act as acceptors. Were this not the case, the radiation-produced change in carrier concentration should be enhanced at the time the donor-type defect anneals. The positively charged donor would have an electrostatic attraction to a negatively charged acceptor. Furthermore, in order to provide the smallest strain in the lattice, the interstitial would find it energetically favorable to be near the

slightly undersized arsenic atom, while the vacancy would like to associate itself with the oversized antimony atom. Since the arsenic atoms are not available for vacancy removal, much higher temperatures are required for annealing in arsenic-doped material than in antimony-doped material since the vacancies must migrate to more distant sites, such as dislocations.

BIBLIOGRAPHY

BIBLIOGRAPHY

Aldington, J. N., and A. J. Meadowcroft, "The Flash Tube and Its Applications," Journal of the Institute of Electrical Engineers (London) 95 (1948), pp. 671-678.

Asada, T., H. Saito, K. Omura, T. Oku, and M. Oka, "Annealing of γ-Ray Damage in Germanium," Journal of the Physical Society of Japan 15 (1960), pp. 93-94.

Baruch, P., "Mobility of Radiation Induced Defects in Germanium," to be published in the Journal of Applied Physics.

Brown, W. L., W. M. Augustyniak, and T. R. Waite, "Annealing of Radiation Defects in Semiconductors," Journal of Applied Physics 30 (1959), pp. 1258-1268.

Brown, W. L., R. C. Fletcher, and K. A. Wright, "Annealing of Bombardment Damage in Germanium: Experimental," Physical Review 92 (1953), pp. 591-596.

Cleland, J. W., J. H. Crawford, Jr., and D. K. Holmes, "Effects of Gamma Radiation on Germanium," Physical Review 102 (1956), pp. 722-724.

Curtis, O. L., Jr., "Radiation Effects on Recombination in Germanium," Journal of Applied Physics 30 (1959), pp. 1174-1180.

Curtis, O. L., Jr., and J. W. Cleland, "Monoenergetic Neutron Irradiation of Germanium," Journal of Applied Physics 31 (1960), pp. 423-427.

Curtis, O. L., Jr., J. W. Cleland, and J. H. Crawford, Jr., "Radiation Induced Recombination Centers in Germanium," Journal of Applied Physics 29 (1958), pp. 1722-1729.

Curtis, O. L., Jr., J. W. Cleland, J. H. Crawford, Jr., and J. C. Pigg, "Effect of Irradiation on the Hole Lifetime of n-Type Germanium," Journal of Applied Physics 28 (1957), pp. 1161-1165.

Curtis, O. L., Jr., and J. H. Crawford, Jr., "Annealing of Radiation-Induced Recombination Centers in Germanium," Bulletin of the American Physical Society (II) 5 (1960), p. 196.

Dresselhaus, G., A. F. Kip, and C. Kittel, "Cyclotron Resonance of Electrons and Holes in Silicon and Germanium Crystals," Physical Review 98 (1955), pp. 368-384.

Gibson, A. F., A. F. Aigrain, and R. E. Burgess (Editors), Progress in Semiconductors (II). New York: John Wiley and Sons, Inc., 1957, pp. 69-107.

Hall, R. N., "Electron-Hole Recombination in Germanium," Physical Review 87 (1952), p. 387.

Herring, C., "Transport Properties of a Many-Valley Semiconductor," Bell System Technical Journal 34 (1955), pp. 237-290.

Hornbeck, J. A., and J. R. Haynes, "Trapping of Minority Carriers in Silicon I. p-Type Silicon," Physical Review 97 (1955), pp. 311-321.

Konopleva, R. F., T. V. Mashovets, and S. M. Ryvkin, "On the Influence of Defects Created by Neutron Irradiation on the Recombination Process in Germanium," Fizika Tverdogo Tela (Supplement II) (1959), pp. 11-21.

Lax, Benjamin, and J. G. Mavroides, "Statistics and Galvanomagnetic Effects in Germanium and Silicon with Warped Energy Surfaces," Physical Review 100 (1955), pp. 1650-1657.

Letaw, H., Jr., W. M. Portnoy, and L. Slifkin, "Self-Diffusion in Germanium," Physical Review 102 (1956), pp. 636-639.

Loferski, J. J., and P. Rappaport, "Electron-Bombardment Induced Recombination Centers in Germanium," Journal of Applied Physics 30 (1959), pp. 1181-1183.

MacKay, J. W., and E. E. Klontz, "Low Temperature Annealing Studies in Ge," Journal of Applied Physics 30 (1959), pp. 1269-1274.

Pauling, L., The Nature of the Chemical Bond. New York: Cornell University Press, 1948, pp. 160-193.

Reiss, H., "Diffusion-Controlled Reactions in Solids," Journal of Applied Physics 30 (1959), pp. 1141-1152.

Ryvkin, S. M., and I. D. Yaroshetskii, "The Influence of Trap Levels on the Relaxation of the Nonequilibrium Conductivity of Germanium Irradiated with Gamma Rays," Fizika Tverdogo Tela 2 (1960), pp. 1966-1780.

Shockley, W., and W. T. Read, Jr., "Statistics of the Recombination of Holes and Electrons," Physical Review 87 (1952), pp. 835-842.

Tyler, W. W., "Deep Level Impurities in Germanium," Journal of the Physics and Chemistry of Solids 8 (1959), pp. 59-65.

Waite, T. R., "Theoretical Treatment of the Kinetics of Diffusion-Limited Reactions," _Physical Review_ 107 (1957), pp. 463-470.

Waite, T. R., "Diffusion-Limited Annealing of Radiation Damage in Germanium," _Physical Review_ 107 (1957), pp. 471-478.

Wertheim, G. K., "Transient Recombination of Excess Carriers in Semiconductors," _Physical Review_ 109 (1958), pp. 1086-1091.

Wertheim, G. K., "Neutron-Bombardment Damage in Silicon," _Physical Review_ 111 (1958), pp. 1500-1505.

Wertheim, G. K., "Recombination Properties of Bombardment Defects in Semiconductors," _Journal of Applied Physics_ 30 (1959), pp. 1166-1171.

Wertheim, G. K., and G. L. Pearson, "Recombination in Plastically Deformed Germanium," _Physical Review_ 107 (1957), pp. 694-698.

ORNL-3108
UC-34 – Physics
TID-4500 (16th ed.)

INTERNAL DISTRIBUTION

1. Biology Library
2. Health Physics Library
3. Reactor Division Library
4-5. Central Research Library
6. ORNL - Y-12 Technical Library
7-26. Laboratory Records Department
27. Laboratory Records, ORNL R.C.
28. J. H. Barrett
29. R. F. Bass
30. W. T. Berg
31. D. S. Billington
32. T. H. Blewitt
33. G. E. Boyd
34. C. T. Butler
35. C. E. Center
36. R. A. Charpie
37. J. W. Cleland
38. R. S. Cockreham
39. Esther Cohn
40. R. R. Coltman
41-50. J. H. Crawford, Jr.
51. F. L. Culler
52-81. O. L. Curtis, Jr.
82. J. H. Frye, Jr.
83. C. S. Harrill
84. A. Hollaender
85. D. K. Holmes
86. A. S. Householder
87. J. T. Howe
88. L. D. Hulett
89. L. H. Jenkins
90. R. G. Jordan (Y-12)
91. W. H. Jordan
92. C. P. Keim
93. M. T. Kelley
94. R. H. Kernohan
95. C. E. Klabunde
96. J. A. Lane
97. T. A. Lincoln
98. S. C. Lind
99. R. S. Livingston
100. H. G. MacPherson
101. C. J. McHargue
102. A. J. Miller
103. K. Z. Morgan
104. J. P. Murray (K-25)
105. M. L. Nelson
106. O. S. Oen
107. S. Othmer
108. V. K. Pare
109. D. Phillips
110. J. C. Pigg
111. P. M. Reyling
112. M. T. Robinson
113. H. C. Schweinler
114. H. E. Seagren
115. S. T. Sekula
116. E. D. Shipley
117. H. Shulman
118. M. J. Skinner
119. A. H. Snell
120. E. Sonder
121. A. L. Southern
122. J. A. Swartout
123. E. H. Taylor
124. D. O. Thompson
125. M. S. Wechsler
126. R. A. Weeks
127. A. M. Weinberg
128. C. E. Winters
129. M. C. Wittels
130. F. W. Young, Jr.
131. Harvey Brooks (consultant)
132. N. Cabrera (consultant)
133. R. L. Sproull (consultant)
134. D. Turnbull (consultant)

EXTERNAL DISTRIBUTION

135. Division of Research and Development, AEC, ORO
136-138. Bell Telephone Laboratories, Murray Hill, New Jersey (1 copy each to W. M. Augustyniak, Walter L. Brown, and G. K. Wertheim)
139-142. University of Tennessee, Knoxville, Tennessee (1 copy each to E. G. Harris, A. H. Nielson, R. D. Present, and J. O. Thomson)
143-144. Sandia Corporation, Sandia Base, Albuquerque, New Mexico (1 copy each to J. W. Easley and Herman Stein)
145. Lincoln Laboratory, Massachusetts Institute of Technology, Cambridge, Massachusetts (Gene F. Dresselhaus)
146. Department of Physics, Rockefeller Hall, Cornell University, Ithaca, New York (James A. Krumhansl)
147. Department of Physics, Arizona State University, Tempe, Arizona (Ben R. Gossick)
148. Department of Mining and Metallurgical Engineering, University of Illinois, Urbana, Illinois (T. A. Read)
149. Department of Physics, The University of North Carolina, Chapel Hill, North Carolina (Lawrence Slifkin)
150-778. Given distribution as shown in TID-4500 (16th ed.) under Physics category (75 copies - OTS)
779. Department of Physics, University of Tennessee, Knoxville, Tennessee (W. E. Deeds)